

Photosystem II electron flow as a measure for
phytoplankton gross primary production

Fotosysteem II elektronentransport als een maat voor
de bruto primaire produktie van fytoplankton

Promotor: dr. W.J. Vredenberg
Hoogleraar in de plantenfysiologie met bijzondere aandacht voor fysische aspecten

Co-promotor: dr. J.F.H. Snel
Universitair docent bij de leerstoelgroep plantenfysiologie

NUG 2701, 2342

Corine Geel

**PHOTOSYSTEM II ELECTRON FLOW AS A MEASURE FOR
PHYTOPLANKTON GROSS PRIMARY PRODUCTION**

Proefschrift

ter verkrijging van de graad van doctor
op gezag van de rector magnificus
van de Landbouwniversiteit Wageningen
dr. C.M. Karssen

in het openbaar te verdedigen
op woensdag 12 november 1997
des namiddags te vier uur in de Aula

ISBN: 947511

The work presented in this thesis was performed at the Wageningen Agricultural University,
Department of Plant Physiology, Arboretumlaan 4, 6703 BD Wageningen, The Netherlands

The investigations were supported by the Cornelus Lely foundation and the National Institute of
Coastal and Marine Management (RIKZ)

Cover design front page: Henk Geel

Cover design back page: comic strip "Heinz" from René Windig and Eddy de Jong

ISBN 90-5485-789-7

BIBLIOTHEEK
LANDBOUWUNIVERSITEIT
WAGENINGEN

STELLINGEN

- 1 De minimale fluorescentie van eukaryote algen is een goede maat voor het lichtabsorberend vermogen van fotosysteem II, mits de spectrale verdeling van het fluorescentie-excitatielicht identiek is aan die van het omgevingslicht.

Dit proefschrift.

- 2 Zolang er onduidelijkheid blijft bestaan over het bruto of netto karakter van fotosynthese metingen met behulp van ^{14}C incubatie is het eenduidiger om fotosynthese metingen te baseren op metingen van de fytoplankton elektronen flux met behulp van fluorescentie.

Dit proefschrift.

Williams et al, J Plankton Res 18(10):1961-1974 (1996).

- 3 De doving van de maximale fluorescentie in het donker bij gelijkblijvende efficiëntie, zoals waargenomen door Ting en Owens, is beter te verklaren met een zogenaamde 'state transition' dan met de door hen gesuggereerde chlororespiratie.

Dit proefschrift.

Ting and Owens, Plant Physiol 101:1323-1330 (1993).

- 4 Het feit dat anno 1996 slechts weinig mensen zich persoonlijk verantwoordelijk voelen voor het milieu wordt geïllustreerd door onder andere de toename van het privé gebruik van elektriciteit en auto, en de toename van de hoeveelheid huishoudelijk afval.

Milieubalans, RIVM (1997).

- 5 Het gesuggereerde vertrek van het hoofdkantoor van Philips uit Eindhoven omdat Eindhoven zich te ver van de financiële centra bevindt is een ontkenning van de mogelijkheden van de huidige communicatie middelen aan de ontwikkeling waarvan Philips zelf bijgedragen heeft.

- 6 De minimalisering van mineralenverliezen in de rundveehouderij kan tot gevolg hebben dat runderen het hele jaar op stal moeten blijven staan. Uit oogpunt van dierwelzijn en humane recreatie is dit een ongewenste ontwikkeling.
- 7 Degene die zich ergert aan een ander is bezig de ander te verbieden wat hij/zij zichzelf niet kan toestaan.

Marinus Knoope, Humanist 6/7/8 (1997).

- 8 Mensen die louter in de geest van het collectivisme grootgebracht worden kunnen onvoldoende hun individualiteit ontwikkelen en zullen als reactie hierop eerder egoïstisch gedrag vertonen dan mensen bij wie hun individualiteit wel voldoende ontwikkeld is.

Guus Kuijer, het geminachte kind.

- 9 Wie tijdens haar zwangerschap niet op de hoogte gesteld wil worden van allerlei rampscenario's aangaande zwangerschap, bevalling en het hebben van jonge kinderen kan het beste het gezelschap van mensen met jonge kinderen vermijden.

Stellingen behorende bij het proefschrift "Photosystem II electron flow as a measure for phytoplankton gross primary production".

Wageningen, 12 november 1997.

Corine Geel

VOORWOORD

Ik wil graag een aantal mensen bedanken voor hun bijdrage aan de totstandkoming van dit proefschrift. Zowel voor mijn wetenschappelijke als voor mijn persoonlijke ontwikkeling heb ik de afgelopen 6 jaren als een leerzame, soms moeizame, maar ook leuke tijd ervaren.

Vooreerst wil ik iedereen bedanken voor de gezelligheid, waardoor ik altijd wel weer zin had om naar Wageningen, en voor twee korte periodes, naar Zeeland af te reizen.

Voor wetenschappelijke en technische ondersteuning wil ik bedanken: de leden van de fotosynthese groep, met name Jan Snel, Wilma Versluis, Wim Vredenberg en natuurlijk Victor Curwiel, Tijmen van Voorthuysen en Gert Schansker; Willem Buurmeijer voor de programmatuur; van de werkplaats Jan van Kreel en Ruth van der Laan; de studenten Marjola Maas v.d. Weijde, Kitty Jansen (ik wacht nog steeds op een foto!) en Martine Segers; mijn broer Martin voor een deel van de figuren; van de begeleidingscommissie Bart Althuis, Kees Peeters, Hans Hofstraat en Jacco Kromkamp; uit Middelburg en Jacobahaven: Louis Peperzak, Martin Steendijk, Arjen Pouwer, Vincent Escaravage en Theo Prins; for the development of the Xe-PAM fluorometer which opened many possibilities for my research project I want to thank dr Schreiber.

Gerrit wil ik bedanken voor zijn geweldig relativeringsvermogen en voor alle eigenschappen die hij in royale mate tentoonspreidt en die ik wel eens te weinig bezit.

CONTENTS

List of abbreviations

1 General introduction	1
1.1 Primary production in marine ecosystems	
1.2 Photosynthetic energy conversion	
1.2.1 Light reactions	
1.2.2 Dark reactions	
1.3 Regulation of PS II electron flow	
1.3.1 Light harvesting	
1.3.2 PS II electron flow	
1.4 Chlororespiration	
1.5 Measurement of primary production	
1.5.1 Increase in biomass	
1.5.2 Carbon uptake, oxygen evolution	
1.5.3 PS II electron flow	
1.6 Outline of the thesis	
2 Simple determination of photosynthetic efficiency and photoinhibition of <i>Dunaliella tertiolecta</i> by saturating pulse fluorescence measurements	11
2.1 Introduction	
2.2 Measurement of saturating pulse fluorescence	
2.3 Experimental application	
2.4 Results and discussion	
2.4.1 Measurement of Φ_{PSII} and q_P	
2.4.2 Determination of photoinhibition	
2.4.3 Modifications for phytoplankton measurement	
2.5 Conclusions	
3 Estimation of oxygen evolution by marine phytoplankton from measurement of the efficiency of photosystem II electron flow	26
3.1 Introduction	
3.2 Materials and methods	
3.3 Results	
3.4 Discussion	
3.5 Conclusions	
4 Measurement of phytoplankton electron flux using a Xe-PAM fluorometer	41
4.1 Introduction	
4.1.1 Comparison of the Xe-PAM and the PAM fluorometers	
4.1.2 Phytoplankton electron flux	

4.2 Materials and methods	
4.3 Results and discussion	
4.3.1 Spectral distribution of the efficiency of PS II electron flow	
4.3.2 F_0 as a measure of PS II excitation	
4.3.3 Determination of the efficiency of PS II electron flow	
4.4 Conclusions	
5 The relation between carbon fixation and photosystem II electron flow in marine phytoplankton	56
5.1 Introduction	
5.2 Materials and methods	
5.3 Results	
5.4 Discussion	
5.5 Conclusions	
6 Estimation of photosynthetic performance of marine phytoplankton in a model ecosystem by means of chlorophyll fluorescence	67
6.1 Introduction	
6.2 Materials and methods	
6.3 Results	
6.4 Discussion	
7 The minimal fluorescence in the dark as a measure for photosystem II excitation in the light: Effects of chlororespiration and state transitions	83
7.1 Introduction	
7.2 Materials and methods	
7.3 Results	
7.4 Discussion	
7.4.1 Effects of chlororespiration on the fluorescence yield	
7.4.2 Effects of state transitions on the fluorescence yield	
7.4.3 How much does F_0' (the light adapted state) differ from F_0 (the dark adapted state)?	
7.5 Conclusions	
8 General discussion	92
8.1 Introduction	
8.2 Fluorescence measurements on phytoplankton samples	
8.3 The relation between PS II electron flow, oxygen evolution and carbon fixation	
8.3.1 Oxygen evolution and carbon fixation	
8.3.2 Minimal fluorescence, F_0	
8.4 Phytoplankton electron flux or phytoplankton carbon flux?	
8.5 Recommendations for future research	
Summary	99

Samenvatting	101
References	103
Curriculum Vitae	110

LIST OF ABBREVIATIONS

A	constant used in the photosynthesis model
B	constant used in the photosynthesis model
C	constant used in the photosynthesis model
chl	chlorophyll <i>a</i> concentration
D	initial slope of phytoplankton carbon flux as a function of phytoplankton electron flux
DPFD	daily photon flux density from 400 to 700 nm
E	constant used in the photosynthesis model
F	actual fluorescence in light adapted state
F_0 ; F_0'	minimal fluorescence in dark adapted and light adapted state respectively
F_M ; F_M'	maximal fluorescence in dark adapted and light adapted state respectively
F_V	variable fluorescence ($F_M - F_0$)
J_C	rate of carbon fixation
J_E	rate of PSII electron flow
J_E^L and J_E^M	rate of PSII electron flow, determined in the laboratory and in the mesocosm respectively
J_O	rate of oxygen evolution
k	constant used in the photosynthesis model
K_d	apparent diffuse light attenuation coefficient
LHC	light harvesting complex
NSDP	net system daily production of oxygen in the mesocosm
n_{PSII}	number of PS II reaction centers
PCF	phytoplankton carbon flux
PEF	phytoplankton electron flux
PFD	photon flux density from 400 to 700 nm
POF	phytoplankton oxygen flux
PPC	daily primary production measured as carbon fixation
PPE^L and PPE^M	daily primary production measured as photosystem II electron flow, using laboratory data and mesocosm data, respectively
PPO	daily primary production determined from the oxygen concentration
PQ	plastoquinone
PS	photosystem
q_N	non-photochemical quenching of fluorescence
q_P	photochemical quenching of fluorescence
Q_A	primary electron acceptor of photosystem II
SDR	system day respiration
Φ_{Po}	the photochemical yield of open PS II reaction centers
Φ_{PSII}	apparent quantum yield of photosystem II electron transport
σ_{PSII}	absorption cross section of photosystem II

1 GENERAL INTRODUCTION

1.1 Primary production in marine ecosystems

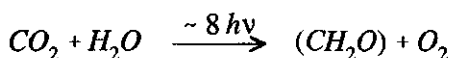
The marine ecosystem contains photoautotrophic and heterotrophic organisms. Phytoplankton and macrophytes belong to the photoautotrophic organisms and convert inorganic carbon into organic matter by means of photosynthesis. This organic matter, which is the basis of the food web, is consumed by heterotrophic organisms like for example protozoans, shrimps, mussels and fishes and by microbes which decompose organic material back to the basic substances like CO_2 , NO_3^- and PO_4^{3-} .

Primary production is defined as the increase in phytoplankton organic matter and can be expressed in two ways. Gross primary production is the increase in organic matter including the organic matter lost in respiration. Net primary production is the organic matter produced minus the organic matter respired. Primary production can be measured as the increase in biomass but can also be derived from the chlorophyll content, photosynthetic carbon fixation or oxygen evolution.

The North Sea ecosystem in general contains the following phytoplankton groups: Cyanophyta (cyanobacteria); Chrysophyta, especially the Prymnesiophyceae (including flagellates and coccolithophorids) and the Bacillariophyceae (diatoms); Phyrophyta (dinoflagellates) and Cryptophyta (Kirk 1994, Reid et al 1990, Hofstraat et al 1994b). Chlorophyta (green algae) are only scarcely present in the North Sea. The cyanobacteria are present in large numbers, but are of minor importance for primary production because of their small size. Both diatoms, flagellates (*Phaeocystis*) and dinoflagellates are major primary producers of the North Sea ecosystem. The Cryptophyta are occasionally significant components of the phytoplankton in coastal waters (Kirk 1994).

1.2 Photosynthetic energy conversion

In photosynthesis light energy is used to convert water (H_2O) and carbon dioxide (CO_2) into carbohydrates:



Photosynthesis consists of two groups of reactions: the light reactions and the dark reactions. In eucaryotes the light reactions take place at the thylakoid membranes in the chloroplast, the dark reactions take place in the stroma of the chloroplast.

1.2.1 Light reactions

The light is absorbed by antenna pigments in the light harvesting complexes (LHC) and the

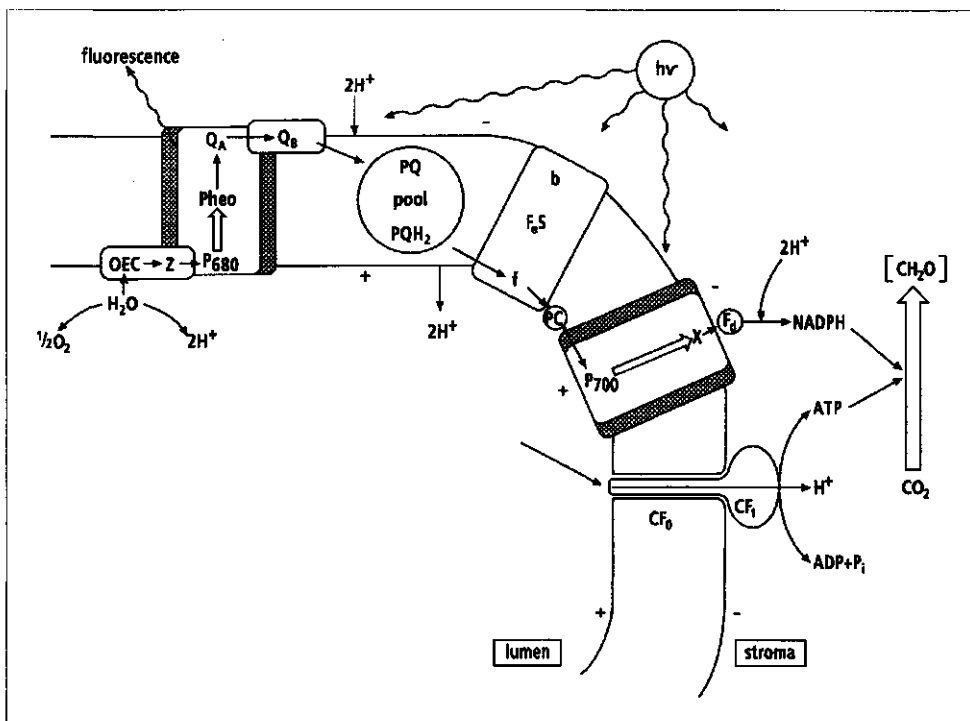


Figure 1.1. Simplified scheme of the photosynthetic electron transport. Z: intermediary electron donor for P_{680}^+ ; pheo: pheophytin, intermediary electron acceptor of P_{680}^+ ; Fe-S: Rieske iron-sulphur protein, part of the cytochrome $b_6 f$ complex; X: intermediary electron acceptor of P_{700}^+ ; Fd: ferredoxin; CF_0 - CF_1 : ATPase complex. Other symbols are explained in the text.

excitation energy is delivered to the P_{700} and the P_{680} reaction centre molecules, imbedded in photosystem I (PS I) and II (PS II) respectively (Fig. 1.1). In the reaction centre of PS I and PS II this excitation energy induces a charge separation. At PS II the bound plastoquinone Q_A is the primary stable electron acceptor. After taking up 2 electrons from Q_A and 2 protons from the stroma the secondary acceptor Q_B dissociates from its binding site at PS II and diffuses into thylakoid membrane, becoming part of the mobile plastoquinone (PQ and PQH_2) pool. Upon binding of PQH_2 to the cytochrome $b_6 f$ complex the protons are released into the lumen and the electrons are transferred to cytochrome f . From cytochrome f the electrons go to plastocyanine (PC) and are finally used to reduce P_{700}^+ . P_{680}^+ is reduced by electrons derived from the splitting of water which results into the liberation of protons and oxygen at the oxygen evolving complex (OEC) of PS II. The proton gradient which is formed is used by the ATPase to form ATP.

Charge separation in PS I initiates a series of redox reactions which result in the reduction of the mobile electron acceptor ferredoxin. $NADP^+$ takes up 2 electrons from ferredoxin (transferred by ferredoxin $NADP^+$ reductase) and 2 protons from the stroma to form $NADPH + H^+$ (Hall and Rao 1987).

In contrast to linear electron flow as described above, in cyclic electron flow the electrons from

ferredoxin are not transferred to NADP^+ but are transferred to PQ, accompanied by the uptake of 2 protons from the stroma per 2 electrons. The formed PQH_2 can be oxidised, releasing the protons in the lumen and delivering the electrons to cytochrome *f*. Cytochrome *f* donates the electrons again to PS I via PC. The stoichiometry in cyclic electron flow is 1 proton translocated per electron.

Light harvesting complexes in phytoplankton

Light harvesting occurs by light harvesting pigment complexes. The LHC of higher plants contains chlorophyll *a* and *b* as the main antenna pigments and the thylakoids are organised in grana stacks. A lot of algae differ from higher plants in their light harvesting pigments and in the organisation of the LHC. In green algae the LHC is comparable to that in higher plants though the grana stacking is less prominent. In the main brown algal groups (coccolithophorids, flagellates, diatoms and dinoflagellates) the thylakoids are grouped per 3. Coccolithophorids, flagellates and diatoms contain the antenna pigments chlorophyll *a*, *c*₁ and *c*₂ and the carotenoid fucoxanthin. Dinoflagellates contain chlorophyll *a* and *c*₂ and the carotenoid peridinin (Kirk 1994). The carotenoids fucoxanthin and peridinin are both efficient in light harvesting (Haxo and Blinks 1950; Goedheer 1970; Prézelin and Haxo 1976). The Cryptophyta contain chlorophyll *a* and *c*₂ and phycobilisomes with either phycoerythrins or phycocyanins as light harvesting pigments. The thylakoid membranes are organized in loosely associated pairs (Kirk 1994). The thylakoids of the procaryotic Cyanobacteria are invaginations of the cell membrane. Cyanobacteria contain chlorophyll *a* and phycobilisome LHCs which contain phycocyanin pigments (Kirk 1994).

Efficiency of PS II electron flow

The efficiency of PS II electron flow, as used here, is defined as the efficiency with which excitation energy is used for photochemistry driving PS II electron flow. In Figure 1.2 a schematic drawing of the processes occurring at the LHC and at the PS II reaction centre, based on the bipartite model of Butler (1978), is given. Light absorbed by the LHC will result in an excited chlorophyll molecule. This excited state (an exciton) can move around between chlorophyll molecules in the LHC. The exciton releases its energy via different pathways: non-radiative energy dissipation, e.g. heat release (rate constant k_D), radiative energy dissipation, e.g. fluorescence (rate constant k_F) or it can transfer its energy to the PS II reaction centre (rate constant k_T). Energy delivered to the reaction centre will result in the excitation of the reaction centre chlorophyll P. P^* can transfer an electron to the primary electron acceptor A, which determines the rate of primary photochemistry (rate constant k_P). Both states P^+-A^- and $\text{P}-\text{A}^-$ (in which P^+ is reduced by the primary donor of PS II) are called closed reaction centres. As long as a reaction centre is closed, it is not able to perform another electron transfer to Q_A , e.g. k_P is zero: P^* cannot perform photochemistry and will transfer its energy back to the LHC (k_L); P^* can also relax via non-radiative energy dissipation in the reaction centre (k_A), but the rate constant of this process is very small making the yield neglectable under normal conditions. Inhibition of photochemistry will therefore result in an increase of heat release, D, and fluorescence, F. The fluorescence yield when all reaction centres are open is called the minimal fluorescence, F_0 . The fluorescence yield when all reaction centres are closed is called the maximal fluorescence, F_M .

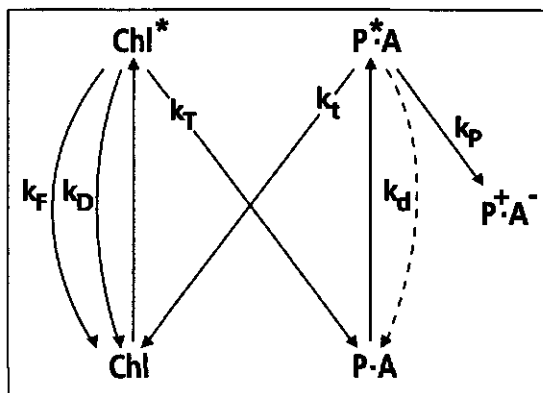


Figure 1.2. primary reactions of PS II according to the model of Butler (1978). Symbols are explained in the text.

The model assumes that all rate constants are constant, except k_p , which can become zero in a closed reaction centre; later observations have shown that k_p can change in response to acidification of the thylakoid lumen (see section 1.3.2). More recent research has shown that although the bipartite model of Butler (1978) is based on an incomplete mechanism, on a ms timescale the model gives good results (for a review see Dau 1994).

Two pathways that are not included in the Butler model are charge recombination and cyclic electron flow in PS II. Charge recombination from the state P^+A^- back to $P-A$ was observed to occur at -196°C (Butler et al 1973, Murata et al 1974) but at room temperature the forward reaction is much faster than the back reaction. Cyclic electron flow in PS II has been suggested to proceed from the state P^+A^- to $P-A$ via electron flow to the donor side of PS II (Prasil et al 1996). The determination of the efficiency of PS II electron flow is hardly influenced by charge recombination and cyclic electron flow in PS II.

1.2.2 Dark reactions

The NADPH and ATP formed in the light reactions are used to reduce carbon dioxide to the level of carbohydrate. A key reaction in the fixation of carbon dioxide is the reaction of carbon dioxide with ribulose 1,5-bisphosphate (RuBP). This reaction is catalysed by the enzyme ribulose 1,5-bisphosphate carboxylase oxygenase (rubisco) and it results in the formation of 2 molecules phosphoglycerate (PGA).

Dissipative dark reactions

In the presence of oxygen rubisco can also act as an oxygenase catalysing the oxygenation of RuBP to 1 PGA and 1 molecule of phosphoglycolate. This reaction is the initiation of photorespiration and is favoured at high oxygen concentrations and/or low carbon dioxide concentrations, and at high temperatures. Phosphoglycolate is not metabolised in the Calvin cycle, but 2 molecules phosphoglycolate are converted into 1 molecule PGA under the consumption of 3 molecules O_2 and the release of 1 molecule CO_2 (Tolbert 1979). As in the

photosynthetic light reaction, preceding the formation of 2 molecules phosphoglycolate, 2 molecules O_2 have been formed the overall stoichiometry of the photosynthetic light reactions and the photorespiratory dark reactions is 1 molecule O_2 taken up per 1 molecule CO_2 released.

Another non-productive pathway is the Mehler-reaction, also named pseudo-cyclic electron flow (Gimmler 1977). In the Mehler-reaction electrons (e^-) coming from ferredoxin are transferred to oxygen to form the superoxide radical ($4O_2 + 4e^- \rightarrow 4O_2^-$). The electrons needed are generated in the photosynthetic light reactions ($2H_2O \rightarrow 4e^- + 4H^+ + O_2$). The superoxide radicals are rapidly converted to the radical H_2O_2 and O_2 ($4O_2^- + 4H^+ \rightarrow 2 H_2O_2 + 2 O_2$) by the enzyme superoxide dismutase. Therefore at this point an uptake of oxygen is found (Asada and Takahashi 1987, Schreiber et al 1995a). In chloroplasts H_2O_2 is scavenged by ascorbate forming monodehydroascorbate (Foyer and Lelandais 1993, Schreiber et al 1995a). This reaction is catalysed by ascorbate peroxidase. The monodehydroascorbate which is formed in this reaction is recycled by monodehydroascorbate reductase (the overall reaction: $2 H_2O_2 + 4e^- + 4H^+ \rightarrow 4 H_2O$). The electrons needed for reduction of monodehydroascorbate are generated in the photosynthetic light reactions ($2 H_2O \rightarrow 4e^- + 4H^+ + O_2$). In the total of these reactions 4 molecules of oxygen and 4 molecules of NADPH are formed but also 4 molecules of oxygen and 4 molecules of NADPH are consumed. It has been suggested that the proton translocation associated with the electron flow to oxygen is important for the regulation of photosynthesis (Björkman and Demmig-Adams 1995). A special case of photosynthetic regulation is the activation of the Calvin cycle which requires a trans thylakoid proton gradient (Schreiber et al 1995a).

Nitrogen metabolism

Furthermore NADPH is not only used in carbon assimilation but, for example, nitrate reduction into ammonium also requires NADPH. Ammonium is the form used in nitrogen metabolism (i.e. amino acid synthesis). For the conversion of NO_3^- to NH_4^+ 8 electrons are needed which might represent as much as one-fourth of the electrons required for the fixation of CO_2 (Lindblad and Guerrero 1993).

1.3 Regulation of PS II electron flow

1.3.1 Light harvesting

In higher plants and green algae changes in the light environment result in state transitions. These state transitions involve changes in energy distribution from LHC II, the major light harvesting pigment protein complex, to PS II and PS I. The state transitions are mediated by phosphorylation of LHC II, resulting in disconnection of LHC II from PS II and attachment to PS I. A reduced PQ-pool, due to a disproportional excitation of PS II, causes activation of the kinase which phosphorylates the light harvesting complex connected to the PS II reaction centre (LHC II). Phosphorylated LHC II's disconnect from the PS II reaction centre, reducing the amount of excitation energy available for photochemistry in PS II (state II). A permanently active phosphatase dephosphorylates LHC II, resulting in the reattachment of LHC II to the PS II reaction

centre in the case the kinase is inactive when the PQ-pool is oxidised (state I) (Allen 1992). The number of LHC's delivering excitation energy to PS II determine the functional absorption cross-section of PS II. A transition from state II to state I is therefore accompanied with a parallel increase of the minimal and the maximal fluorescence (Malkin et al 1986).

The regulation of energy distribution in marine phytoplankton species is as yet not as extensively examined as in higher plants though some aspects have been described in the literature. For the diatom *Phaeodactylum tricornutum* it was found that 510 nm light, which is absorbed mainly by the fucoxanthin of the major antenna complex, is not delivered preferentially to PS II but is more equally distributed between the photosystems (Owens 1986b). The energy distribution between PS II and PS I was suggested to be regulated by ionic distributions rather than by the PQ pool redox state. Furthermore, the mechanism regulating energy distribution between PS II and PS I was found to be rather light intensity dependent than light quality dependent (Owens 1986b). Regulation of energy distribution to PS I and PS II by state transitions independent of wavelength but dependent on the photon flux density was also found in the yellow green alga *Pleurochloris meiringensis* (Büchel et al 1988, Büchel and Wilhelm 1990). In the brown macrophyte *Macrocystis periferia* an increase of F_m of about 20 % going from a light mainly absorbed by PS II (0.9 W m^{-2} 540 nm light) adapted state to a light mainly absorbed by PS I (3.5 W m^{-2} 700 nm light, additional to the light II) adapted state was found (Fork et al 1991). The effect of light I and II on F_0 was much smaller. The halftimes of the transitions (about 10 min for a state I to II transition, about 5 min for a state II to I transition) are comparable to what was found for higher plants (Allen 1992). The transition from state I to state II led to a decrease of -196°C fluorescence of both PS II and PS I. Fork et al (1991) calculated the distribution of light II between PS I and PS II and found an almost even distribution of light II to both photosystems in both states. In cyanobacteria state transitions due to phosphorylation of the phycobilisomes, were found to regulate energy distribution (Allen 1992). The transition however is much faster than in higher plants (Dominy and Williams 1987). Recent results suggest that state transitions in cyanobacteria are a consequence of changes in the intensity of the irradiance rather than the spectrum of the irradiance (Rouag and Dominy 1994).

The process of state transitions in higher plants, green algae and cyanobacteria is relatively well understood. The occurrence and regulation of state transitions in important phytoplankton groups (e.g. coccolithophorids, flagellates, diatoms and dinoflagellates) has not been investigated in great detail as are the consequences for estimation of PS II electron flow from chlorophyll fluorescence measurements.

1.3.2 PS II electron flow

At low photon flux densities (PFD) the rate of photosynthesis increases almost linear with the photon flux density. This implies that at low PFD all the absorbed energy in principal can be used for photochemistry with a nearly constant efficiency. At high PFD's the rate of photosynthesis is saturated. Under this condition photochemistry works at its maximal rate and excessive energy should be dissipated to prevent damage on the photosynthetic apparatus, in particular PS II (Critchley 1981). Besides storage in photosynthetic products there are 3 other ways to dissipate energy: i) via energy consumption in metabolic processes that do not result in energy storage.

An example is photorespiration (Björkman and Demmig-Adams 1995, section 1.2.2) but also Mehler reaction (see section 1.2.2) is suggested to function in dissipation of excessive energy (Björkman and Demmig-Adams 1995, Schreiber et al 1995a); ii) reemission of photons as fluorescence. However, the amount of excitation energy which can be dissipated in fluorescence is small (below 4 % of the total) and can be neglected for most practical purposes; iii) thermal dissipation of the energy in the pigment bed. This dissipation pathway is very important in regulation of PS II electron flow (Björkman and Demmig-Adams 1995).

In the light a proton gradient across the thylakoid membrane is formed, which in higher plants and green algae induces the formation of zeaxanthin from violaxanthin. It is suggested that both the proton gradient and the presence of zeaxanthin in thylakoid membranes cause a change in the conformation of the association of the pigment molecules in the antenna complex. This conformational change is responsible for an increase of the heat release in the antenna complex (via an increase of k_0) (Bilger and Björkman 1994, Björkman and Demmig-Adams 1995). For brown algae it is suggested that increased heat release in the antenna complex is correlated to the conversion of diadinoxanthin to diatoxanthin (Oilazola et al 1994). The increase of heat release results in a reduction of the amount of fluorescence. Therefore fluorescence can be used to monitor both changes in photochemistry and in heat release (Schreiber et al 1986, Krause and Weis 1991).

1.4 Chlororespiration

In chloroplasts of *Chlamydomonas reinhardtii* inhibition of dark respiration (measured as an increase of $^{18}\text{O}_2$) due to short saturating flashes was found by Peltier et al (1987). The respiration was insensitive to DCMU, an inhibitor of photosynthetic electron transport, and antimycin A, an inhibitor of the cytochrome $b_6 f$ complex, and was inhibited by cyanide, an inhibitor of cytochrome oxidase. This endogenous respiratory process, which was named chlororespiration, was suggested to make use of an thylakoid NADPH-dehydrogenase, the PQ-pool, a hypothetical cytochrome b/c complex and a hypothetical cytochrome oxidase (Peltier and Schmidt 1991). In fluorescence experiments it was found that antimycin A significantly increased the redox state of PS II acceptors in dark adapted *Chlamydomonas reinhardtii* (Ravenel and Peltier 1991). NADPH-dehydrogenase activity in the chloroplast was confirmed by Seidel-Guyenot et al (1996) in *P. meiringensis* and by Cuello et al (1995) in barley. Thusfar, however, cytochrome oxidase activity in the chloroplast has not been demonstrated. The electron flow in the chlororespiratory pathway is supposed to create a trans-thylakoid proton gradient. In *P. tricornutum* an increase of F_0 and F_M was found after addition of uncouplers of the proton gradient across the thylakoid membrane (CCCP and nigericin) and after addition of antimycin A or by anaerobiosis (Ting and Owens 1993). This increase of F_0 and F_M was explained by dissipation or prevention of a chlororespiration dependent pH gradient in the dark. The data of Ting and Owens (1993), however, suggest that F_v/F_M did not increase. This would be expected to be the case when energy dependent quenching is involved.

Chlororespiration might decrease the F_0 and F_M , observed in the dark, due to membrane

energization and it might increase the apparent F_0 , observed in the dark, due to reduction of Q_A . Therefore chlororespiration might disturb interpretation of the fluorescence data with respect to photosynthesis.

1.5 Estimation of primary production

Primary production can be estimated in several ways, e.g. the increase in biomass (cell numbers, dry weight), biovolume, chlorophyll content, or via the determination of the photosynthetic reaction by carbon fixation, oxygen evolution or by PSII electron transport.

1.5.1 Increase in biomass

The increase in cell numbers by counting under a microscope gives in precise information on species composition and cell numbers. Cells can be counted more rapidly in a Coulter counter which, however, cannot distinguish between phytoplankton cells and heterotrophic cells. In Coulter counter measurements the spheric equivalent diameter of the cell is also estimated and this information can be used to estimate the biovolume. With flow cytometry it is possible to analyse individual cells and use their optical properties for identification. In this way phytoplankton cells were distinguished from heterotrophic cells and a rough separation in groups of species has been achieved by Hofstra et al (1990).

The chlorophyll concentration of a phytoplankton sample is best determined after extraction via absorption or fluorescence measurements.

The measured increase in biomass should be corrected for the grazing of heterotrophic organisms. Furthermore for all of these methods it should be noted that algae are flexible organisms and the size and geometry of an algal cell is not a constant, neither is the chemical composition of the cell. Therefore, the results obtained with measuring biomass increase depend both on the method used and on the physiological state of the algae in the sample.

1.5.2 Carbon uptake, oxygen evolution

An estimation of determining primary production is measuring the photosynthetic conversion of inorganic carbon into organic matter (biomass). Thus far this has mainly been done by measuring carbon uptake (using labelled bicarbonate, ^{14}C) or oxygen evolution. Oxygen evolution measurements give net photosynthesis because discrimination between oxygen produced at the oxygen evolving complex of PS II and oxygen taken up during respiration (e.g. mitochondrial respiration, photorespiration and Mehler reaction) cannot be made. Carbon fixation measurements can estimate either gross or net photosynthesis depending on the duration of the incubation with ^{14}C (Williams et al 1996).

Net photosynthesis data account for photosynthetic and respiratory activity in the light period. For a conversion of these data into primary production the respiration during the night period should also be taken into account.

1.5.3 PS II electron flow by means of chlorophyll fluorescence

The PS II fluorescence yield depends on the rate of photosynthesis. Based on this phenomenon a method was developed to measure the efficiency PS II electron flow, Φ_{PSII} , with fluorescence parameters (Genty et al 1989). The efficiency of PS II electron flow at any irradiance condition can be determined from the actual fluorescence, F , measured at the ambient irradiance and the maximal fluorescence, F_M' , measured when an additional multiple turnover saturating flash was given:

$$\Phi_{PSII} = \frac{F_M' - F}{F_M'} \quad (1.1)$$

A more comprehensive description of this derivation and of other parameters is given in Chapter 2. When the efficiency of PS II electron flow is known, the rate of PS II electron transport can be calculated as the product of Φ_{PSII} and the photon flux density absorbed by PS II.

1.6 Outline of the thesis

In Chapter 2 the saturating pulse method for determining PS II efficiency is reviewed and applied to cultures of the green alga *Dunaliella tertiolecta*. Photochemical and non-photochemical quenching and the actual and maximal efficiency of PS II were determined under varying growth light intensities. Efficiency of PS II correlated well with the growth rates of the cultures. It was concluded that the saturating pulse method is promising for determination of phytoplankton growth, but the lack of sensitivity of the PAM fluorometer, about a factor 1000 too low for application in the marine environment, might be a severe limitation. A further requirement is the establishment and calibration of the relation between PS II electron flow and primary production of the major phytoplankton groups involved in marine primary production.

Chapter 3 describes comparative measurements on the relation between PS II electron flow estimated as Φ_{PSII} times the photon flux density (PFD) and photosynthetic oxygen evolution of 5 marine algal species, which are members of the main phytoplankton groups. The relation between oxygen evolution and PS II electron flow was found to be approximately linear at low and mediate photon flux densities. At high photon flux densities the relation is shown to be non-linear. The non-linearity is not related to photorespiration but to a Mehler-type of oxygen reduction or light dependent respiration. The relation between PS II electron flow and oxygen evolution could be modelled by including an extra oxygen uptake term in the model of Eilers and Peeters (1988). The initial slope of the relation between the rate of oxygen evolution and the rate of PS II electron transport was found to be species dependent. This species dependence was suggested to be related to differences in PS II absorption cross-section.

The extremely sensitive Xe-PAM fluorometer, built for this project by Dr U. Schreiber, is employed in chapter 4 to develop a method for estimation of the absorption cross-section of PS II using the minimal fluorescence F_0 . The concept of phytoplankton electron flux was introduced, which is the total amount of PS II electron flow in a phytoplankton sample. The relationship between the phytoplankton electron flux and the rate of oxygen production of the same

phytoplankton sample was similar for cultures of *D. tertiolecta* and *Phaeodactylum tricornutum*.

In Chapter 5 the phytoplankton electron flux (PEF) is compared with the phytoplankton carbon flux (PCF) in cultures of 3 marine algal species. The relation showed a similar curvilinearity as found for the comparison of the rate of oxygen evolution and the rate of PS II electron flow in Chapter 3. The ratio of PCF and PEF differed by a factor 1.5 which is smaller than the variation found in the ratio of oxygen production and electron flow in Chapter 3.

In Chapter 6 hard- and soft-ware (Xe-PAM and home build measuring unit; PPMON and PEF concept) were tested under field conditions in a small outdoor artificial ecosystem (mesocosm) where PS II electron flow was continuously monitored for three weeks. 2 phytoplankton blooms were observed and during these blooms the relation between PEF and PCF measured in the mesocosm was similar to that in samples measured in the laboratory.

Chapter 7 describes experiments to assess aspects of phytoplankton physiology, e.g., chlororespiration and state transitions, which might affect the minimal fluorescence F_0 and consequently the estimation of PEF. It is concluded that under our conditions the error was below 10 %.

Finally, Chapter 8 discusses prospects and limitations of the fluorescence methods we applied to determine the primary phytoplankton production in a marine ecosystem. The data obtained with fluorescence measurements are discussed in relation to those obtained from estimates on primary carbon fixation or oxygen production.

2 SIMPLE DETERMINATION OF PHOTOSYNTHETIC EFFICIENCY AND PHOTOINHIBITION OF *DUNALIELLA TERTIOLECTA* BY SATURATING PULSE FLUORESCENCE MEASUREMENTS

2.1 Introduction

Fluorescence measurements have become widely applied in the determination of phytoplankton biomass. Based on the registration of fluorescence emission and excitation characteristics of phytoplankton communities, taxa can be roughly identified (Yentsch and Yentsch 1979, Yentsch and Phinney 1985a,b, Hilton et al 1989). The measurement of chlorophyll fluorescence intensity has found general acceptance for the estimation of autotrophic phytoplankton biomass (Heaney 1978, Butterwick et al. 1982, Falkowski and Kiefer 1985). An important advantage of this approach is that *in situ* measurements on photosynthetic organisms are possible. To gain insight in the distribution (both horizontally, over large areas, and vertically, in the water column) of phytoplankton, *in situ* measurements are indispensable.

It appears, however, that the correlation between chlorophyll *a* fluorescence intensity and phytoplankton biomass, usually approximated by chemical measurement of the total amount of extracted chlorophyll *a*, is, in many instances, not very good (Falkowski and Kiefer 1985). In particular, when one tries to correlate data acquired under different circumstances, e.g. at different depths, in different water masses or at different times of the day, the quantitative agreement between the chlorophyll *a* concentrations as determined by extraction and by fluorescence may be poor. This is mainly due to the fact that the fluorescence which is measured predominantly stems from chlorophyll *a* molecules that are part of the photosynthetic apparatus of the cell; this apparatus is a dynamic system which can respond rapidly to changes in the environmental circumstances. Pollutant stress, light intensity and temperature may thus strongly influence the fluorescence yield (Falkowski and Kiefer 1985, Falkowski et al. 1986, Lichtenthaler and Rinderle 1988). Thus, chlorophyll *a* fluorescence intensity, which can be examined by determination of the amount of fluorescence per molecule of chlorophyll *a* (i.e. the fluorescence quantum yield), can also be used to obtain information on the condition of the photosynthetic apparatus. This means that, in addition to estimates of total biomass, other information can be derived from phytoplankton fluorescence characteristics: estimates can be obtained of the photosynthetic efficiency and, via that, of the primary production and environmental stress. These aspects are considered in more detail in the following section.

The present paper will describe the principles and applications of the saturating pulse fluorescence technique for determination of photosynthetic characteristics of phytoplankton. This method has mainly been applied to investigate higher plants, and can be used to obtain a quantitative estimate of the photochemical efficiency of the photosynthetic system (Schreiber 1983, Renger and Schreiber 1986). Photoinhibitory effects and the amounts of photochemical and non-photochemical quenching can also be determined (Schreiber et al 1986). Measurement

of the photochemical efficiency can be done directly and is suitable for *in situ* application (Genty et al 1989, Falkowski and Kolber 1990). As such, it has important advantages over the ^{14}C -incorporation measurement, which is largely agreed upon as the standard method for determining photochemical efficiency when the phytoplankton concentration is low, as is generally the case in marine applications (Peterson 1980, Dring and Jewson 1982). For higher plants and in eutrophied situations, oxygen measurements can also be applied, which are much more easily applicable from an experimental point of view (Bryan et al 1976). Determination of photoinhibitory effects and of photochemical and non-photochemical quenching requires dark adaptation prior to the measurement, and are hence less suited for dynamic *in situ* measurements.

Experiments in this study were done on *Dunaliella tertiolecta* laboratory cultures with a dedicated, commercially available instrument that was designed for measurement of leaves (Schreiber 1986). The applicability of the saturating pulse fluorescence technique for marine phytoplankton will be demonstrated, and modifications that are required to make the instrument suitable for *in situ* purposes will be discussed. Firstly, however, the principles of the saturating pulse fluorescence measurement are described.

2.2 Measurement of saturating pulse fluorescence

The fluorescence that is measured at ambient temperatures stems almost exclusively from chlorophyll associated with the antennae of photosystem (PS) II. The fluorescent yield of PS I is low because photochemistry here is a particularly efficient competitor, in addition to the other non-radiative decay processes like thermal emission and triplet formation, unless measurements are done at low temperatures (Strasser and Butler 1977, Briantais et al 1986). Chlorophyll associated with the photochemical reaction centres represents only a very small fraction of the total chlorophyll content of phytoplankton and, in addition, has a very low fluorescence quantum yield.

The fluorescence yield of PS II chlorophyll, however, is highly variable. It is strongly influenced by the physiological state of the phytoplankton. The excited states that are produced by light absorption can be deactivated by 4 processes: (1) photosynthetic energy conversion, which requires energy transfer to the reaction center and subsequent electron transport followed by interaction with PS I, (2) triplet formation, (3) radiationless processes and (4) radiative transfer, the process that is accompanied by fluorescence. The fluorescence emission hence provides information on the photochemical processes in PS II. When the photochemical reaction centers are "open", i.e. available to efficiently trap the excited state energy and to be involved in photochemical energy conversion, the yield of the non-photochemical processes (2-4) will be low. On the other hand, when the reaction centers are closed the photochemical yield is very low and the non-photochemical processes become important. The fluorescence yield therefore varies inversely with the yield of photochemistry: it consists of a constant part and a variable part, which is determined by the state of the photochemical reaction center (open or closed). The state of the reaction centers is influenced by environmental circumstances (light history, nutrient status,

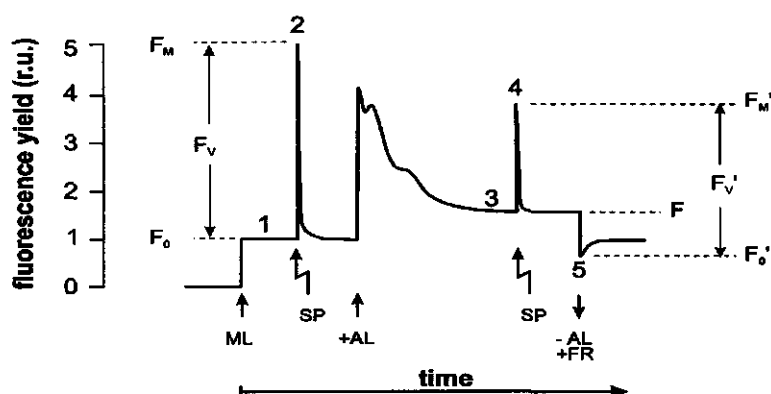


Figure 2.1. Schematic representation of the saturating pulse fluorescence method (Van Kooten and Snel 1990). 5 different states of the photosynthetic system are defined in the course of a full experiment. At the onset of the experiment the dark adapted states F_0 (1) and F_M (2) are defined by using modulated measuring light (ML) only and an additional saturating pulse (SP) respectively, for the 2 parameters. Next, the sample is illuminated with actinic light (AL) and a fluorescence induction (or Kautsky) curve is obtained. In the steady state F (3) and F_M' (4) can be determined by again measuring with modulated measuring light and an additional saturating pulse, now in combination with the actinic light. Finally, the actinic light source is extinguished and far-red illumination is applied to reach F_0' (5). To determine the photochemical efficiency according to the method of Genty et al (1989) it is sufficiently to determine F_M' and F under steady state conditions.

presence of pollutant stress). It is just this dependence which makes simple, straightforward, *in situ* fluorescence intensity measurements difficult to use for phytoplankton chlorophyll determinations.

On the other hand fluorescence measurements can be used to monitor the photosynthetic processes. The saturating pulse method that is used in this paper allows information on these processes to be obtained by application of a refined experimental scheme. In Figure 2.1 the principles of the saturating pulse method are illustrated. The method is based on the application of 3 different excitation schemes to the phytoplankton. The chlorophyll fluorescence is measured using a low power, modulated, light emitting diode for excitation. The fluorescence induced by this probe beam is selectively registered by application of phase resolved detection. In addition,

a constant, variable intensity, white light source may be used for actinic illumination of the sample. To investigate the photosynthetic system, a very high intensity pulse of white light may also be applied, which can saturate the photochemical reaction centers.

The full technique shown in Figure 2.1 provides 4 useful parameters (see also Genty et al 1989):

(1) Photochemical quenching, q_P . Photochemical quenching of fluorescence is caused by the transfer of excited state energy to the photochemical reaction centers, where it is available for photochemical energy conversion. In dark adapted phytoplankton the PS II reaction centers are all open and photochemical quenching is maximal. The fluorescence intensity at this point is designated F_0 . When a short pulse of intense light is given, all PS II reaction centers are closed within a few hundred ms. During the pulse the fluorescence intensity reaches its maximum value F_M . During the illumination with the actinic light source, or under ambient light, q_P can be determined by measuring the normalised difference between the maximum and the actual fluorescence yield:

$$q_P = \frac{F'_M - F}{F'_M - F_0'} \quad (2.1)$$

where F'_M = the maximum fluorescence intensity that is obtained by saturation of the reaction centers under steady state conditions; F = the normal fluorescence intensity in the steady state; and F_0' = the fluorescence intensity that is obtained directly after the actinic light source has been switched off; in addition illumination by far-red light is applied, which is predominantly absorbed by PS I and results in reopening of intact PS II reaction centers by reoxidation of the quinone acceptor Q_A .

(2) Non-photochemical quenching, q_N . Non-photochemical quenching is used to describe all quenching processes of PS II chlorophyll fluorescence processes that are not related to photochemistry. It mainly involves nonradiative, dissipative, processes that are for instance induced by the build-up of a pH gradient across the thylakoid membrane (' ΔpH -quenching'). Non-photochemical quenching can only be determined when F_M is available from dark-adapted samples; it is defined as the normalised decrease of the maximal fluorescence yield, with respect to the dark adapted situation:

$$q_N = 1 - \frac{F'_M - F_0'}{F_M - F_0} \quad (2.2)$$

(3) The photochemical yield of open PS II reaction centers, F_v/F_M . This ratio equals the product of the probabilities of excitation transfer between antennae and PS II reaction center, and vice versa (e.g. Butler 1978). If non-radiative transfer in the reaction center is significantly smaller than the back transfer to the antennae pigments, the yield of photochemistry of the open PS II reaction centers is given by:

$$\Phi_{P_0} = \frac{F_V}{F_M} = \frac{F_M - F_0}{F_M} \quad (2.3)$$

It appears that Φ_{P_0} is a good indicator of photoinhibition. Light induced damage to the PS II reaction center leads to lowering of the photochemical yield of the reaction centers (Björkman 1987). To assess photoinhibition prolonged dark adaptation of the sample must be applied prior to the measurement to fully remove the effects of non-photochemical quenching. The recovery of the photosynthetic system from photoinhibitory effects often takes a long time, typically many hours.

(4) The photochemical efficiency of PS II per absorbed photon, or photon yield, Φ_{PSII} . The method is based on the assumption that the photon yield is given by the product of the efficiency of an open PS II reaction center and the fraction of open reaction centers (Genty et al 1989):

$$\Phi_{PSII} = \frac{F'_M - F'_0}{F'_M} \times \frac{F'_M - F}{F'_M - F'_0} = \frac{F'_M - F}{F'_M} \quad (2.4)$$

Since in steady state the flux of the electrons in PS I and PS II should be equal, the photon yield of PS II gives a good estimation of the efficiency of the linear electron flow in the photosynthetic apparatus. The overall rate of electron flow J_E [$\mu\text{mol e} (\mu\text{mol PS II})^{-1} \text{s}^{-1}$], can be calculated by multiplying the photon yield with the amount of photons absorbed by PS II:

$$J_E = \Phi_{PSII} \sigma_{PSII} PFD \quad (2.5)$$

where σ_{PSII} = the absorption cross section of PS II; and PFD = the photon flux of the photosynthetically active radiation. As we were not able to determine σ_{PSII} directly, the (relative) J_E was estimated by the product $\Phi_{PSII} \cdot PFD$. This is a reasonable estimate: according to Kolber et al (1988) the absorption cross section of *D. tertiolecta* does not change by more than 14-17% in the light range of 20-200 μE .

The saturating pulse fluorescent approach can be applied in conjunction with the ^{14}C -method, which is conventionally used for primary production measurements in the marine environment. An important advantage of the fluorescence technique over the ^{14}C -method is that the former measurement gives information on the instantaneous photosynthetic status and can be applied *in situ* (i.e., in the sea water at a particular location, measurements, for instance time series, can be performed). The measurement can be done directly as it does not require dark adaptation. To obtain absolute rates, calibration with ^{14}C -incorporation measurements may be required.

An alternative optical approach, dubbed pump-and-probe fluorescence, can be used to measure properties similar to those measured with the saturating pulse fluorescence method used in this study (Falkowski and Kiefer 1985, Falkowski and Kolber 1990). The main difference between the two methods is the procedure used to determine F_M and F'_M , which can produce different results. In particular, as the pump-and-probe technique only uses a single, short pump pulse only a single turn-over of the PS II reaction centers is effected, which results in reduction of Q_A only. In the saturating pulse approach a longer intense pulse is applied, which results in total

reduction of Q_A and of the PQ pool. Therefore F_M and F_M' in general will be somewhat lower in the pump-and-probe measurement. The trends determined by both methods, however, may be similar. For comparison of the 2 methods see Schreiber et al (1995b).

2.3 Experimental application

Table 2.1. Photon flux densities of photosynthetically active radiation under which the *D. tertiolecta* cultures were grown

Culture #	PFD ($\mu\text{mol m}^{-2} \text{s}^{-1}$)
1	22.6
2	42.1
3	66.0
4	92.3
5	107.4
6	137.3
7	214.3

The chlorophyte *D. tertiolecta* was grown at 15 °C in an f/2 medium (McLachlan, 1975) under a 14 h light/ 10 h dark cycle. The cultures were kept in culture bottles, which were placed in plastic containers with white, diffuse reflecting walls, covered by suitable neutral density (gray) attenuation filters to obtain 7 different light intensities. An incubator (Gallenkamp Orbital INR-401) equipped with fluorescent tubes operating at a full light intensity of 300-400 $\mu\text{mol m}^{-2} \text{s}^{-1}$ was used. Light intensities in the containers were measured with a Photodyne 88 XLA spherical sensor. The intensities under which the cultures were grown are given in Table 2.1.

The growth rate of the cultures was determined by means of a flow cytometer, especially constructed for use with phytoplankton; the cytometer measured the concentration of particles with red chlorophyll fluorescence ($> 670 \text{ nm}$) under excitation with an Ar-ion laser operated at 529 nm (Hofstraet et al 1990).

Saturating pulse fluorescence measurements were done with a pulse amplitude modulation fluorimeter (PAM, produced by Walz, Effeltrich, FRG, as developed by U. Schreiber, see Schreiber 1986). The PAM consists of 4 units, the settings of which were optimized before the actual experiment was started. Firstly, the modulated measuring light intensity provided by a pulsed LED in the 101-ED unit of the PAM, peaking at 650-660 nm, had to be chosen so as to obtain enough sensitivity, yet to be low enough to prevent induction of significant variable fluorescence.

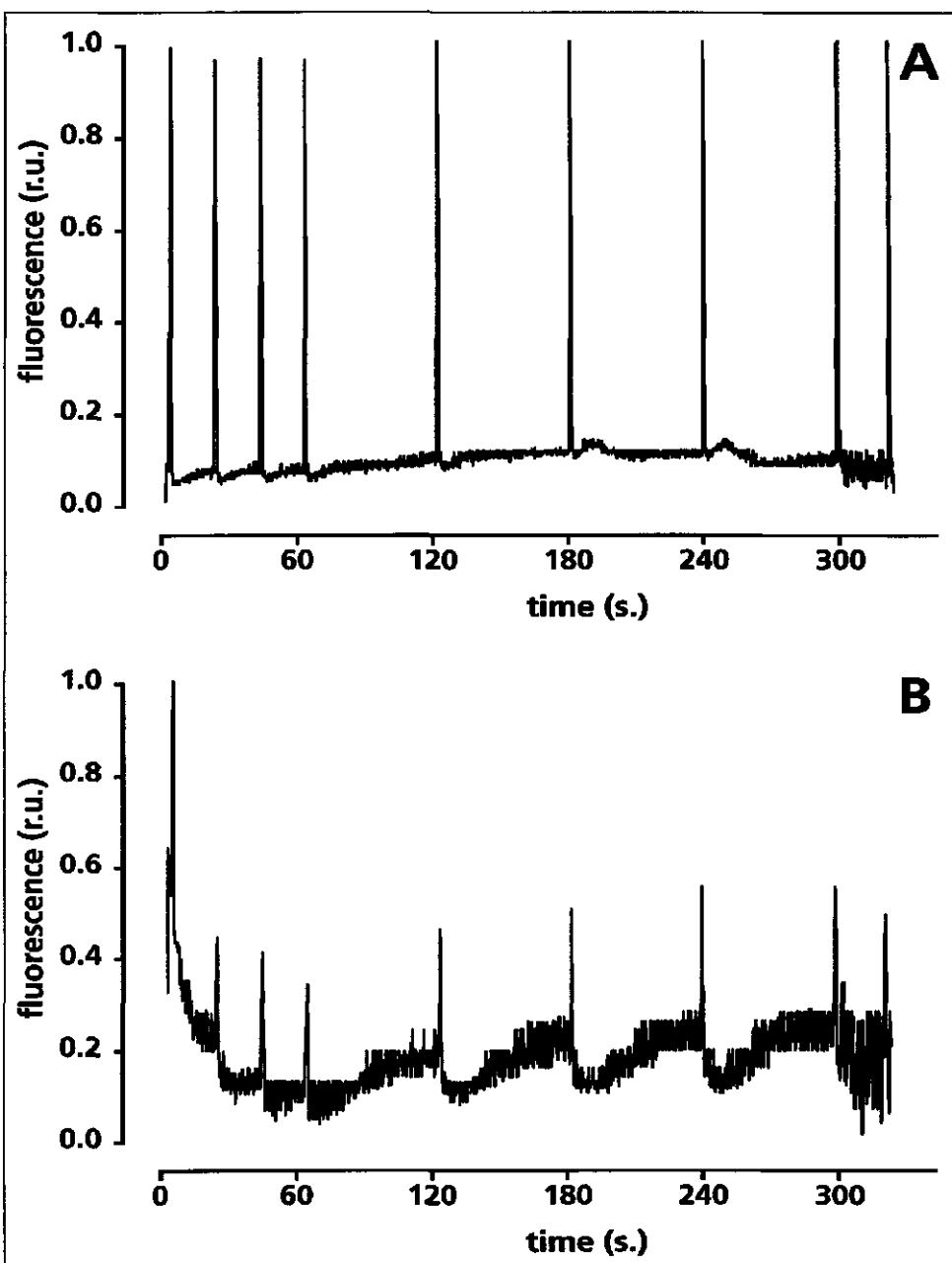


Figure 2.2. Typical results of saturating pulse fluorescence measurements for 2 cultures of *D. tertiolecta* grown under (A) low ($66.0 \mu\text{mol m}^{-2} \text{s}^{-1}$) and (B) high ($214.3 \mu\text{mol m}^{-2} \text{s}^{-1}$) light intensity. Cultures were measured 17 d after commencing the experiment. See text and Table 2.2 for more details.

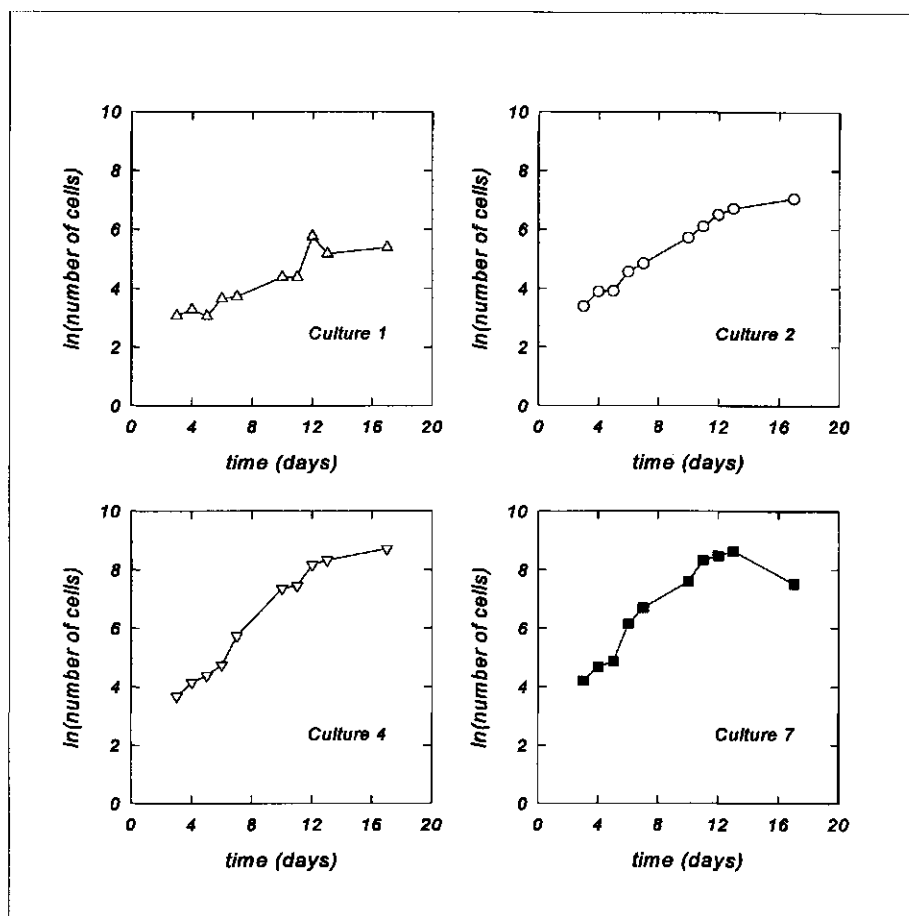


Figure 2.3. Increase in *D. tertiolecta* cell numbers in the cultures, as determined by flow cytometry. Curves are shown for 4 typical cultures; the corresponding light intensities are given in Table 2.1.

Secondly, the actinic illumination from the KL-1500 lamp, controlled by the PAM 102 unit, was chosen to match the total light intensity under which the different cultures had been grown, as determined by a UDT PIN-10 photodiode. The matching was accomplished by applying the available settings of the actinic light source in combination with a number of Oriel neutral density filters. The spectral intensity distribution of the KL-1500 light source and that of the incubator were measured with a calibrated, spherical sensor, using 10 nm full-width-at-half-maximum bandpass filters to measure the absolute light intensity every 20 nm. The intensity distributions of the two light sources did not match completely, the KL-1500 source being more intense in the orange and red part of the spectrum. Thirdly, the intense, saturating light-pulse of the KL-1500 light source, controlled by the PAM 103 unit, was optimized to ensure complete closure of the PS II reaction centers by observing the time resolved fluorescence signal as obtained by the

modulated measuring light. At the same time actinic effects resulting from the saturating pulse should be absent; this was accomplished by application of a 700 ms pulse at an intensity of more than 2000 W m^{-2} . Finally, far-red illumination ($> 730 \text{ nm}$) was applied to reopen the PS II reaction centers following a saturating pulse. Data acquisition and handling were performed by the dedicated program 'FLUORESC', developed at the department of Plant Physiology, Wageningen Agricultural University.

The measuring procedure was executed on a daily basis and commenced exactly 3 h after the light in the incubator was switched on. Samples were taken from the flasks in the incubator and put in the MKS-101 cuvette (provided by Walz, Effeltrich, FRG) with minimal light exposure. Subsequently, the measurement was started with the actinic light intensity of the PAM matching that to which the sample had been exposed in the incubator. Due to the transfer to the measuring cuvette the sample had been subjected to a change in light climate. Hence, the sample was irradiated with the actinic light source for 5 minutes before the actual measurement of F_M' and F . To confirm that after this adaptation time the steady state condition was reached, fluorescence and, at regular intervals, saturating pulse measurements were done during actinic illumination. Following this sequence the actinic light was switched off and another series of readings of fluorescence and saturating pulse fluorescence was done in the dark, to check for possible measurement induced quenching effects. For the measurements in the dark the pulse rate of the LED in the 101-ED unit of the PAM, used for induction of the fluorescence, was changed from 100 kHz to 1.6 kHz, to prevent any actinic effects.

In a separate experiment, samples were dark adapted for 15 minutes to remove any energy dependent quenching and subsequently F_v/F_M was measured to determine photoinhibition effects. F_v/F_M was independent of the chlorophyll *a* concentration between 0.5-40 μg chlorophyll/ml (unpublished results). Dilute samples (less than 10^6 cells/ml, corresponding to less than 1 μg chlorophyll/ml) were concentrated by centrifugation at 3,000 g for 5 min. Centrifugation did not affect the rate of photosynthesis.

2.4 Results and discussion

2.4.1 Measurement of Φ_{PSII} and q_p

First, the applicability of the saturation pulse method for the measurement of Φ_p and q_p was studied; this measurement does not require dark adaptation of the phytoplankton. As can be inferred from Equation (1), determination of F_M' , F and F_0' , all parameters which can be obtained under steady state conditions, suffices for determination of Φ_{PSII} and q_p .

The fluorescence induction kinetics obtained from two cultures that had been grown for 17 days under low and high light conditions, respectively, are shown in Figure 2.2. Figure 2.2A shows the fluorescence transient for low light adapted phytoplankton (culture 3). At this light intensity the sample is still growing exponentially (see Fig. 2.3). The fluorescence induction kinetics indicate that the phytoplankton returns to a steady state almost immediately after the light pulse. In contrast, for the high light adapted cultures in the stationary phase (culture 7, Fig. 2.3) a strong reduction of the effect of closing the reaction centers with a saturating pulse is

Table 2.2. Photosynthetic characteristics for the 2 *D. tertiolecta* cultures shown in Figure 2.2

Culture #	PPFD ($\mu\text{mol m}^{-2} \text{s}^{-1}$)	q_N	q_P	Φ_{PSII}	F_V/F_M
3	66.0	0.37	0.96	0.58	0.69
7	214.3	0.61	0.81	0.25	0.42

observed once the sample is re-illuminated. The relatively short time in which the phytoplankton is kept in the dark prior to the measurement for the high light case appears to be sufficient to allow some recuperation of the light-induced non-photochemical quenching. Also, for the high light sample the saturating pulse appears to cause some transient quenching effects. The difference between the samples grown under relatively low and relatively high light regimes is striking (see Table 2.2). The low light sample, which is in the exponential growth phase, shows a significantly higher photochemical efficiency than the high light sample, which is in a steady state. Photochemical quenching, which can also be calculated from the direct measurement (under actinic illumination), appears to be somewhat higher for the low light adapted sample. Both observations indicate that photosynthetic energy conversion is more efficient in the low light situation (see also Kolber et al 1990). The curve in Figure 2.2B also suggests a much higher contribution of non-photochemical quenching in the high light intensity case. However, as no lengthy dark adaptation was done, data for q_N cannot be considered conclusive. Residual non-photochemical effects can still be present; dark adaptation will remove these effects, while more persistent photoinhibitory effects will remain. Non-photochemical (or energy dependent) quenching will be more important for the high light case, so that the difference in the values obtained for q_N given in Table 2.2 will be more pronounced when the samples are dark adapted for a longer time.

When cultures grown under different light intensities are followed over time, observations similar to those mentioned above are made. In Figure 2.4A the development of Φ_{PSII} with time is presented. Five days after the culture has been started, the 6 cultures (cultures 2 to 7, Table 2.1) had more or less similar values for Φ_{PSII} (0.64-0.74). All cultures are growing exponentially. After 17 d a clear difference, depending on the light intensity, had become apparent. At that time Φ_{PSII} ranges from 0.30-0.67. The 2 cultures grown under the lowest light intensities are still in exponential growth after 17 d. Indeed, the value of Φ_{PSII} determined for these cultures appeared to have hardly decreased. Cultures 4 and 5 show exponential growth until Day 13. Cultures 6 and 7 enter the stationary (growth) phase around Day 11, the time at which Φ_{PSII} starts to decrease.

Φ_{PSII} only gives an estimate of the efficiency of the electron flow in PS II. The overall rate of electron flow, J_E , which represents the photosynthetic activity of the phytoplankton, can be calculated by multiplying Φ_{PSII} with the amount of photons absorbed by PS II. If we assume equal absorption cross sections for the different cultures, the (relative) J_E can be approximated by the

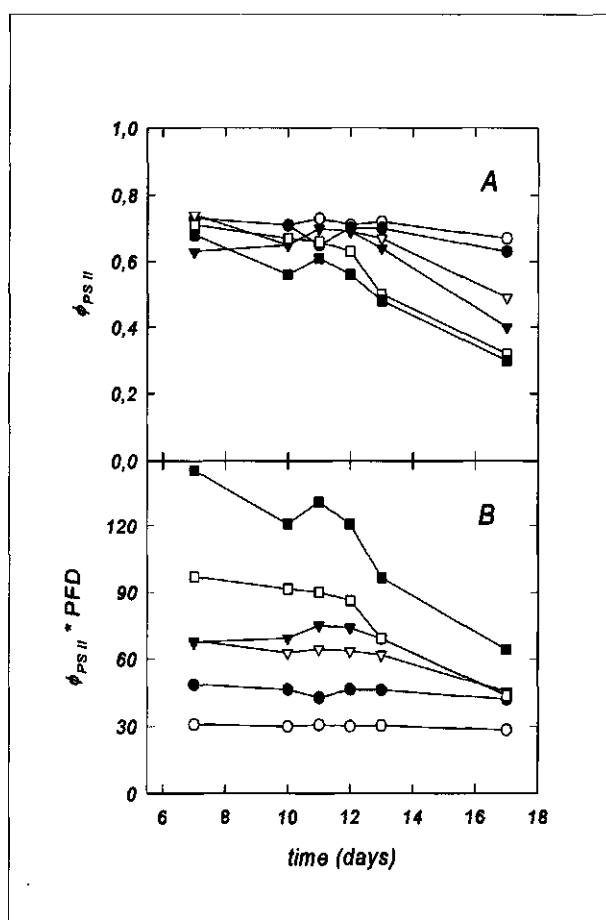


Figure 2.4. Development of (A) $\Phi_{PS II}$ and (B) $\Phi_{PS II} \cdot PFD$ with the time for *D.* the cultures 2 to 7, grown under light intensities given in Table 2.1. Culture 2: (○); culture 3: (●); culture 4: (▽); culture 5: (▼); culture 6: (□) and culture 7: (■).

product of $\Phi_{PS II}$ and the integrated intensity of the light used to culture the samples. Figure 2.4B shows the product $\Phi_{PS II} \cdot PFD$ as a function of incubation time for the different cultures. $\Phi_{PS II} \cdot PFD$ is an approximation of the linear electron flow in PS II, assuming that the absorption cross section is equal for all cultures. Clearly, the high light cultures show significantly higher overall rates in the first phase of the experiment. The 2 cultures grown at the lowest light intensities show constant J_E during the course of the experiment.

A relation between the photosynthetic activity and the growth rate of the phytoplankton cultures is expected. Figure 2.5 shows the relation between $\Phi_{PS II} \cdot PFD$ (the estimated electron transport) and the measured growth rate of the cultures during the exponential growth phase. The relation is clear: at low electron transport rates (i.e., at light levels below $100 \mu\text{mol m}^{-2} \text{s}^{-1}$)

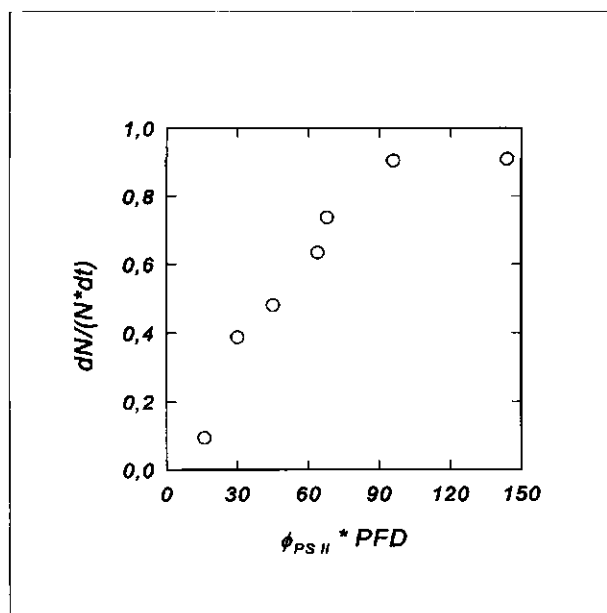


Figure 2.5. Relation between $\phi_{PSII} \cdot PFD$ and *D. tertiolecta* growth rate. Both ϕ_{PSII} and the growth rate were determined as averages during the exponential growth phase; N = cell number.

the exponential growth rate is more or less determined by the light intensity. At higher light levels the growth rate approaches a limiting exponential value of about 1. Extrapolation to zero electron transport ($\phi_{PSII} \cdot PFD = 0$) indicates no growth, as expected.

The above clearly indicates the applicability of the saturating pulse fluorescence technique for the estimation of the photochemical efficiency of PS II, and hence of the total photosynthetic activity of phytoplankton. The results suggest that this approach can be a useful alternative for the ^{14}C -incorporation technique that is normally used to measure primary productivity (Peterson 1980, Dring and Jewson 1982). Indeed, Genty et al (1989) have reported very good correlations between the photochemical yield as determined by the saturating pulse technique and the quantum yield of CO_2 -assimilation as determined by the ^{14}C -incorporation technique. The saturating pulse technique and the pump-probe technique (Falkowski and Kolber 1990) have several advantages over the latter method. Firstly, they do not require radioactive substances. Secondly, they can be applied directly, without incubation as required for the ^{14}C -technique. Therefore, they are less cumbersome and more efficient and can even be applied *in situ*, so that the photosynthetic activity of phytoplankton can be monitored, for example, over a certain period of time. On the other hand the ^{14}C -method directly monitors the incorporation of CO_2 in the phytoplankton and therefore gives more straightforward information on the photosynthetic energy conversion process. The fluorescence techniques described here give direct information on photosynthetic electron flow, as they are based solely on measurement of PS II fluorescence.

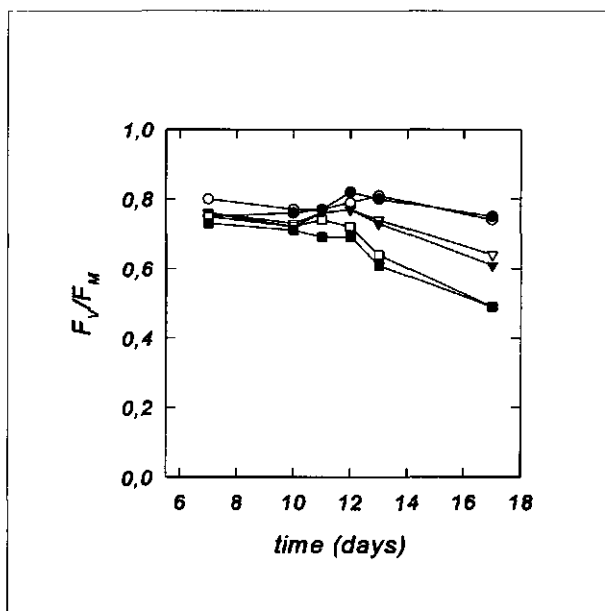


Figure 2.6. Development of the parameter F_v/F_m , representative of the extent of photoinhibition, with time for *D. tertiolecta* cultures 2 to 7 according to Table 2.1. Culture 2: (○); culture 3: (●); culture 4: (▽); culture 5: (▼); culture 6: (□) and culture 7: (■).

With these techniques, therefore, it is not possible to distinguish between energy storage in the Calvin cycle and that in other assimilation pathways (e.g., N-reduction, photorespiration). Another advantage of the ^{14}C -method is that it provides a time-averaged (e.g. daily) rate of primary production, which can be useful for certain applications. In this respect the 2 approaches, the fluorescence-based methods and the ^{14}C -method are complementary. Presumably, in future applications one would perform most measurements with the fluorescence technique, but would take several samples for ^{14}C -incorporation analysis to calibrate Φ_{PSII} in terms of biomass production.

2.4.2 Determination of photoinhibition

As indicated above, the photoinhibition can be estimated from the ratio of the variable and maximum fluorescence $F_v/F_m = (F_m - F_0)/F_m$. This ratio is a measure of the photochemical yield in open reaction centers (Björkman, 1987). Due to primary damage to the PS II reaction center, the variable fluorescence especially is reduced. Photoinhibition can be determined only when all transient quenching processes have been allowed to relax. Hence, following transfer of the samples from the illuminated containers, the samples are dark adapted for 15 minutes, which is sufficient to remove any photochemical or energy-dependent quenching. Then F_0 and F_m are measured, the latter by using a short pulse of saturating light.

In Figure 2.6 F_v/F_m has been determined for cultures 2 to 7 (Table 2.1) during the course of

the experiment. In the first phase of the experiment, when all the cultures are still growing exponentially, differences in the ratio are small: all cultures show values between 0.73 and 0.80. However, after 12 d of growth, significant differences are observed. In particular the cultures that are grown under high light conditions start to give indications of photoinhibitory effects, the F_v/F_m ratio dropping to a mere 0.4 for the 2 cultures exposed to the highest light conditions. At the same time the growth curves for these cultures show clear non-exponential growth behaviour, and even a small decline in cell numbers for the last day of the experiment. The fact that in exponentially growing cultures F_v/F_m is almost as high as 0.8 suggests that even at the relatively high cell concentrations used in the measurements, saturation of fluorescence and reabsorption effects are not important. For other phytoplankton species such as *Phaeodactylum tricornutum* and *Rhodomonas sp.* values of F_v/F_m of 0.7 and higher were observed (Geel et al, to be published). F_v/F_m is highly correlated with Φ_{PSII} , which suggests that chlororespiration should have only a minor influence.

The example shown in Figure 2.6 illustrates the potential of this technique as a simple means to monitor photoinhibitory effects in phytoplankton. Using the saturating pulse fluorescence technique P/I curves can easily be made. As the measurement is based on a relative approach, the method appears to be extremely robust. The repeatability of the determination of F_v/F_m is better than 1%. However, due to the insensitivity of the PAM fluorimeter applied to phytoplankton measurement, it is crucial to implement corrections for the effect of stray light. This effect cannot be neglected; it has a particularly strong influence on the determination of F_o , but it can easily be corrected for.

2.4.3 Modifications for phytoplankton measurement

A final problem of the saturating pulse technique as realized in the PAM-fluorimeter is that the instrument was specifically designed for studies on higher plants. Therefore, it is not sufficiently sensitive for study of phytoplankton. In our study we found that the concentration of *D. tertiolecta* should exceed 10^6 cells ml^{-1} in order for good results to be obtained with the PAM. At this concentration Φ_{PSII} can still be determined with a repeatability of better than 5%, as the determination is a relative one and therefore relatively robust. However, for applications on field samples or for dilute cultures the sensitivity is 3 to 4 orders of magnitude too low. In the laboratory the range of the instrument can be extended for most phytoplankton species by centrifugation. For field samples this approach cannot be applied. However, the sensitivity of the instrument can probably be improved significantly by relatively straightforward modifications. The present instrument has been designed for application to plants and leaves. It uses excitation in the 650-660 nm region and detection >710 nm. For phytoplankton, where the chlorophyll concentration is much lower, excitation in the blue and detection >670 nm would already yield a tremendous increase in sensitivity. In addition, the volume of interaction between light and phytoplankton is very small. For phytoplankton dispersed in surface water at relatively low concentration a much larger volume of interaction would also lead to a significant increase in sensitivity. Finally, some improvements in the data acquisition and transfer can be implemented.

Recent experiments with a modified PAM instrument, incorporating the changes suggested above and, in addition, a pulsed Xenon flash lamp as excitation source have shown that the

required improvements in sensitivity can indeed be realized (Schreiber, personal communication). A modified PAM instrument is presently being built, and will be used for further study.

2.5 Conclusions

The saturating pulse fluorescence technique appears to be a method that can be successfully used for the non-destructive measurement of important photosynthetic characteristics of *D. tertiolecta*. It allows for the simple and direct measurement of photosynthetic efficiency, of photoinhibitory effects and of fluorescence quenching processes. For some parameters the samples must be dark adapted prior to the measurement. The saturating pulse fluorescence approach and the pump and probe technique (Falkowski and Kolber 1990), seem to offer useful extensions to the conventionally used techniques. For instance ^{14}C -uptake measurements require the use of radioactive material, supply time-integrated photosynthetic data and cannot be used for *in situ* monitoring applications. Oxygen measurements, which may be used for *in situ* applications, are not sufficiently sensitive for marine use.

However, several improvements still have to be made in the design of the PAM fluorimeter. First and foremost the sensitivity of the instrument, which was developed for plant studies, must be improved to enable measurement of field samples. Also, the measurements done with the saturating pulse technique have to be compared with those of the conventional techniques, as has already been done (with good results) for plants.

3 ESTIMATION OF OXYGEN EVOLUTION BY MARINE PHYTOPLANKTON FROM MEASUREMENT OF THE EFFICIENCY OF PHOTOSYSTEM II ELECTRON FLOW

3.1 Introduction

Chlorophyll *a* fluorescence has found wide application in the analysis of photosynthesis (Krause and Weis 1991). Using pulse amplitude modulation (Schreiber et al 1986, Schreiber et al 1993) or pump and probe techniques (Mauzerall 1972, Falkowski and Kiefer 1985), it has become possible to determine the efficiency of PS II electron transport. A good correlation between the efficiency of PS II electron transport and the efficiency of carbon uptake was demonstrated in barley and maize under non-photorespiratory conditions (Genty et al 1989). This correlation might also be very useful in estimating carbon fixation or photosynthetic oxygen evolution of phytoplankton by means of chlorophyll fluorescence. The fluorescence measurement only lasts a few seconds and might be specially suited for *in situ* measurements to monitor the efficiency of PS II under the ambient irradiance. This in contrast with measurements of oxygen evolution or carbon fixation on samples with low phytoplankton concentrations, which usually require large samples and long light incubation times (2-6 hours) in a laboratory set-up or in bottle-enclosures in the natural environment (Hall and Moll 1975, Falkowski and Kolber 1990).

The relationship between the efficiency of PS II electron transport (Φ_{PSII}) and the efficiency of carbon dioxide uptake has been examined under a variety of conditions in mainly higher plants and green algae. The linear relationship was confirmed in C4 plants (Krall and Edwards 1990) and in several C3 plants under non-photorespiratory conditions (Harbinson et al 1990). A non-linear relationship was found in the presence of 20 % oxygen in C3 plants (Harbinson et al 1990). Öquist and Chow (1992) reported a single curvilinear relationship at high CO₂ levels where photorespiration is reduced but where Mehler-type oxygen reduction still might occur. More recently, Genty et al (1992) eliminated the contributions of oxygen uptake by photorespiration and Mehler reaction by measuring ¹⁸O₂ in mass-spectrometric measurements in bean leaves and confirmed the linear relationship between electron flow and photosynthetic oxygen evolution. At high irradiance a larger reduction in the efficiency of oxygen evolution than in the efficiency of PS II electron transport has been found in *Dunaliella tertiolecta* (Falkowski et al 1986, Rees et al 1992). This phenomenon was suggested to be caused by cyclic electron flow around PS II (Falkowski et al 1986). Rees et al (1992) have excluded photorespiration as a possible electron sink linked to oxygen uptake and proposed non-assimilatory electron flow, either linear whole chain or cyclic around PS II, to be the cause of the non-linearity.

At very low irradiances, an additional non-linearity has been observed, which has been explained at least partly by respiration (Oberhuber et al 1993) or by the presence of inactive PS II centres which lower the yield of oxygen evolution more than the yield of PS II electron transport (Hormann et al 1994).

The rate of photosynthetic oxygen evolution can be calculated from the estimated rate of PS II

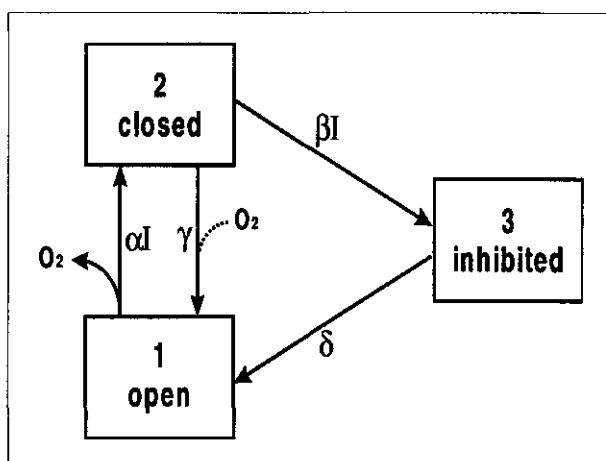


Figure 3.1. The photosynthesis model showing the three states of the 'photosynthetic factories' (Eilers and Peeters 1988). The modification (dotted line) emphasizes oxygen consumption driven by linear electron flow.

electron transport ($\Phi_{PSII} \cdot PFD$) using σ_{PSII} , the absorption cross-section of PSII. The results of Krall and Edwards (1990) suggest that the absorption cross-section is almost identical in three different C4 plants (maize, *Panicum maximum*, *P. miliaceum*) but different in the C3 plant (wheat) measured, although all plants were cultured at the same irradiance. Other researchers found that the effective absorption cross-section of PSII is dependent on the growth irradiance (Ley and Mauzerall 1982, Kolber et al 1988) and can change rapidly in fluctuating light by means of state transitions (Kroon 1994). The effective absorption cross-section of PSII furthermore is dependent on the nutrient availability and the C3 species involved (Kolber et al 1988). Falkowski and Kolber (1990) found a good correlation between the estimated rate of PS II electron transport and the rate of carbon fixation in phytoplankton using a pump and probe fluorescence method to estimate the effective absorption cross-section of PSII. This close correlation between PS II electron flow and carbon fixation suggests that algal growth and PS II electron flow are correlated as well, which was demonstrated in a *Dunaliella tertiolecta* laboratory experiment (Hofstra et al 1994a).

In order to assess the usefulness of the fluorescence method to estimate primary production in marine phytoplankton we examined both the rate of PS II electron transport determined by fluorescence and the rate of oxygen evolution in several marine algae under varying light conditions. The data were modelled with a modified version of the model of Eilers and Peeters (1988) to account for oxygen consuming processes. The relation between the rate of PSII electron flow and the rate of oxygen evolution was curvilinear and is dependent on species and experimental conditions. The observed non-linearity at high irradiances is probably not caused by photorespiration.

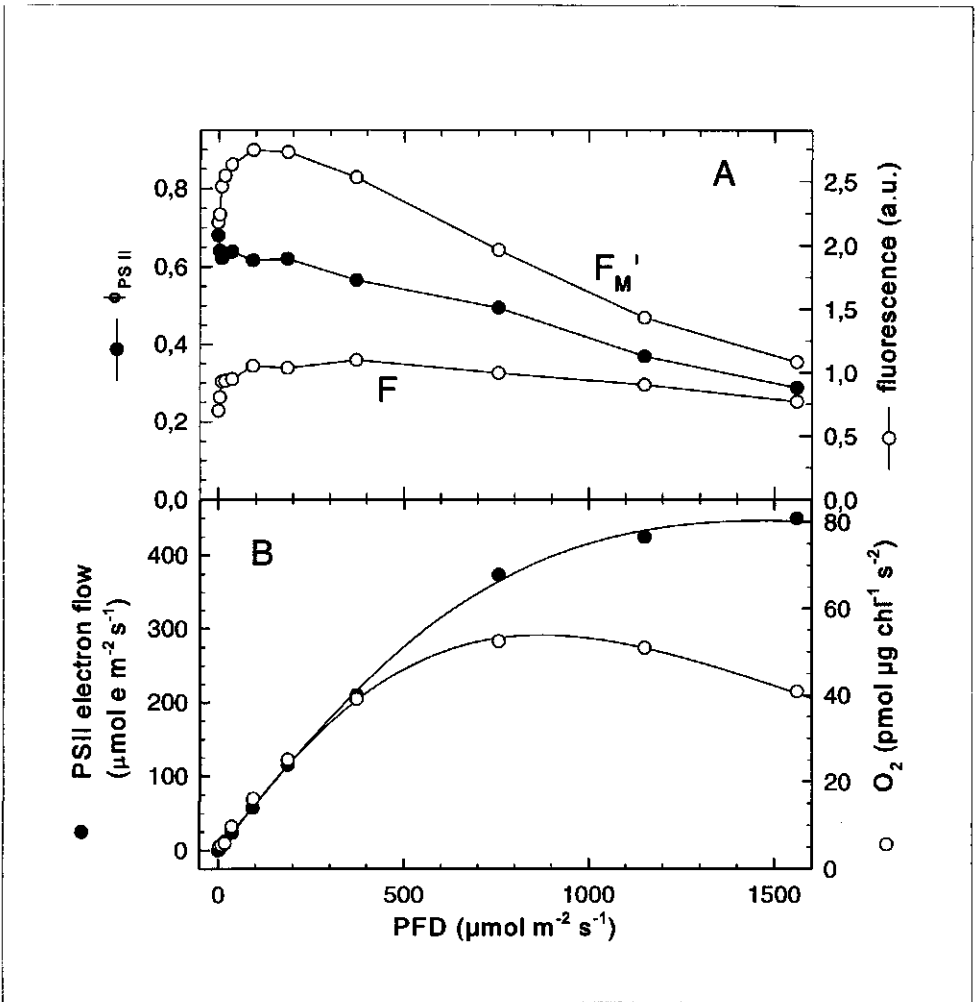


Figure 3.2. A: The actual (\circ) and maximal (\circ) fluorescence levels and the efficiency of PS II electron transport Φ_{PSII} (\bullet) as a function of the irradiance. B: The rate of oxygen evolution (\circ) and the estimated rate of PS II electron transport (\bullet) as a function of the irradiance. The experiment was done with *P. tricornutum* at 20 °C with a single sample using the Xe-PAM fluorometer and the Hansatech DW2/2 oxygen electrode chamber. Growth temperature: 20°C. Lines represent fits according to the photosynthesis model of *Eilers and Peeters* (1988) adapted to allow for electron flow driven oxygen uptake (see text for more details).

3.2 Materials and methods

The marine algae *Phaeodactylum tricornutum*, *Dunaliella tertiolecta*, *Tetraselmis sp.*, *Isochrysis sp.* and *Rhodomonas sp.* were kindly supplied by L. Peperzak of the National Institute of Coastal and Marine Management. The algae were grown in unialgal batch cultures in f/2 medium at pH

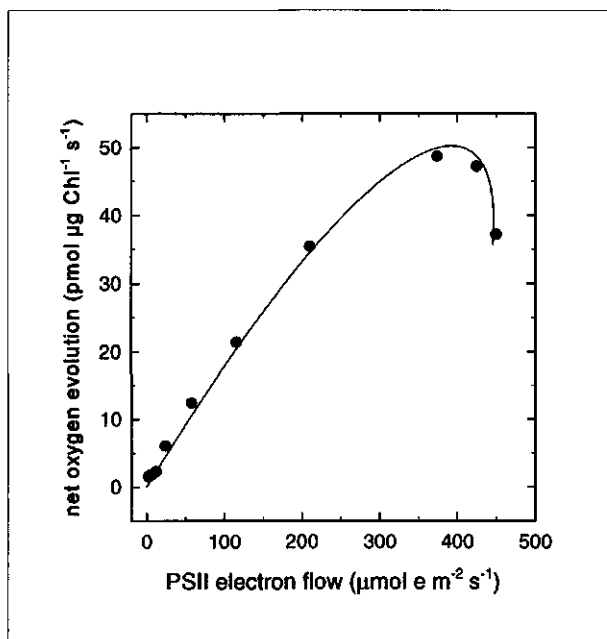


Figure 3.3. The relationship between oxygen evolution and estimated PS II electron transport in *P. tricornutum*. Data are from Figure 3.2B and the line represents the fit according to the model of *Eilers and Peeters* (1988) modified as described in Figure 3.2.

7.4 (MacLachlan 1975) in artificial seawater (35 g seasalts l^{-1} , Sigma seasalts). The cultures were kept at 20 °C or 25 °C and $100 \mu\text{mol m}^{-2} \text{s}^{-1}$ continuous irradiance. They were mixed by bubbling with air enriched in CO_2 . The cells were kept in the exponential growth phase as determined spectrophotometrically at 680 nm.

The algae were harvested by centrifugation and used at a final concentration of 0.5-7 μg chlorophyll a ml^{-1} . The algae were dark adapted for 30 min prior to the start of the measurement. Oxygen and fluorescence were measured in steady state which was reached after 5 to 10 minutes. Measurements were made at the growing temperature. Unless stated otherwise, a new sample was taken for every measurement.

Oxygen and fluorescence were measured simultaneously in a DW2/2 oxygen electrode chamber (Hansatech, Kings Lynn, Norfolk, UK). Oxygen measurements were controlled using the CBD1 control box (Hansatech). Net oxygen evolution was calculated from the rate of oxygen increase minus the dark respiration. The efficiency of photosystem II electron transport was determined with excitation at 650 nm and detection above 700 nm using the PAM Chlorophyll Fluorometer (Heinz Walz, Effeltrich, Germany) or with broadband excitation from 400-560 nm (Xenon flashlamp plus 4mm Schott BG39) and emission detected above 650 nm (Balzer R65 plus Schott RG645) using a slightly modified version of the Xe-PAM fluorometer (Schreiber et al

1993). The PAM and Xe-PAM fluorometer gave similar results for the efficiency of PSII electron flow (Geel unpublished results). The signal to noise ratio of the PAM measurements was comparable to the measurements shown in Hofstra et al (1994). The signal to noise ratio of the Xe-PAM measurements was much higher due to the high sensitivity of the Xe-PAM fluorometer (Schreiber et al 1993). Using the PAM fluorometer the LS2 light source (Hansatech) and neutral density filters (Schott) were used to illuminate the sample and saturating light pulses ($6000 \mu\text{mol m}^{-2} \text{s}^{-1}$) were given with a FL-103 Fiber Illuminator (Walz). The Xe-PAM fluorometer is equipped with two halogen lamps which were used for actinic and saturating light. The saturating light was filtered through a 650 nm short-pass filter (Balzers DT Cyan special) and was used at an intensity of $6000 \mu\text{mol m}^{-2} \text{s}^{-1}$, the actinic irradiance was adjusted with neutral density filters. Light saturation was checked by comparing F_M in the absence and in the presence of DCMU. The fluorescence measurements were corrected for a background signal caused by scattering of the excitation light, filter fluorescence or electrical artifacts which significantly affect the results at low chlorophyll concentrations. Fluorescence nomenclature was according to Van Kooten and Snel (1990). The efficiency of PSII electron flow was calculated as $(F_M' - F)/F_M'$. The rate of electron transport was estimated by the product of the efficiency of photosystem II and the photon flux density (PFD). The chlorophyll *a* concentration was determined after extraction with boiling ethanol according to Nusch (1980). The rates of oxygen evolution and electron transport were varied by changing the irradiance. Photon flux density from 400 to 700 nm was measured with a Skye photometer equipped with a quantum sensor.

The rates of PS II electron flow and oxygen evolution were fitted by the phytoplankton photosynthesis model proposed by Eilers and Peeters (1988). The model assumes that a photosynthetic unit can exist in one of the three following states: open, closed or inhibited, existing in fractions x_1 , x_2 and x_3 , respectively (see Fig. 3.1). Absorption of light by a unit in state 1 results with a probability α in a photochemical event leading to oxygen production and conversion into a closed unit (state 2). Excitation of the closed state results in an inhibited state (state 3) with probability β which is much smaller than α . The closed unit is reopened by the dark reactions associated with carbon assimilation with a rate constant γ . The inhibited state is converted into the open state with rate constant δ . The probability for recovery of photoinhibition δ is much smaller than the probability for photosynthesis dark reactions γ . A system of differential Equations can be obtained from Figure 3.1:

$$\frac{dx_1}{dt} = -\alpha I x_1 + \gamma x_2 + \delta x_3 \quad (3.1)$$

$$\frac{dx_2}{dt} = \alpha I x_1 - (\beta I + \gamma) x_2 \quad (3.2)$$

$$\frac{dx_3}{dt} = \beta I x_2 - \delta x_3 \quad (3.3)$$

To simplify the equations, δx_3 and $\beta I x_3$ can be omitted in the Equations (3.1) and (3.2) (see

Eilers and Peeters 1988). The steady state solution for the rate of electron flow (J_E) is given by:

$$J_E = \frac{\alpha\gamma\delta I}{(\alpha\beta I^2 + \alpha\delta I + \gamma\delta)} \quad (3.4)$$

Substituting $A = \beta/(\gamma\delta)$, $B = (\alpha + \beta)/(\alpha\gamma)$ and $C = \alpha^{-1}$ the equation is simplified to:

$$J_E = \frac{I}{(AI^2 + BI + C)} \quad (3.5)$$

Oxygen evolution data were fitted using k to account for the PSII absorption cross-section and for the stoichiometry of oxygen evolution and one additional parameter E describing oxygen consumption. A part of the enzymatic reactions leading to reopening (rate constant γ) of closed units was assumed to be associated with oxygen consumption. The ratio of the rate constants of oxygen uptake and oxygen production was assumed to be proportional to the redox state of ferredoxin. The redox state of ferredoxin is in equilibrium with the 'redox state' x_2/x_1 of the photosynthetic factories.

$$\frac{\gamma_{OC}}{\gamma_{OP}} = (x_2/x_1) E \quad (3.6)$$

with γ_{OC} , γ_{OP} : rate constants of oxygen consumption and production, respectively and E , a proportionality constant.

Furthermore, we assumed that the sum of the rate constants was constant and equal to γ :

$$\gamma_{OC} + \gamma_{OP} = \gamma \quad (3.7)$$

With $\beta \ll \alpha$ and $\delta \ll \gamma$ the following expression can be derived:

$$x_2 = \left(\frac{\alpha I}{\gamma}\right) x_1 \quad (3.8)$$

The relative rate constants γ_{OC} and γ_{OP} can now be calculated. Net oxygen evolution (J_{O-net}) is the sum of oxygen production (γ_{OP}) and oxygen consumption (γ_{OC}). We assumed that oxygen consumption was caused by Mehler reaction. This reaction uses only 2 electrons per oxygen molecule whereas oxygen production is accompanied with the release of 4 electrons per molecule. Therefore net oxygen evolution is given as:

$$J_{O-net} = kx_2(\gamma_{OP} - 2\gamma_{OC}) \quad (3.9)$$

The experimentally observed rate of oxygen evolution (J_O) can now be described by the following equation:

$$J_O = \frac{kI(C - 2BEI)}{(AI^2 + BI + C)(BIE + C)} \quad (3.10)$$

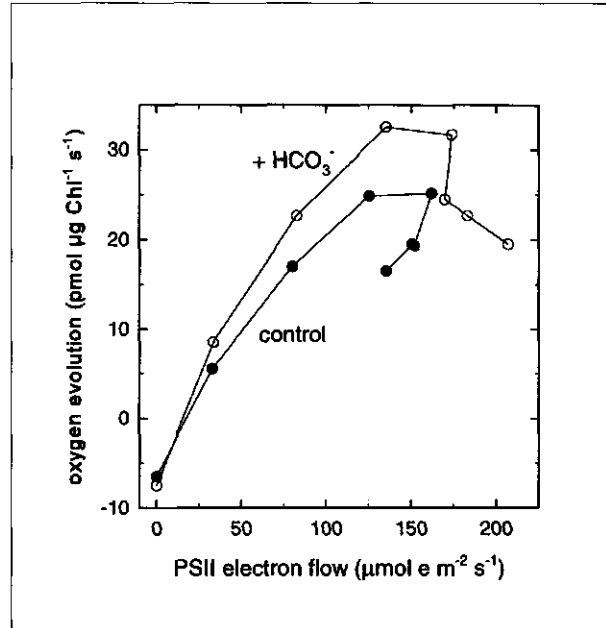


Figure 3.4. The relationship between oxygen evolution and estimated PS II electron transport in *P. tricornutum* grown at 25 °C with (○) and without (●) addition of 0.625 Mm HCO_3^- . The measurements were done at 25 °C using the PAM Chlorophyll Fluorometer, other conditions as in Figure 3.1.

with k : fraction of incident photons absorbed by PSII, as determined by the absolute absorption cross-section, divided by the number of electrons required for watersplitting.

The fitting procedure was performed in MathCad 6.0 *plus* (MathSoft, Cambridge, Mass., USA) and started with fitting Equation (3.5) to the PS II electron flow data as a function of irradiance by optimizing the model parameters A , B and C . Keeping A , B , and C constant, k was optimized assuming a linear slope of oxygen evolution to irradiance at low irradiances. Finally E was optimized by fitting the total set of oxygen evolution data to Equation (3.10), keeping all other parameters constant.

3.3 Results

The steady state rates of oxygen evolution and the actual (F) and the maximal (F_m) fluorescence levels have been determined in a number of marine algae over a range of light intensities. Figure 3.2A shows the efficiency of PS II electron transport and the actual and the maximal fluorescence levels as a function of the irradiance in *P. tricornutum*. The quantum efficiency of PS II electron transport is about 0.68 in the dark and decreases to about 0.3 at $1560 \mu\text{mol m}^{-2} \text{s}^{-1}$. In contrast

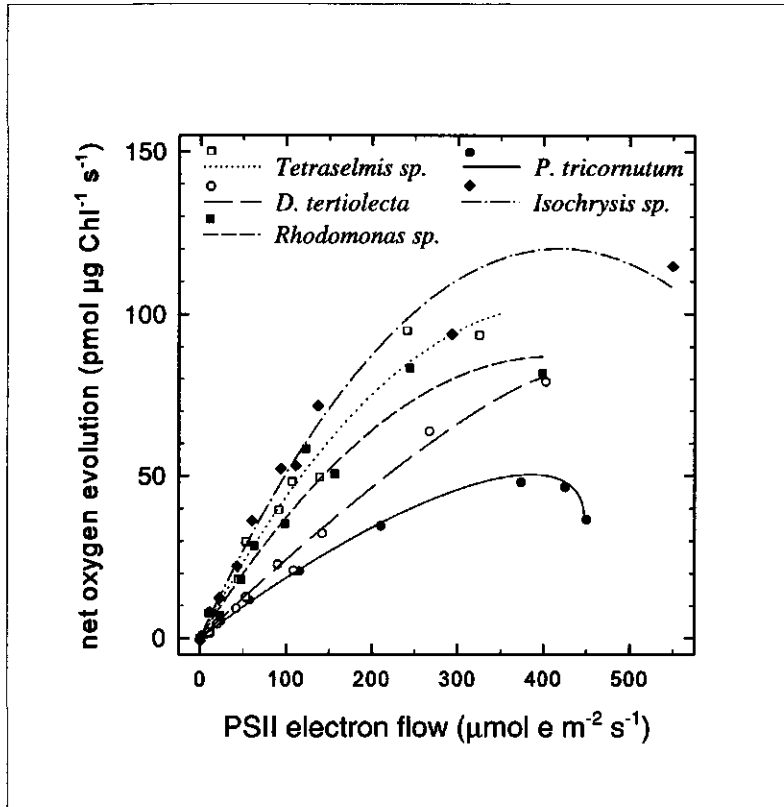


Figure 3.5. The relationship between oxygen evolution and estimated PS II electron transport in the marine algae *P. tricornutum* (●), *D. tertiolecta* (○), *Tetraselmis* sp. (□), *Rhodomonas* sp. (■) and *Isochrysis* sp. (◆). Experiments were done using the PAM Chlorophyll Fluorometer, other conditions as in Figure 3.1.

to higher plants not only F but also F_M' increases when a dark adapted sample is illuminated with up to about $100 \mu\text{mol m}^{-2} \text{s}^{-1}$. This is in line with observations from Falkowski et al (1986) who found higher maximal fluorescence values at intermediate irradiances (about $100 \mu\text{mol m}^{-2} \text{s}^{-1}$) compared to low irradiances ($< 1 \mu\text{mol m}^{-2} \text{s}^{-1}$) in *Skeletonema costatum*, *Thalassiosira weissflogii* and *Isochrysis galbana* using the pump and probe method. Ting and Owens (1993) interpreted comparable results in *P. tricornutum* as energy dependent fluorescence quenching. From 100 to $1560 \mu\text{mol m}^{-2} \text{s}^{-1}$ both levels are reduced. This means that fluorescence quenching analysis as described earlier (Schreiber et al 1986, Van Kooten and Snel 1990) is not possible as the maximal fluorescence level in the dark (F_M) is lower than the maximal fluorescence in the light (F_M') leading to negative non-photochemical quenching coefficients. The method described to determine the efficiency of PS II from the actual and maximal fluorescence levels in the light (Genty et al 1989) does not depend on the maximal fluorescence in the dark and is therefore unaffected by the increase in F_M' observed in Figure 3.2A.

The estimated rate of PS II electron transport and the rate of oxygen evolution are shown in Figure 3.2B as a function of the irradiance. The rate of oxygen evolution increases with increasing irradiance until a maximum is reached at about $800 \mu\text{mol m}^{-2} \text{s}^{-1}$. At higher irradiances the rate of oxygen evolution decreases. The estimated rate of PS II electron transport also increases in *P. tricornutum* with increasing irradiance but saturation is not yet observed at $1560 \mu\text{mol m}^{-2} \text{s}^{-1}$. The fitted lines indicate that the modified model of Eilers and Peeters (1988) can give a good description of both PS II electron flow and oxygen evolution data.

Table 3.1. Summary of the parameters resulting from a fit of the model to the estimated rates of PS II electron flow and oxygen evolution shown in Figure 3.4.

	Φ_{PSII}^1	$C'(\alpha)$	A s^2	$B(-Y^1)$ s	k	E
<i>Rhodomonas sp.</i>	0.80	0.828	1.29E-7	1.18E-4	0.424	0.210
<i>Tetraselmis sp.</i>	0.76	0.716	9.42E-7	7.20E-4	0.407	0.217
<i>D. tertiolecta</i>	0.73	0.713	5.47E-7	5.14E-4	0.239	0.154
<i>Isochrysis sp.</i>	0.81	0.781	0	5.32E-4	0.442	0.545
<i>P. tricornutum</i>	0.64	0.637	6.18E-07	2.45E-4	0.225	1.16

¹ Φ_{PSII} measured at low light ($<15 \mu\text{mol m}^{-2} \text{s}^{-1}$)

Figure 3.3 shows the relationship between oxygen evolution and the estimated rate of PS II electron transport for *P. tricornutum*. The relationship is approximately linear at low and moderate photosynthetic rates corresponding to light intensities up to about $400 \mu\text{mol m}^{-2} \text{s}^{-1}$ (cf. Fig. 3.2B). At high photosynthetic rates the decrease of the rate of oxygen evolution results in a non-linear relationship at high irradiance. As this decrease in the rate of oxygen evolution is not accompanied by a decrease in the rate of PS II electron transport, it must be caused by oxygen consuming processes linked to linear electron flow, e.g., Mehler reaction or photorespiration.

We examined the role of photorespiration by addition of bicarbonate to the medium to suppress oxygenation of ribulose 1,6-diphosphate. The effect of additional bicarbonate on the relation between PS II electron transport and oxygen evolution is shown in Figure 3.4. The addition of bicarbonate results in both a higher maximal rate of oxygen evolution and a higher maximal rate of PS II electron transport. The irradiance at which the relation between the rate of PS II electron transport and the rate of oxygen evolution becomes non-linear (about $250 \mu\text{mol m}^{-2} \text{s}^{-1}$, not shown) is, however, not significantly influenced by the HCO_3^- concentration. Similar effects were observed in *Tetraselmis sp.* (Geel unpublished results) and we therefore conclude that under our experimental conditions photorespiration is not the major cause for the non-linearity observed at high irradiance.

Figure 3.5 shows the relation between the rate of oxygen evolution and the estimated rate of

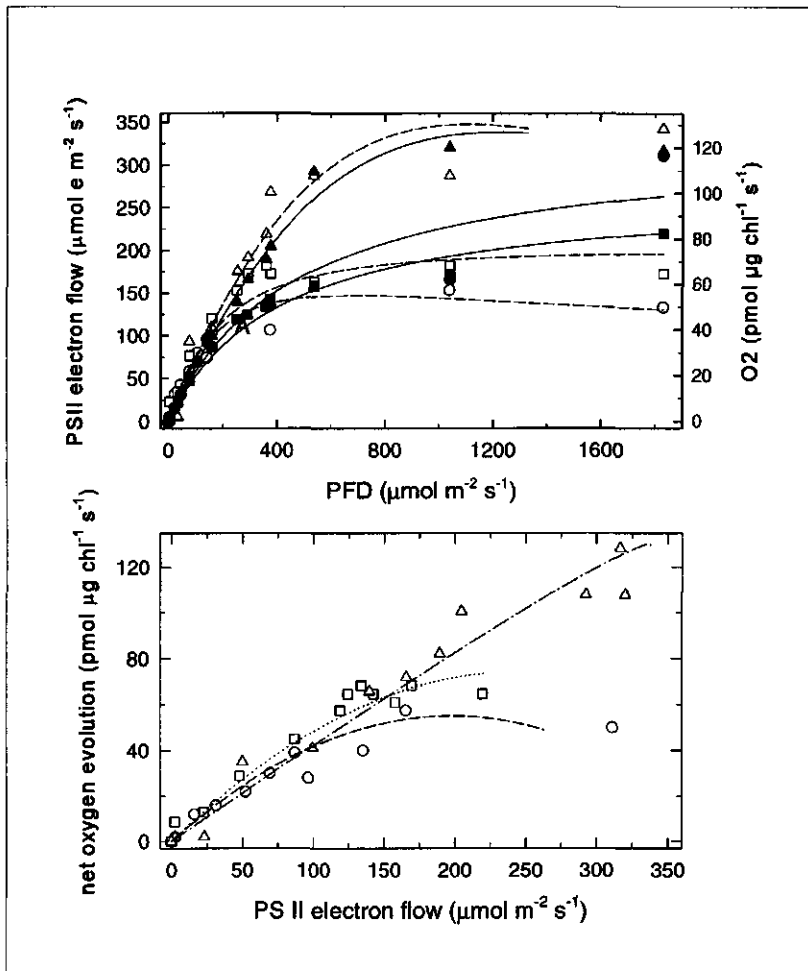


Figure 3.6. A: The rate of oxygen evolution (open symbols) and the rate of PS II electron transport (closed symbols) as a function of the irradiance at 10 °C (●, ○), 15 °C (■, □) and 20 °C (▲, △). The solid lines represent the fits of PS II electron flow and the dashed lines fits of oxygen evolution. B: The relationship between oxygen evolution and estimated PS II electron transport in *P. tricornutum*. Symbols: 10 °C (○), 15 °C (□) and 20 °C (△). The combined fits are shown as lines: 10 °C (---), 15 °C (····) and 20 °C (----). Each measurement was done with a separate sample, other conditions as in Figure 3.1.

PS II electron transport for *P. tricornutum* and four other species. At low rates an approximately linear relationship between oxygen evolution and PS II electron transport is observed. At high rates the relation is more non-linear. In general we find saturation of the rate of oxygen evolution which is not accompanied by a simultaneous saturation of the estimated rate of PS II electron

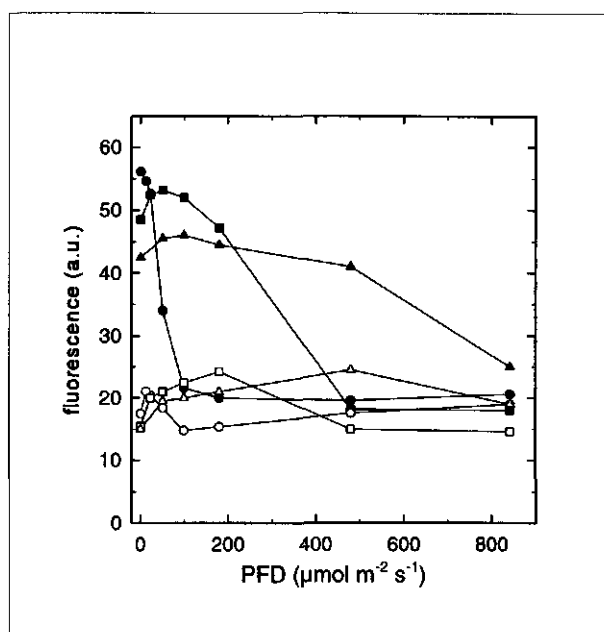


Figure 3.7. Actual (open symbols) and maximum (closed symbols) fluorescence levels as a function of the irradiance at 5°C (●,○), 15°C (■,□) and 25 °C (▲,△). Conditions as in Figure 3.4.

transport. The irradiance at which deviation from linearity starts is different for the different algal species examined and varies from 200 $\mu\text{mol m}^{-2} \text{s}^{-1}$ in *Isochrysis*, to 400 $\mu\text{mol m}^{-2} \text{s}^{-1}$ in *P. tricornutum*, about 500 $\mu\text{mol m}^{-2} \text{s}^{-1}$ in *Tetraselmis sp.* and *Rhodomonas sp.* and no saturation until 1000 $\mu\text{mol m}^{-2} \text{s}^{-1}$ in *D. tertiolecta*. Table 3.1 summarizes the results of the fit procedures. The value of the probability α of photochemistry in an open unit is quite similar to the value of the quantum efficiency of PSII measured at low light, albeit slightly smaller in most cases. Assuming $\alpha \gg \beta$, γ equals B' . Table 3.1 shows that the rate constant γ for the dark conversion of closed to open units is much more species dependent and differs almost an order of magnitude between *Rhodomonas sp.* and *P. tricornutum*. The proportionality constant k for the relation between the estimated rate of PS II electron transport and the rate of oxygen evolution is clearly species-dependent and varies by a factor of 2 between the species.

In Figure 3.6A the effect of temperature on the rates of PS II electron transport and oxygen evolution in *P. tricornutum* is shown. Both the maximal rate of PS II electron transport and the maximal rate of oxygen evolution decrease with decreasing temperature. The initial slope of the relation between the estimated rate of PS II electron transport and the rate of oxygen evolution is independent of temperature (Fig. 3.6B). The light dependence of the actual and maximum fluorescence levels (F and F_m') is shown in Figure 3.7 at various temperatures. At 15 and 25 °C the fluorescence levels F and F_m' increase at low to medium irradiances and decrease again at

higher irradiances. The irradiances at which the maxima are reached decrease with decreasing temperature; at 5 °C the light-induced increase of F_M' is no longer observed. The temperature effects on F and F_M result in an increase of the F_V/F_M with decreasing temperature from 0.61 at 25 °C to 0.67 at 5 °C (Table 3.2).

Table 3.2. The F_V/F_M of dark adapted *P. tricornutum* grown at 20 °C as a function of the incubation temperature. F_0 and F_M were measured after 30 minutes dark adaptation in the measuring cuvette with the Xe-PAM fluorometer using 10 replicate samples at each temperature.

Temperature (°C)	$F_V/F_M \pm \text{STD}$
5	0.671 ± 0.004
10	0.673 ± 0.004
15	0.645 ± 0.006
20	0.636 ± 0.006
25	0.612 ± 0.006
30	0.550 ± 0.012

3.4 Discussion

Under the conditions examined here (normal and increased HCO_3^- concentration, different temperatures) we found in different algal species a linear relation between the rate of oxygen evolution and the estimated rate of PS II electron transport at irradiances up to 200 (*Isochrysis sp.*) or 1000 $\mu\text{mol m}^{-2} \text{s}^{-1}$ (*D. tertiolecta*), but mostly to irradiances of about 400 $\mu\text{mol m}^{-2} \text{s}^{-1}$. This is in the range of the typical mean irradiances in a seawater column (Kirk 1994). Furthermore the range of linearity extends to an irradiance which is 2 to 5 times higher than the irradiance at which the species were grown. This range in which a linear relationship was found is wider than in Rees et al (1992), who demonstrated non-linearity in the relation between oxygen evolution and PS II electron transport at irradiances comparable to those at which the algae were grown.

The non-linear relationship at high irradiances resembles the results of Harbinson et al (1990) and Krall and Edwards (1990) with higher plants. In experiments using higher plant thylakoids and artificial electron acceptors Hormann et al (1994) have demonstrated a good relationship between the ratio $(F_M' - F)/F_M'$ and the quantum yield of PS II electron flow. For their

experiments this means that the non-linearity is not caused by cyclic electron flow within PSII, but must be due to the non-assimilatory electron flow associated with oxygen uptake. Falkowski et al (1986) suggested that cyclic electron flow around PSII might explain the dissimilarity between the normalized flash-induced increase in the fluorescence yield and the normalized rate of oxygen evolution in a number of eucaryotic algae. In their experiments, however, contributions from photorespiration or Mehler reaction were not taken into consideration. In a more recent publication Prasil et al (1996) provided evidence for uncoupling of linear PSII electron flow and oxygen evolution, but their conclusions were based on fluorescence and oxygen measurements using 150 μ s flash trains resulting in a single turnover per PSII reaction center. Under these conditions PSII photochemistry and oxygen evolution can be uncoupled, depending on the state of the watersplitting system which was not measured in the light. In our conditions a multi-turnover light-pulse was used to close the PSII reaction center diminishing the dependence of the redox-state of the watersplitting system at the start of the saturating light pulse. We, therefore, regard the results of Prasil et al (1996) not as conclusive evidence for the occurrence of cyclic PSII electron flow *in vivo*. As cyclic electron transport in PSII is expected to occur within the reaction centre, its kinetics should be similar in thylakoids or intact algae. Therefore we think that the results of Hormann et al (1994) might be used to dismiss the explanation of cyclic electron transport in our experiments.

The non-linear relationship was not influenced by addition of extra HCO_3^- in our experiments (Fig. 3.4) indicating that photorespiration is not involved. Bicarbonate addition did stimulate oxygen evolution somewhat, indicating that some photorespiration was present in control conditions (Fig. 3.3). While photorespiration was reduced by the increased carbon dioxide concentration, the Mehler reaction should not be affected by the addition of bicarbonate. This would favour a role of the Mehler reaction which is dependent on reduced ferredoxin. As the detoxification of reduced oxygen species results in the formation of molecular oxygen, this detoxification process should not be very effective under our conditions. This is in line with the results of Rees et al (1992) who found a stronger decrease in the quantum yield of oxygen evolution than in the quantum yield of PS II electron transport under non-photorespiratory conditions in *Dunaliella C9AA*. They suggested that their results give evidence for non-assimilatory electron flow. Results of Kana in plankton from estuarine surface waters and in cyanobacteria confirm the possibility of increased Mehler-reaction-oxygen-uptake at high irradiances (Kana 1990, Kana 1992, Kana 1993). An increased Mehler reaction corresponds with a more reduced ferredoxin, which is in correspondence with the extension of the model with the oxygen uptake component. Extra oxygen uptake also might be caused by an increase of mitochondrial respiration in the light as Weger et al (1989) found in the diatom *Thalassiosira weissflogii*. They found that light respiration was as high as 30 % of maximal photosynthesis. Results of Beardall et al (1994) show an increased oxygen consumption just after the light is put out compared to the dark adapted state. In the line of these results our assumption that mitochondrial respiration rates are constant at all light intensities leads to an underestimation of photosynthetic oxygen evolution at high irradiances, which may be the cause of (part of) the non-linearity between oxygen evolution and PSII electron flow. However, non-linearity was also found in the comparison of PSII electron flow data with short term carbon fixation data in a

natural seawater sample (C Geel unpublished results), which suggests that increased mitochondrial respiration is not the only cause of the non-linearity. The non-linearity in the low light region observed by Öquist and Chow (1992), Oberhuber et al (1993) and Hormann et al (1994) was also present in our measurements. The underlying mechanism of this non-linearity has not yet been elucidated. In microalgae rates of light-dependent mitochondrial respiration involved in ammonium assimilation might be high enough to affect the relation between steady state oxygen evolution and photosynthetic electron flow (Weger et al 1988). The ratio of the estimated rate of electron transport and the rate of oxygen evolution is not dependent on temperature in *P. tricornutum* (Fig. 3.6) and *Tetraselmis sp.*. These results are not in agreement with findings in *Dunaliella C9AA* where a stronger decrease in the quantum yield of oxygen evolution than in the quantum yield of PS II electron transport at low temperature has been reported (Rees et al 1992).

Both F_v/F_m and F_m increase with decreasing temperature (Table 3.2 and Fig. 3.7). An explanation might be found in energy-dependent quenching induced by chlororespiration which is believed to be associated with proton translocation across the thylakoid membrane during oxidation of the plastoquinone pool at the expense of stromal NADPH (Peltier and Schmidt 1991). This proton gradient was suggested to be the cause of the low F_m and F_v/F_m levels in *P. tricornutum* in the dark (Ting and Owens 1993). In our case the lower rate of enzymatic processes at low temperatures might lead to a decrease of the activity of the chlororespiratory pathway which in turn might lead to a lower proton gradient across the thylakoid membrane in the dark a decreased energy-dependent quenching and an increased value of F_m and F_v/F_m . However, in the presence of the uncouplers, nigericine or CCCP we did not observe higher F_v/F_m values indicative of less energy dependent quenching in *P. tricornutum* (C Geel see Chapter 7). This observation suggests that chlororespiration is not involved in lowering F_v/F_m in *P. tricornutum*. A lower temperature might lead to a larger absorption cross-section of PSII which in turn could decrease PSI fluorescence contribution resulting in a higher F_v/F_m . An increase in σ_{PSII} should lead to an increased initial slope of the oxygen evolution as a function of the rate of PSII electron flow. Based on the relation between PSII electron flow and oxygen evolution (Fig. 3.6B) the change in the absorption cross section can not be large.

At low light, the ratio of estimated PS II electron transport and oxygen evolution, k , varies a more than a factor 2 between the different species examined (Fig.3.5 and Table 3.1). The ratio between the estimated PSII electron transport and the oxygen evolution might vary less than a factor 2 when the rate of PSII electron flow is calculated as the product of the efficiency of PSII electron transport, the irradiance and the absorption cross-section of photosystem II, σ_{PSII} . As photosynthetic electrons are not only used in carbon reduction but also in the reduction of nitrate to ammonium, the nitrogen source also might affect the slope of the relation between the rate of PS II electron transport and the rate of oxygen evolution (Weger et al 1988, Holmes et al 1989, Huppe and Turpin 1994). For accurate predictions of phytoplankton oxygen evolution or carbon fixation from *in situ* chlorophyll fluorescence measurements frequent calibrations in the laboratory will therefore be required to determine the ratio between the estimated rate of PS II electron flow and oxygen evolution or carbon fixation. The model of Eilers and Peeters (1988), as modified here, can provide a good tool to estimate oxygen evolution at high irradiance where

the relation is non-linear.

3.5 Conclusions

The relationship between photosynthetic oxygen evolution and PS II electron flow as estimated by simple chlorophyll fluorescence measurements is shown to be non-linear in a number of marine algae. At low and moderate irradiances the relationship is almost linear and oxygen evolution and estimated PSII electron flow are well correlated. The relationship is more non-linear at high irradiances and the non-linearity is suggested to be related to oxygen consumption other than photorespiration as it is not affected by addition of bicarbonate. The relationship can be described by a photosynthesis model modified to allow for oxygen uptake. The relationship between oxygen evolution and estimated PS II electron flow under limiting light is shown to be not dependent on temperature between 10 and 20°C.

4 MEASUREMENT OF PHYTOPLANKTON ELECTRON FLUX USING A Xe-PAM FLUOROMETER

4.1 Introduction

In Chapter 3 the rate of PS II electron flow, estimated as the product of the efficiency of PS II electron flow and the ambient photon flux density, has been compared with the rate of oxygen evolution per amount of chlorophyll in several marine algal species. For each species a different relation was found. Therefore it is not possible to predict the photosynthetic oxygen evolution of a phytoplankton sample from a single measurement of the efficiency of PS II electron flow. For the determination of the absolute amount of PS II electron flow of a phytoplankton sample the functional absorption cross-section of PS II has to be determined as well. Another problem in the determination of the phytoplankton electron flux, PEF, is the low sensitivity of the PAM fluorometer which prevents its use for fluorescence measurements on marine phytoplankton at the concentrations which are found in the natural environment. A new fluorometer was developed which uses a Xenon flash lamp for excitation (Schreiber et al 1993). This apparatus, the Xe-PAM fluorometer, is much more sensitive than the PAM fluorometer, especially when it is used with the PPMON program which was dedicated for controlling the operation of the data logger and the analysis of the output data. Also, due to the white excitation light of the Xenon flash lamp we are able to estimate also the absorption cross-section under certain conditions. In this Chapter we have examined the possibilities and limitations of this system and the conditions under which correct measurements of the efficiency of PSII electron flow and the functional absorption cross-section of PS II can be made.

4.1.1 Comparison of the Xe-PAM and the PAM fluorometers

The PAM fluorometer

The PAM fluorometer has been developed for plant studies (Schreiber 1986). It uses red excitation from a light emitting diode (LED) which peaks at about 650 nm. Measuring light above 680 nm is rejected with a short pass filter (Balzers DT Cyan). Fluorescence emission is measured with a photodiode detector which is screened by a long pass filter (1 mm Schott RG9) that transmits light above 700 nm. Stray light from the LED and from the actinic light, and low wavelength fluorescence generated by the actinic light is rejected by the long pass filter. Fluorescence originating from the modulated measuring light is selective separated from all other fluorescence components by the window amplifier used in the pulse-amplitude-modulation technique. The 650 nm measuring light excites chlorophyll *a* which is present in PS II and PS I and chlorophyll *b* which mainly resides in PS II. The fluorescence emerges from both PS II and PS I. PS II fluorescence peaks at about 680 nm. The fluorescence yield of PS I is not variable and it peaks at about 730 nm (Holzwarth 1990, Krause and Weis 1991) but the fluorescence yield is much lower than the fluorescence yield of PS II. Therefore still most of the fluorescence measured with the PAM fluorometer originates from PS II. Although fluorescence is only detected at

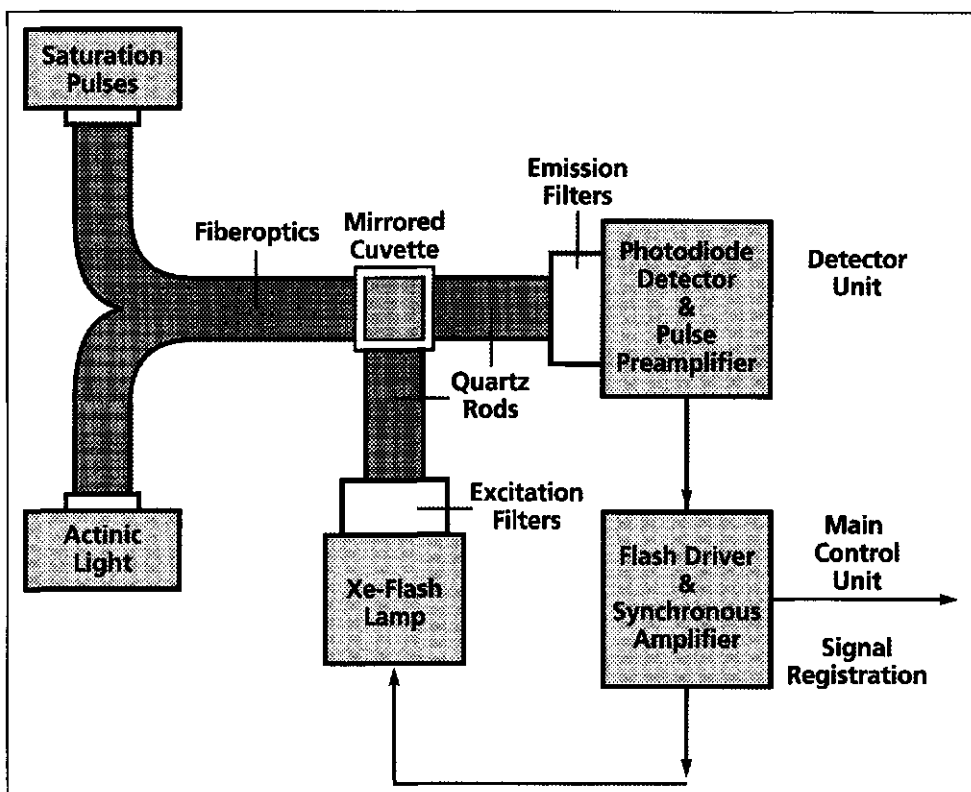


Figure 4.1. Experimental set-up of the Xe-PAM fluorometer in its standard optical configuration. Modified from Schreiber et al (1993).

wavelengths above 700 nm the setup is sufficiently sensitive for higher plants.

The Xe-PAM fluorometer

The custom version of the Xe-PAM fluorometer (Schreiber et al 1993) developed for this project, uses a Xenon flash lamp for excitation and a photodiode detector for detection. The white measuring light of the Xenon lamp in our set-up is usually restricted to a range of 400 to 560 nm by a colour filter (Schott BG39, 4 mm) and fluorescence can be detected from 650 nm upwards. The detector is protected from actinic and measuring light by a combination of a dichroic filter (Balzers R65) and a long pass filter (Schott RG645). The new fluorescence excitation and detection range improved the sensitivity of the apparatus significantly by 2 ways: i) both the excitation and detection range are enlarged allowing more pigments to be excited: chlorophyll is excited in the Soret band, but also accessory pigments like the carotenoids fucoxanthin and peridinin and the phycobilisome pigment phycoerythrin (Kirk 1994) are excited; furthermore nearly the whole chlorophyll fluorescence emission band is measured; ii) interference of excitation light and fluorescence detection is minimized.

The Xenon flash lamp can only properly operate at a frequency below or equal to 128 Hz which

is much lower than the frequencies used with the LED in the PAM fluorometer. However, as the flash intensity of the Xenon lamp is higher than that of the LED, the Xe-PAM gives a higher fluorescence signal and is thus more sensitive. It must be kept in mind, however, that a single measuring pulse should not excite more than a few percent of the PS II reaction centres in order to prevent actinic effects.

The Xe-PAM is equipped with quartz rods which are much more efficient in light transmission than the fibre optics used in the PAM. The Xe-PAM is now optimized for use with algal and chloroplast suspensions in a fluorescence cuvette with 1 ml effective sample volume. The quartz rods for excitation and detection are positioned at an angle of 90° reducing the amount of measuring light that reaches the detector. For the same reason the quartz rod for the actinic light and the saturating light pulse is also positioned at an angle of 90° with the detector (Fig. 4.1).

Even though the excitation and detection wavelengths can be well separated using an appropriate filter set and the construction of the measuring set up is optimized for minimal stray light, a background signal may be usually measured. The signal from algal samples can be corrected for this background signal by zeroing the signal in a blank sample with the zero compensation connected to the measuring light switch.

The spectral composition of the measuring light will influence the background signal. Blue measuring light itself will hardly contribute to the background signal as the detector usually measures light above 650 nm. However, if the optical path contains fluorescing substances other than chlorophyll, blue measuring light may lead to fluorescence emission not related to chlorophyll. Red measuring light is more difficult to reject with the long pass filter and stray light will therefore contribute to the background signal, but on the other hand red light will hardly excite other fluorescing substances.

With the Xe-PAM variable fluorescence can be measured on samples with a chlorophyll concentration as low as $0.02 \mu\text{g l}^{-1}$ (Schreiber et al 1993) whereas the PAM fluorometer requires a chlorophyll concentration of about $1 \mu\text{g ml}^{-1}$ for measurable fluorescence traces (Chapter 3).

4.1.2 Phytoplankton electron flux

The absolute phytoplankton electron flow in an algal sample is dependent on several parameters of the algal photosystems and of the environment. First, the ambient photon flux density will pose an upper limit to the rate of PS II electron transport. The PEF of an algal sample is determined by the capacity of the algae to absorb this light which is described by the functional absorption cross-section of PS II, $\sigma_{\text{PS II}}$, and the overlap between the spectrum of the absorption cross-section and the spectrum of the ambient photon flux density. Furthermore the PEF is determined by the capacity of the algae to use the excitation energy for electron transport, described by $\phi_{\text{PS II}}$, and by the number of PS II reaction centres, $n_{\text{PS II}}$, present in the sample.

4.2 Materials and methods

Culturing the algae

The marine algae *Phaeodactylum tricornutum* and *Dunaliella tertiolecta* were grown in batch cultures in f/2 medium at pH 7.4 (Machlachlan 1975) in artificial seawater (35 g sea salts l⁻¹, Sigma sea salts). The cultures were kept at 20 °C and 100 $\mu\text{mol m}^{-2} \text{s}^{-1}$ continuous irradiation. They were mixed by bubbling with air.

Preparation of the phytoplankton samples

Samples used to determine the maximal efficiency of PS II electron transport were dark adapted for about 15 min prior to the measurement. Light adaptation of samples to measure the steady state efficiency of PS II electron flow lasted about 10 min. Concentration of the algae, when necessary, was achieved by centrifugation and resuspension in fresh medium. All measurements were carried out at 20 °C.

Fluorescence measurements with a Xe-PAM fluorometer

The measurements were carried out with a Xe-PAM fluorometer (see also Chapter 3) at a modulation frequency of 16 Hz. The fluorometer was used in combination with a PC equipped with a data logger (Keighley model 576). A dedicated program PPMON (Phytoplankton Photosynthesis MONitor, Lovoan Software and Education, Wageningen, The Netherlands) controlled the operation of the data logger and the analysis of the output-data. Fluorescence parameters were determined as described in Chapter 3.

The PPMON program

PPMON, written in TURBO PASCAL 6.0, is a dedicated program for fluorescence and/or oxygen measurements. Applications for fluorescence measurement are described here only. Several parameters can be controlled by the program: the time at which the measuring light is put on, the number of saturating light pulses, the length of the saturating light pulse, the repetition frequency of the saturating light pulse and the time when the actinic light is put on or off. The baseline is determined before the measuring light is put on. The F level is determined during a time interval of 0.2 s which ends 0.1 s before the saturating light pulse is turned on. The maximal fluorescence is determined during each saturating light pulse. The period over which the baseline and the F level are determined can be chosen. Furthermore the program enables averaging data and can make corrections for blanc samples. The program is able to repeat a given procedure over a long period resulting in semi-continuous measurements. The program calculates $\Phi_{\text{PS II}}$ from the baseline, the F level and the F_M' level.

Determination of fluorescence excitation and emission spectra

Excitation and emission spectra of F_0 and F_M were measured using filter combinations shown in Table 4.1. A single sample was used to measure a complete excitation spectrum. Emission spectra of F_0 and F_M were measured by varying the detection wavelength. Excitation was performed with broad band measuring light (400 to 560 nm, BG39, Schott). Detection was

performed at 670 nm (670 nm bandpass filter, 10 nm bandwidth, Balzers), 680 nm (680 nm bandpass filter, 20 nm band width, Oriel), 705 nm (705 nm bandpass filter 15 nm band width, Balzers), 730 nm (730 nm bandpass filter, 20 nm band width, Oriel) and 750 nm (750 nm bandpass filter, 11 nm band width, Balzers).

Table 4.1. Description of excitation and detection wavelengths and applied colour filters
Numbered filters are specified as follows: I: BG39; II RG645; III: 430 nm bandpass filter, 12 nm bandwidth; IV: 475 nm bandpass filter, 6 nm band width; V: 530 nm bandpass filter, 10 nm bandwidth; VI: 550 nm bandpass filter, 7 nm bandwidth; VII: 625 nm bandpass filter, 9 nm bandwidth; IX: 705 nm bandpass filter; 15 nm bandwidth; X: R65, dichroic filter; XI: B42, dichroic filter; XII: G49/59, dichroic filter; XIII: 655 nm shortpass filter; XIV: 650 nm bandpass filter, 20 nm bandwidth; XV: 680 nm bandpass filter, 10 nm bandwidth. Filters were supplied by Schott (I and II), Balzers (III to XII) and Oriel (XIII to XV).

Excitation		Detection	
band (nm)	filters	band (nm)	filters
400-560	I	>650	X; II
430	III; XI; I	>650	X; II
480	IV; I	>650	X; II
530	V; XII; I	>650	X; II
550	VI; XII, I	>650	X; II
625	VIII; XIII	6801	X; II; XV
625	VIII; XIII	7052	X; II; IX
650	XIV; XIII	705	X; II; IX

¹ This detection range was used for *D. tertiolecta*.

² This detection range was used for *P. tricornutum*.

Determination of phytoplankton electron transport and oxygen evolution

Samples were dark adapted for 30 min. NaHCO₃ was added after the dark adaptation to a final concentration of 0.625 mM. Oxygen and fluorescence measurements were done as described in Chapter 3 for the Xe-PAM fluorometer. The chlorophyll *a* concentration was determined as described in Chapter 2.

Determining the effect of the measuring light intensity on the efficiency of PS II electron flow

The measuring light intensity was varied by using neutral density filters. Samples were diluted to a concentration of 10 µg chlorophyll *a* per ml and dark adapted. At each measuring light intensity a series of 5 or 10 measurements was made using 2 samples. The control measurement was done on the non-diluted sample.

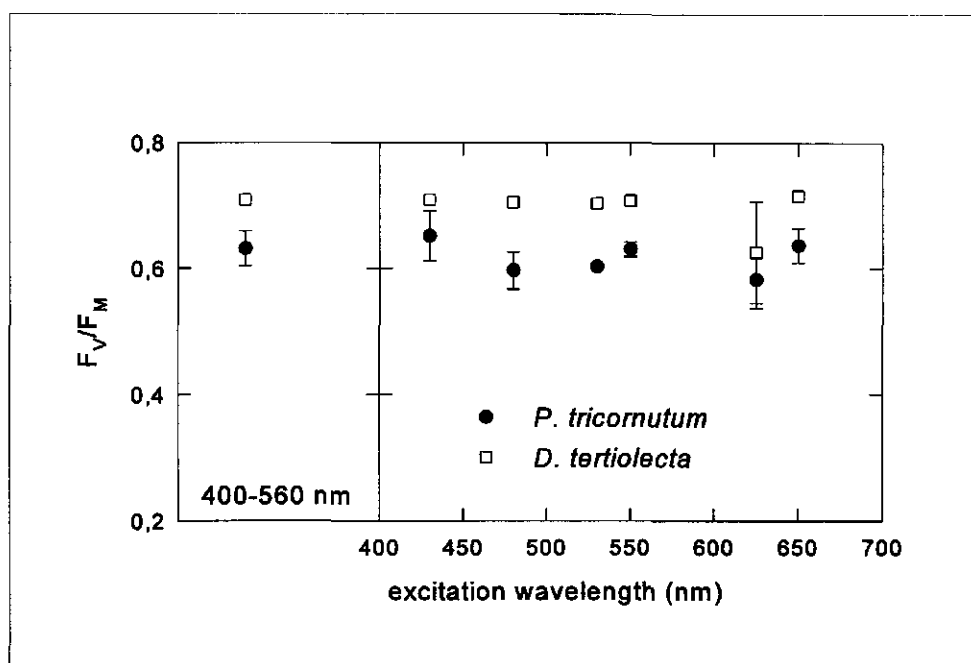


Figure 4.2. Measured efficiency of PS II electron flow in the dark as a function of wavelength of the measuring light. Data are shown for *D. tertiolecta* and *P. tricornutum*. Each series was repeated 2 (*D. tertiolecta*) or 4 (*P. tricornutum*) times. Error bars represent the standard deviation.

Determining the effect of the saturating light pulse on the efficiency of PS II electron flow

The effect of the intensity of the saturating light pulse on the observed maximal fluorescence was examined in dark adapted samples. For each intensity 4 samples were measured and averaged. The saturating light pulses lasted 1 s. The effect of the length of the saturating light pulse was examined in dark adapted samples using a 10 s saturating light pulse. The average of 10 measurements on different samples were taken. The saturating light pulses lasted 10 s. The comparison of the effect of the saturating light pulse and of the addition of DCMU was examined in samples which were dark adapted for 45 min. DCMU was added in the dark at a final concentration of 10 μM . For each experiment 3 samples were measured and averaged.

4.3 Results and discussion

The phytoplankton electron flux in a sample is determined by the ambient photon flux density, the size and optical properties of the light harvesting complexes of each photosystem, the number of PS II reaction centres which are capable for electron transport and the efficiency of the photosystems in converting the excitation energy into electron transport. This is described in

Equation (4.1):

$$PEF = n_{PSII} PFD_A \int_{400}^{700} I_A(\lambda) \sigma_{PSII}(\lambda) \phi_{PSII}(\lambda) d(\lambda) \quad (4.1)$$

With PEF: phytoplankton electron flux; n_{PSII} : the number of PS II reaction centres; PFD_A : the ambient photon flux density ($\mu\text{mol m}^{-2} \text{s}^{-1}$); $I_A(\lambda)$: the spectral distribution function of the ambient light; $\sigma_{PSII}(\lambda)$: the spectral distribution function of the PS II absorption cross-section and $\phi_{PSII}(\lambda)$: the spectral distribution function of the efficiency of PS II electron flow (electron per photon).

4.3.1 Spectral distribution of the efficiency of PS II electron flow

The efficiency of PSII electron flow was tested on its dependency on the wavelength of the measuring light. If the efficiency of PS II electron flow is independent on the wavelength of the

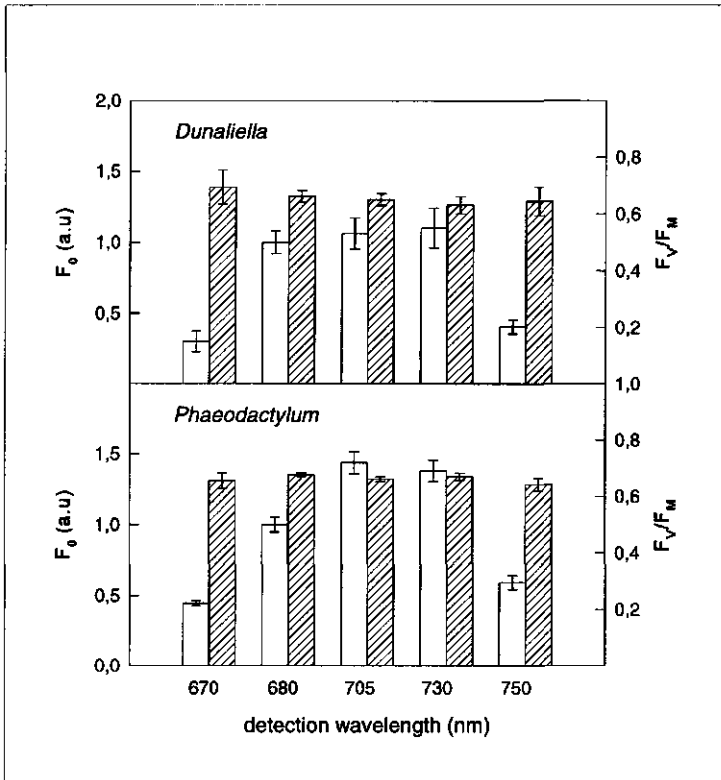


Figure 4.3. Measured minimal fluorescence (white boxes) and maximal efficiency of PS II electron flow (dashed boxes) in the dark as a function of the emission wavelength. Data are shown for *D. tertiolecta* and *P. tricornutum*. Error bars represent the standard deviation. Samples were concentrated 20 times by centrifugation.

measuring light Equation (4.1) can be simplified by taking ϕ_{PSII} out the integral function. In Figure 4.2 F_V/F_M obtained with broad band measuring light (400-560 nm) is compared with that obtained with narrow band measuring light of 430, 480, 530, 550, 625 and 650 nm. In *D*.

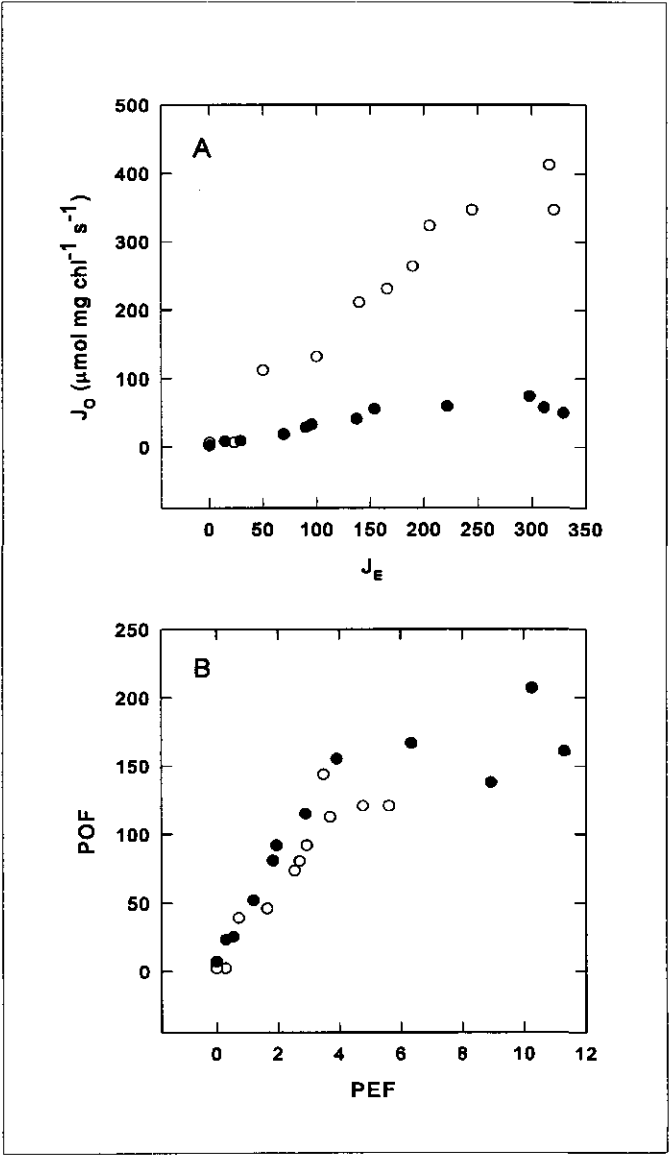


Figure 4.4. A: oxygen evolution per chlorophyll (J_O) as a function of PS II electron flow per PS II reaction centre (J_E). *P. tricornutum*: \circ ; *D. tertiolecta*: \bullet . B: phytoplankton oxygen evolution (POF) as a function of phytoplankton electron flux (PEF). Symbols as in A.

tertiolecta all F_v/F_m values are invariable within the standard deviation except for the value measured at measuring light of 625 nm. In *P. tricornutum* we used a higher detection wavelength (at 705 instead of 680 nm) for the 625 excitation. This resulted in an F_v/F_m value invariable for the wavelength bands used. Previous experiments on the quantum yield for oxygen evolution (mol oxygen per mol photons absorbed) in the alga *Chlorella* showed some spectral dependency as a lower quantum yield was found at about 480 nm than for the other wavelengths, which was assigned to absorption of carotenes (Lawlor 1993). However, fluorescence measurements are more directly related to that fraction of the absorbed photons as only the absorbed photons that reach the chlorophyll pool contribute to F_v/F_m . On the basis of our F_v/F_m measurements we conclude that Φ_{PSII} is not dependent on the excitation wavelength once the excitation reaches the chlorophyll pool, both in *D. tertiolecta* and in *P. tricornutum*.

We also examined the relation between Φ_{PSII} and the wavelength range of fluorescence detection (Fig. 4.3). Both in *D. tertiolecta* and in *P. tricornutum* Φ_{PSII} is independent on the detection range. Genty et al (1990) found a higher maximal efficiency of PS II electron flow at 690 nm as compared to 730 nm in barley and maize. A decrease in F_v/F_m at higher detection wavelengths was found by these authors to be accompanied with an increase in the relative amount of non-quenchable minimal fluorescence at 730 nm. In a leaf reabsorption of PS II fluorescence emission is relatively high and this will lead to a relatively large contribution of non variable PS I fluorescence at wavelengths above 700 nm. As our algal samples are much more dilute the process of reabsorption does not affect the apparent emission spectrum. In Figure 4.3 also the minimal fluorescence is shown. The minimal fluorescence was highest from 680 to 730 nm for *D. tertiolecta* and from 705 to 730 nm for *P. tricornutum*. This is comparable with the room temperature fluorescence emission spectra of *P. tricornutum* found by Goedheer (1973) and Owens (1986a).

As under our conditions the measured efficiency of PS II electron flow is independent on the excitation wavelength the spectral distribution fraction $\Phi_{PSII}(\lambda)$ is constant and Equation (4.1) can be simplified to:

$$PEF = n_{PSII} \Phi_{PSII} PFD_A \int_{400}^{700} I_A(\lambda) \sigma_{PSII}(\lambda) d(\lambda) \quad (4.2)$$

4.3.2 F_0 as a measure of PS II excitation

In this paragraph we will focus on the number of PS II reaction centres, n_{PSII} , and the spectral distribution function of both the ambient irradiance and the functional absorption cross-section. We suggest that the product of these terms can be estimated from F_0 which can be described by an Equation similar to PEF:

$$F_0 = n_{PSII} \Phi_{F_0} PFD_M \int_{400}^{700} I_M(\lambda) \sigma_{PSII}(\lambda) d(\lambda) \quad (4.3)$$

With Φ_{F_0} : the efficiency by which absorbed photons lead to minimal fluorescence (photon per photon); PFD_M : the photon flux density of the measuring light and $I_M(\lambda)$: the spectral distribution function of the measuring light.

In the case that the spectral distribution functions $I_A(\lambda)$ and $I_M(\lambda)$ are identical, the integral term can be eliminated from Equations (4.2) and (4.3):

$$PEF = F_0 \Phi_{PSII} PFD_A \frac{1}{\Phi_{F_0} PFD_M} \quad (4.4)$$

The spectral distribution function of the ambient light and the measuring light are dependent on the light source. In our experiments with the Xe-PAM fluorometer the ambient light is supplied with a halogen lamp which has a continuous white spectrum. The measuring light of the Xe-PAM fluorometer is a Xenon-flash lamp. This lamp also shows a continuous white spectrum, but it normally is filtered with a blue green colour filter (BG 39). Therefore the spectra of the ambient light and the measuring light, although not exactly the same, are not too different.

Φ_{F_0} is generally assumed to be constant. In the case that the measuring light photon flux density is kept constant, these two parameters can be taken together to form the constant $m = (\Phi_{F_0} * PFD_M)^{-1}$. Therefore the relation of Equation (4.4) can be simplified to the following Equation:

$$PEF = m F_0 \Phi_{PSII} PFD_A \quad (4.5)$$

Equation (4.5) is only valid if the amount of fluorescence which is detected is proportional to the amount of fluorescence emission under all conditions. If the optical pathway of the measurement is changed Equation (4.5) is not valid anymore. The amount of light absorbed by the sample is not relevant as long as the optical paths for actinic and measuring light are similar. The product of $m \cdot F_0$ can be regarded as a measure for the amount of light intercepted by PSII in the sample:

$$m F_0 = n_{PSII} \int_{400}^{700} I_M(\lambda) \sigma_{PSII}(\lambda) d(\lambda) \quad (4.6)$$

To check the approximation described by Equation (4.5) we have done measurements on both the electron flux per PS II, J_E , and the phytoplankton electron flux, PEF and compared them with respectively the oxygen evolution per unit of chlorophyll, J_O , and with the phytoplankton oxygen flux, POF (Fig. 4.4). In *P. tricornutum* much higher J_O values are found at comparable J_E values than in *D. tertiolecta*. In the comparison of J_E with J_O it is implicitly assumed that the number of PS II reaction centres is proportional to the amount of chlorophyll *a*. This is only true when each reaction centre is associated by a constant amount of chlorophyll *a* under all conditions. This has been shown not to be true (Gallagher et al 1984, Wilhelm 1993). *D. tertiolecta* contains chlorophyll *a* and *b* as photosynthetic ally active pigments, *P. tricornutum* contains chlorophyll *a* and *c* and fucoxanthin (Owens and Wold 1986). In the right panel of Figure 4.4 the phytoplankton oxygen flux and the phytoplankton electron flux are compared for both species. The adapted method described in Equation (4.5) leads to similar relations between oxygen evolution and electron transport in both species. Therefore we conclude that the use of the minimal fluorescence, to which all photosynthetic ally active pigments contribute, leads to a better estimate for the amount of PS II reaction centres than chlorophyll *a*.

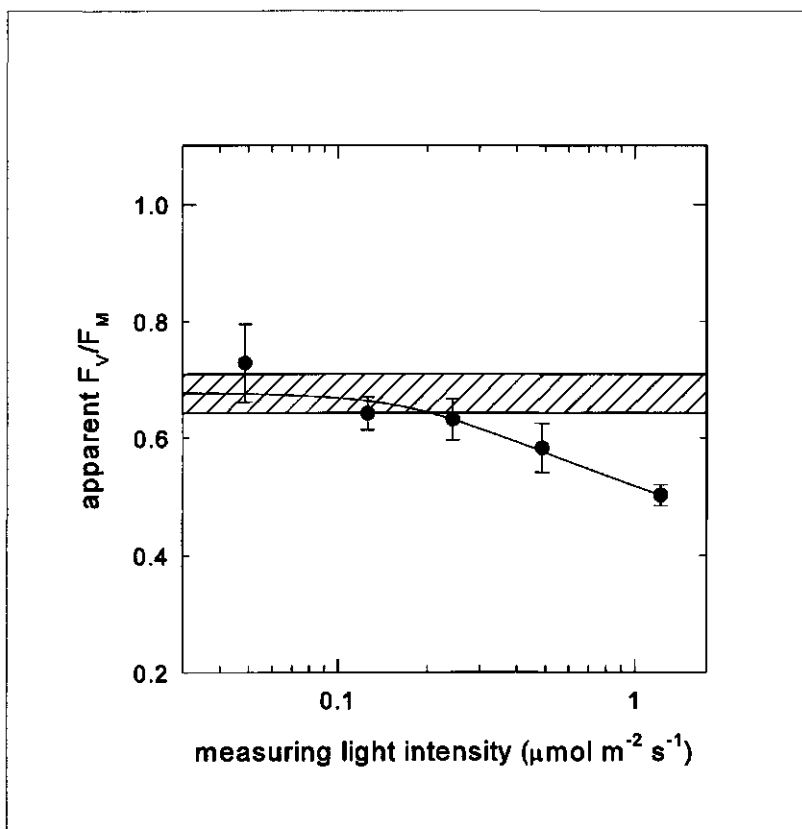


Figure 4.5. F_v/F_m as a function of measuring light intensity in *P. tricornutum*. The grey box indicates the true Φ_{PSII} value $\pm 5\%$.

4.3.3 Determination of the efficiency of PS II electron flow

Effect of measuring light intensity on variation in efficiency of PS II electron flow

For a correct determination of the efficiency of PS II it is essential to consider the effect of the intensity of the measuring light intensity. A high measuring light intensity will result in a higher fluorescence signal and therefore in a higher signal to noise ratio than a low measuring light intensity. However, as the measuring light is absorbed by the photosystems it also changes their reduction state. Therefore the measuring light intensity should be low enough not to change the reduction state of PS II noticeable. The efficiency of PS II electron flow is given as a function of the measuring light intensity for *Phaeodactylum tricornutum* (Fig. 4.5). At low measuring light intensities Φ_{PSII} stabilizes at about 0.67. At high measuring light intensities lower values of Φ_{PSII} are found. This decrease is due to the reduction of the PQ pool, caused by the measuring light. The true efficiency of PS II electron flow was determined with high precision in a non-diluted sample. The grey box represents the area of this Φ_{PSII} plus or minus 5%. It can be seen that the

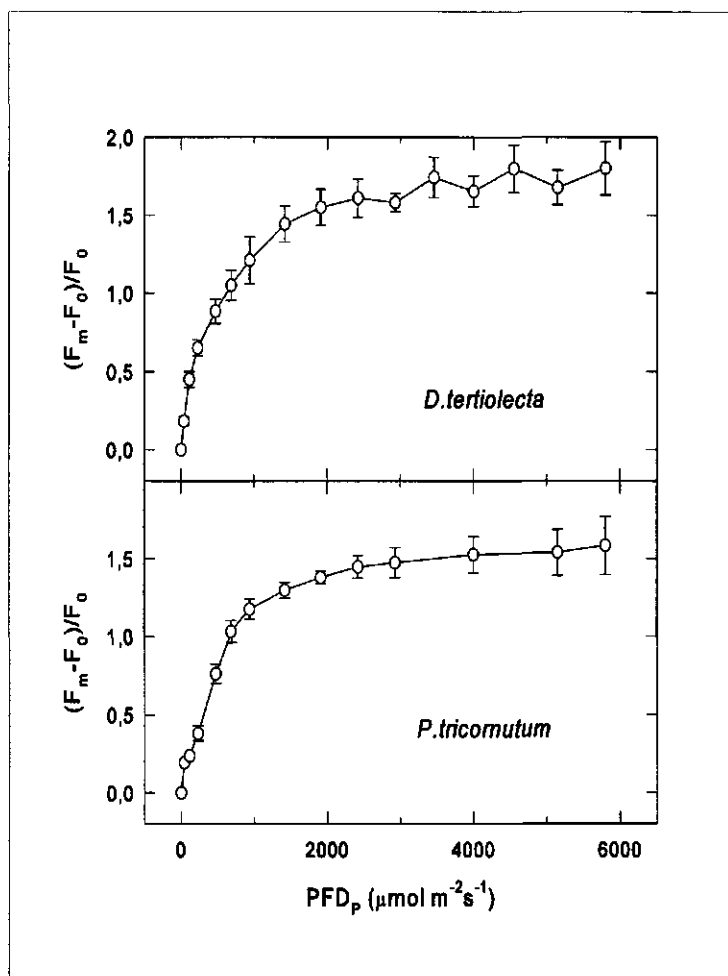


Figure 4.6. Normalized fluorescence $((F_m - F_0)/F_0)$ as a function of the intensity of the saturating light pulse. Samples are averaged 4 (*D. tertiolecta*) or 3 (*P. tricornutum*) times.

intermediate measuring light intensities (between about 0.05 and 0.25 $\mu\text{mol m}^{-2} \text{s}^{-1}$) give the best values for Φ_{PSII} . It should be noted that the lower limit of measuring light intensities leading to acceptable Φ_{PSII} values is also determined by the concentration of the sample. Furthermore it should be noted that in many cases the measurements are not restricted by the variation in the measurement itself but by the biological variation between samples.

Effect of saturating light pulse on the determination of efficiency of PS II electron flow

For a correct determination of the maximal fluorescence level the saturating light pulse should be intense enough and last long enough to cause a complete reduction of the PQ-pool (Ting and Owens 1992). On the other hand too high an intensity of light might induce undesired

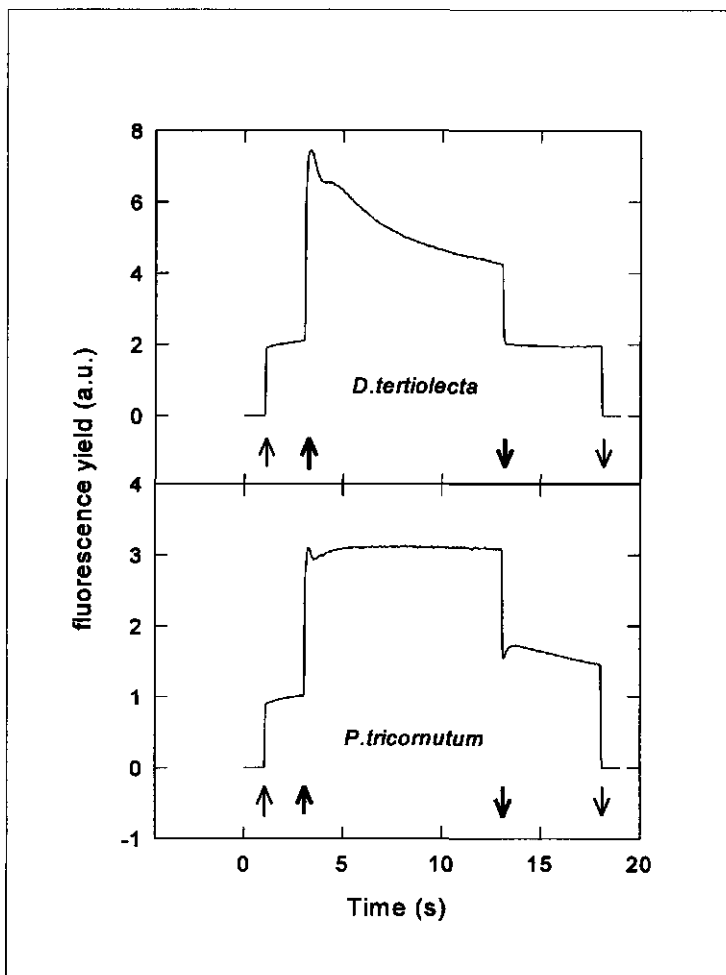


Figure 4.7. Effect of duration of a saturating light pulse on the maximal fluorescence. Duration of the saturating light pulse: 10 s. Data are shown for *D. tertiolecta* and *P. tricornutum*. Measuring light on: ↑ and off: ↓. Saturating light pulse on: ↑↑ and off: ↓↓. The saturating light pulse was given with a continuous white lamp and a shutter. Curves are the average of 10 measurements with different samples

fluorescence quenching in the phytoplankton (Krause and Weis 1991). In Figure 4.6 the maximal fluorescence is shown as a function of the intensity of the saturating light pulse. Both in *D. tertiolecta* and *P. tricornutum* saturation is reached at about $3000 \mu\text{mol m}^{-2} \text{s}^{-1}$. For *P. tricornutum* previously a higher level of $6000 \mu\text{mol m}^{-2} \text{s}^{-1}$ was found to be necessary (Ting and Owens 1992).

In Figure 4.7 the fluorescence behaviour during a long saturating light pulse is shown for *D.*

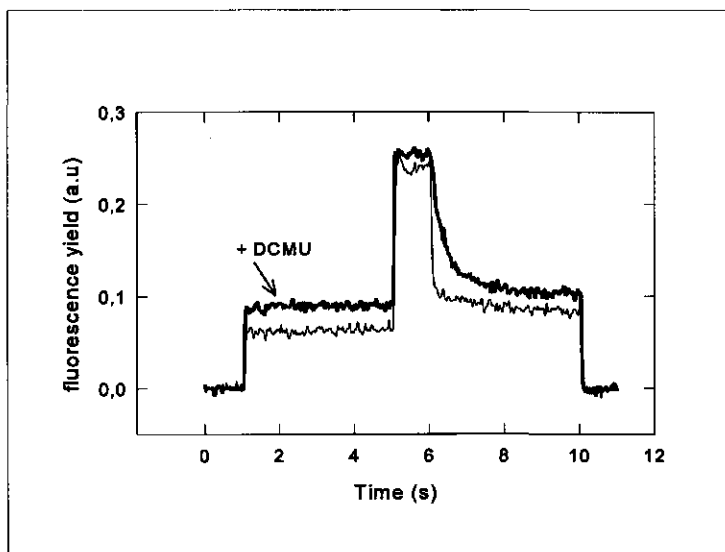


Figure 4.8. Effect of DCMU on measured fluorescence of *P. tricornutum*. The saturating light pulse was given with a continuous white lamp and a shutter.

tertiolecta and *P. tricornutum*. *D. tertiolecta* shows a maximum at 0.5 s after the start of the saturating light pulse and a high quenching of 50 % in 10 s afterwards. When the saturating light pulse is turned off the fluorescence almost immediately decreases to the minimal fluorescence level which was attained before the saturating light pulse. *P. tricornutum* shows a very stable maximal fluorescence, except for a small decrease between 0.5 and 1 s after the onset of the saturating light. When the saturating light pulse is turned off the fluorescence decreases rapidly to a level almost 2 times higher than the minimal fluorescence, increases somewhat and finally decreases very slowly to the minimal fluorescence. The induction of quenching during the saturating light pulse as found in *D. tertiolecta* should be avoided when more measurements of $\Phi_{PS II}$ have to be made on the same sample. It affects the energization of the algal sample and thus affects the observed $\Phi_{PS II}$. Although *P. tricornutum* does not show this quenching during a long saturating light pulse, the fluorescence pattern found after the saturating light pulse has turned off suggests that in *P. tricornutum* the saturating light pulse also induced some changes in the photosynthetic system. Under the conditions used here (continuous white lamp and a shutter) a duration of the saturating light pulse of 0.5 s is enough to reach saturation. When the saturating light pulse is provided by turning on a halogen lamp a longer time is needed as the lamp itself takes about 300 ms to reach the maximal photon flux density.

Saturation of photosynthesis by the saturating light pulse was checked with DCMU. DCMU binds to the Q_B binding place on PS II and inhibits linear electron transport through PS II (Krause and Weis 1991). Closing of PS II reaction centres occurs already at low light intensities in the presence of DCMU. An example of a fluorescence trace with and without DCMU is shown in Figure 4.8. The DCMU sample shows a higher steady state fluorescence than the sample without DCMU suggesting that the measuring light already causes a noticeable reduction of Q_A in the presence

of DCMU. Also saturation of photosynthesis due to the saturating light pulse is faster in the presence of DCMU. Both the sample with and without DCMU reach the same maximal fluorescence. Therefore we conclude that in this experiment the photon flux density of the saturating light pulse was high enough to reach saturation.

4.4 Conclusions

In this chapter we have shown that with certain limitations it is possible to determine the phytoplankton electron flux in an algal sample. The efficiency of PS II electron flow is independent on the excitation wavelength under the conditions used. The accuracy in the determination of $\Phi_{PS II}$ is dependent on the light intensity of the measuring light which should be high enough for a good signal to noise ratio and low enough to minimize actinic effects of the measuring light. The accuracy with which $\Phi_{PS II}$ can be determined is dependent on the intensity and the duration of the saturating light pulse. The intensity of the saturating light pulse of the Xe-PAM was found to be high enough for saturation of photosynthesis of the algae under our conditions. The relationship between PS II electron flux and oxygen evolution expressed on a chlorophyll basis differed by a factor 4 in the diatom *P. tricornutum* and the green flagellate *D. tertiolecta*. Applying Equation (4.5) a similar relationship between PEF and the POF was found for the diatom *P. tricornutum* and green flagellate *D. tertiolecta*.

5 THE RELATION BETWEEN CARBON FIXATION AND PHOTOSYSTEM II ELECTRON FLOW IN MARINE PHYTOPLANKTON

5.1 Introduction

In Chapter 3 a curvi-linear relationship between photosynthetic oxygen evolution and PSII electron flow was found in several marine algae. The non-linearity, which was most obvious at high photon flux densities, was shown not to be related to photorespiration and could be described with a photosynthesis model modified to take oxygen consumption into account. In the marine environment where the phytoplankton content is very low ^{14}C fixation measurements are more suited to determine photosynthesis than oxygen evolution measurements. This is because the measurement of ^{14}C fixation is much more sensitive than the measurement of oxygen evolution by using oxygen electrodes. Photosynthetic oxygen evolution data in a natural seawater sample will be contaminated by the respiration of bacteria and zooplankton. ^{14}C fixation measurements in phytoplankton might result in gross or net photosynthesis depending on the duration of the incubation. The recycling of respiratory carbon dioxide was found to be high (Williams et al 1996). Photosynthetic oxygen evolution is almost directly coupled to electron transport at PS II but the coupling between PS II electron flow and photosynthetic carbon fixation is more indirect. Carbon fixation is dependent on the ATP and NADPH which are formed by linear electron flow in the electron transport chain in the photosynthetic membrane. Carbon reduction, however, is not the only sink for ATP and NADPH. Therefore the relationship between carbon fixation and PSII electron flow might be expected to be more complex than the relationship between oxygen evolution and PSII electron flow (Kroon et al 1993). So the next step in our research was to examine the relation between carbon fixation and PSII electron flow.

In Chapter 3 results of the relation between the efficiency of PS II electron flow and the efficiency of carbon fixation in higher plants have been described. Under optimal growing conditions and non-photorespiratory conditions they found a linear relationship between the efficiency of PS II electron flow and the efficiency of carbon fixation (Genty et al. 1989; Harbinson et al 1990, Krall and Edwards 1990, Oberhuber et al 1993). Photorespiration led to a non-linear relationship between the efficiency of PS II electron flow and the efficiency of carbon fixation (Harbinson et al 1990, Krall and Edwards 1990). Cyclic electron transport was shown to be unimportant under conditions where linear electron flow is not suppressed (Harbinson et al 1990, Prasil et al 1996). However, more recent results with maize showed a much larger variability in the relation between the efficiency of PS II electron flow and the efficiency of carbon fixation (Baker et al 1995). From these experiments with outdoors growing maize Baker et al. suggested that other sinks than carbon reduction might be important under these non-optimal growing conditions. A possible sink might be the Mehler reaction as suggested by Öquist and Chow (1992) (see also Chapter 3). Using ^{18}O isotopes Kana (1990, 1992, 1993) indeed found an increased oxygen uptake in the light compared to the dark in phytoplankton from estuarine

surface waters and in cyanobacteria. As the oxygen uptake in the cyanobacteria was inhibited by DCMU he attributed it to the Mehler-reaction. Another sink for photosynthetically formed ATP and NADPH might be nitrate reduction (Huppe and Turpin 1994). Furthermore an increased mitochondrial respiration in the light compared to the dark as was suggested by Weger et al (1989) and Beardall et al (1994) might explain part of the non-linearity in the relation between PS II electron flow and carbon fixation. New experiments from Xue et al (1996) show that light induces both an increase in oxygen consumption and a decrease in carbon dioxide production. This would lead to a different relation between carbon fixation and PS II electron flow than between oxygen evolution and PS II electron flow.

In marine phytoplankton samples from the Atlantic ocean Falkowski and Kolber (1990) and Kolber and Falkowski (1993) have found a reasonable correlation between the rate of carbon fixation and the rate of PSII electron flow. They estimated the product of the number of closed PS II reaction centres and the effective absorption cross-section of PS II with the pump and probe fluorescence method to calculate the rate of PS II electron flow. The variation they found in the relation between the rate of carbon fixation and the rate of PS II electron flow is somewhat smaller than the variation found in the results of Baker et al (1995).

We determined both carbon fixation and PSII electron flow in 3 different marine algae. The phytoplankton electron flux, PEF, was estimated by the product of the efficiency of PSII electron flow, Φ_{PSII} , the photon flux density, PFD, and the minimal fluorescence of the algae in the dark, F_0 . The phytoplankton carbon flux, PCF, was determined directly as carbon fixation per m^3 . We also examined whether a preincubation of the algae at a given photon flux densities did influence the relation between carbon fixation and PSII electron flow.

In general we found that the relation between PCF and PEF resembles the relation between oxygen evolution and PSII electron flow as found in Chapter 3. The relation between PCF and PEF at low photon flux densities is more or less the same for all 3 species.

5.2 Materials and methods

Culturing conditions

Dilute and nutrient-replete, non-axenic monocultures of *Isochrysis sp.* and *Phaeocystis sp.* macroflagellates (Prymnesiophyceae), and *Skeletonema costatum* (Bacillariophyceae), were grown in f/2 medium at 10° C and 69 $\mu mol m^{-2} s^{-1}$ in a 12:12 light-dark cycle. At the start of the experiments, the cultures had been in the light for 6 hours.

Incubation of the phytoplankton samples

120 ml phytoplankton samples were incubated in flasks at 8 discrete photon flux densities (0, 11, 24, 54, 136, 281, 664 and 1530 $\mu mol m^{-2} s^{-1}$) at 12° C in a thermostated incubator. At each photon flux density 9 samples were incubated of which 8 samples were used for the carbon fixation measurements (Fig. 5.1). All samples were put in the incubator at $t = 0$. $NaH^{14}CO_3$ was added at $t = 0$ to sample 1. At $t = 0.5$ (hr) sample 1 was harvested and treated for the determination of the carbon incorporation in organic substances (see below). The carbon fixation

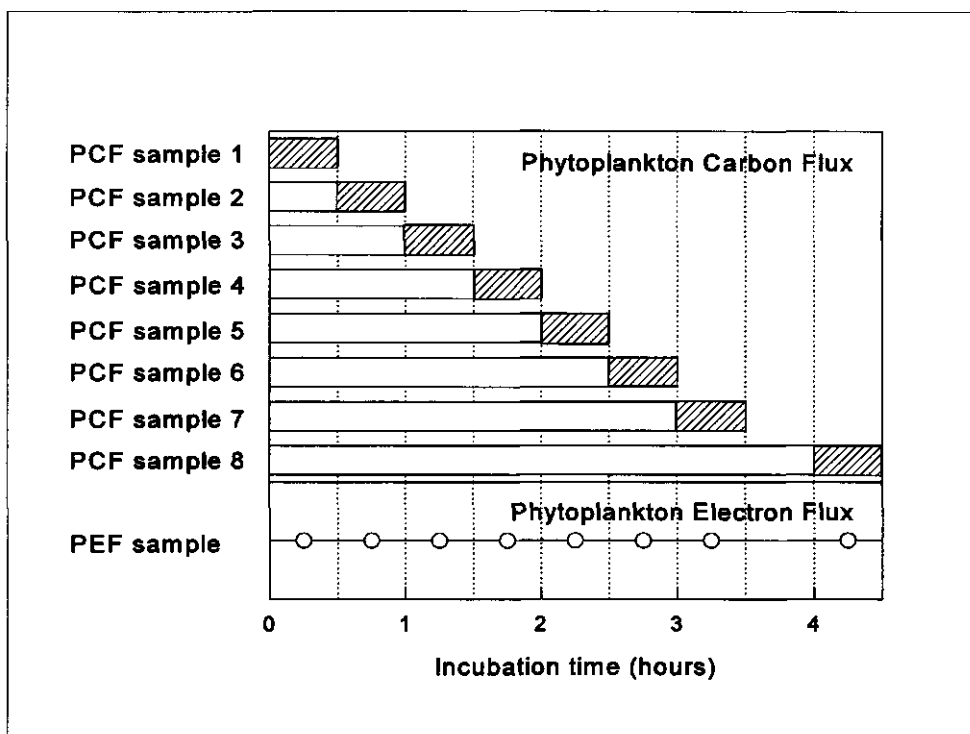


Figure 5.1. Incubation scheme of 9 samples for carbon fixation measurements and fluorescence measurements. For each photon flux density 8 samples for carbon fixation were put in the incubator at $t=0$. For PS II electron flow measurements 1 sample per photon flux density was put in the incubator. Carbon fixation was measured in the periods indicated with a grey box. PS II electron flow was determined at the times indicated with \circ . After subsampling 2 ml the flask with the sample for PS II electron flow measurements was put back in the incubator.

in sample 1 of each photon flux density was estimated during the period from $t = 0$ to $t = 0.5$. Also at $t = 0.5$ $\text{NaH}^{14}\text{CO}_3$ was added to sample 2. Sample 2 was subsequently harvested at $t = 1$ and treated as sample 1, etcetera. The shaded boxes in Figure 5.1 represent the period in which the incorporation of $\text{NaH}^{14}\text{CO}_3$ was occurring for all samples. For the fluorescence measurements only one flask per photon flux density (sample number 9) was used (Figure 5.1). On the indicated times 2 ml was taken out of the flask to measure the efficiency of PS II electron flow. The flask was put back into the incubator to continue the incubation. The sampling and measurement of the efficiency of PS II electron flow occurred in the middle of each carbon fixation period.

Carbon fixation

Phytoplankton samples were incubated at 8 photon flux densities as described before. The incubation with $\text{NaH}^{14}\text{CO}_3$ lasted 0.5 hours for each sample. After this period the sample was taken out of the incubator, inorganic carbon was removed by acidification and the carbon

incorporation in organic substances was measured (Escaravage et al 1996). The phytoplankton carbon flux, PCF, was calculated from the ^{14}C uptake in $\text{Bq m}^{-3} \text{ s}^{-1}$.

Fluorescence measurements

The Xe-PAM fluorometer was used as described in Chapters 3 and 4. Fluorescence parameters were determined as described in Chapter 3.

For the measurement of the efficiency of PS II electron flow in the light the phytoplankton samples were incubated as described before. The 2 ml samples were transferred rapidly from the incubator to the Xe-PAM cuvette, readapted to the incubation irradiance for another 30 seconds and $\Phi_{\text{PS II}}$ was measured.

The phytoplankton electron flux, PEF, was calculated as the product of the efficiency of PSII electron flow, Φ_{PSII} , the photon flux density, PFD, and the minimal fluorescence of the dark adapted sample, F_0 , determined at the beginning of the experiment (see also Chapter 4). In order to establish the extent of the photoinhibitory damage of the samples incubated in the light at $1530 \mu\text{mol m}^{-2} \text{ s}^{-1}$ these 2 ml samples were dark adapted for one hour at 18°C after the measurement. Then the maximal efficiency of PS II electron flow of these samples was measured and compared with the maximal efficiency measured before the light incubation.

Modelling

The PEF was fitted to the photosynthesis model of Eilers and Peeters (1988) yielding three fit parameters A_E , B_E and C_E . The PCF was fitted separately to the same model yielding the fit parameters A_C , B_C and C_C . The fitting procedure was performed in Mathcad 6.0+ (MathSoft, Cambridge, MA, USA) using a least squares method.

5.3 Results

In Figure 5.2 PEF and PCF, measured after various preincubation times, are shown for the 3 species. The differences in maximal PEF and PCF between these 3 species is dependent on the specific activity of the species and on the concentration of the algae in the sample. At low to intermediate photon flux densities (0 to about $200 \mu\text{mol m}^{-2} \text{ s}^{-1}$) PEF increases linear with the photon flux density in all 3 species. In the incubations from 0 to 0.5 hour and from 0.5 to 1 hour PEF is not saturated at the highest photon flux density in *Isochrysis*. In the longer incubations a saturation level is reached at about $300 \mu\text{mol m}^{-2} \text{ s}^{-1}$. In *Phaeocystis* the PEF reaches a saturation level at about $300 \mu\text{mol m}^{-2} \text{ s}^{-1}$ for all incubation periods. In *S. costatum* saturation of PEF does not occur in this range of photon flux densities. The PCF in these 3 species also shows a linear increase with the photon flux density at low photon flux densities. The PCF in *Isochrysis* saturates at about $650 \mu\text{mol m}^{-2} \text{ s}^{-1}$ in the short time incubations but after longer incubations saturation occurs already at $300 \mu\text{mol m}^{-2} \text{ s}^{-1}$ or less. In *Phaeocystis* saturation of PCF is around $300 \mu\text{mol m}^{-2} \text{ s}^{-1}$ independent of the incubation period. Saturation of PCF in *S. costatum* occurs at about $650 \mu\text{mol m}^{-2} \text{ s}^{-1}$ after short time incubations and between 300 and $650 \mu\text{mol m}^{-2} \text{ s}^{-1}$ after longer incubation periods. Both PEF and PCF are independent on the duration of the

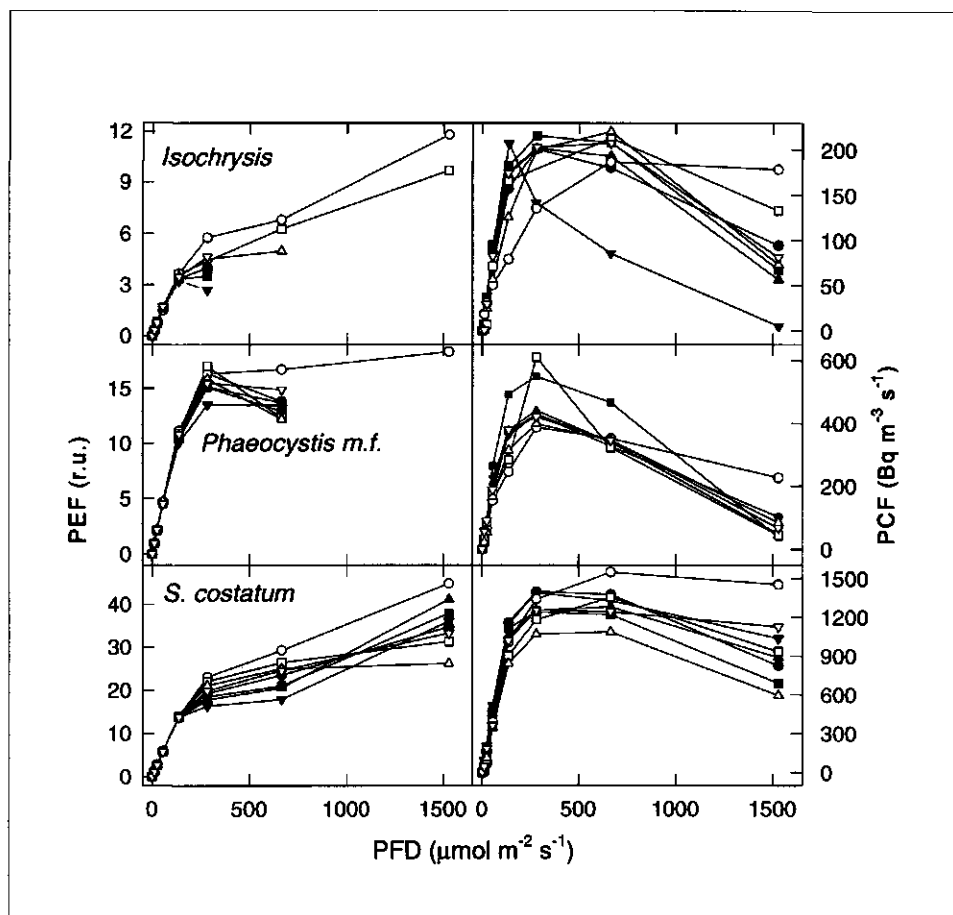


Figure 5.2. Phytoplankton electron flux (PEF, left panel) and phytoplankton carbon flux (PCF, right panel) as a function of the photon flux density. Incubation period from 0 to 30 min: ○; from 30 to 60 min: □; from 60 to 90 min: △; from 90 to 120 min: ▽; from 120 to 150 min: ●; from 150 to 180 min: ■; from 180 to 210 min: ▲; from 240 to 270 min: ▼. Some of the PEF data measured at the two highest irradiances in *Isochrysis* and *Phaeocystis* were discarded as they were not reliable due to the relatively low signal to noise ratio.

incubation, except for the incubation from 0 to 0.5 hr which shows higher values for PEF and PCF compared to the later experiments.

The data of Figure 5.2 suggest that the relation between the PCF and the PEF is complex for all 3 species. As at low to intermediate photon flux densities both PCF and PEF increase linearly with the photon flux density, the relation between PCF and PEF will be linear too. At high photon flux densities this linearity is lost.

In carbon fixation measurements a two hours incubation period is quite common for field

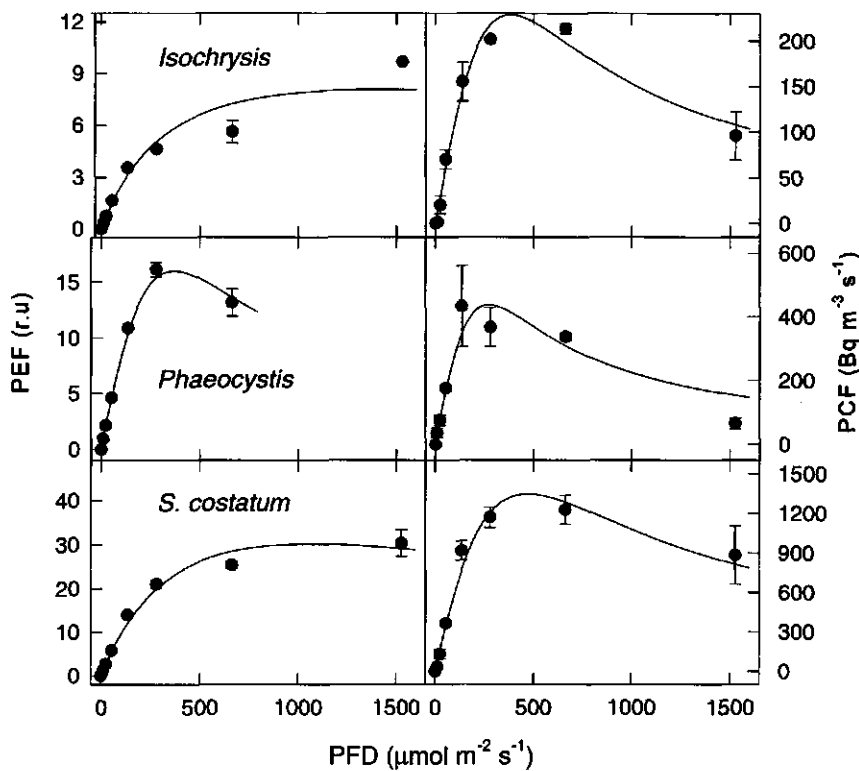


Figure 5.3. Phytoplankton electron flux (PEF, left panels) and phytoplankton carbon flux (PCF, right panels) as a function of the photon flux density. Each data point is the average of data from samples 2 to 4 (see Fig. 5.1) from the data points from 0.5 to 2 hours of incubation. The fit of these data points to the model of Eilers and Peeters (1988) is given by the solid line.

measurements (Escaravage et al 1996). In Figure 5.2 it can be seen, however, that the data from the first incubation period differ from the data of the other periods in almost each experiment. Therefore we choose to omit the data from the first incubation period and average PEF and PCF data from 0.5 to 2 hr incubation periods (Fig. 5.3). In most cases the fitted line is within the standard deviation of the data points. The PEF could be determined with a low standard deviation at low to medium photon flux densities, but the standard deviation increases somewhat at higher photon flux densities. In general the standard deviation in the PCF values is higher than in the PEF values. The fits of the model of Eilers and Peeters (1988) to the average PEF and PCF are shown by the solid line.

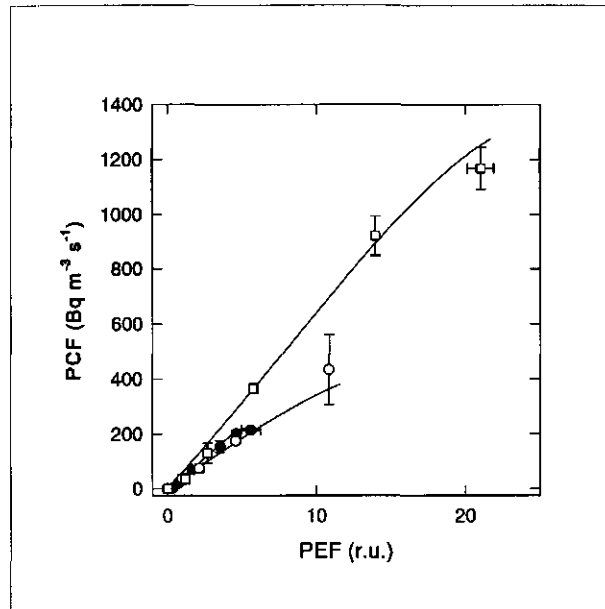


Figure 5.4. Phytoplankton carbon flux (PCF) as a function of phytoplankton electron flux (PEF). Data from Fig. 5.3. *Isochrysis*: ●; *Phaeocystis*: ○; *S. costatum*: □. The fit of the model of Eilers and Peeters (1988) to these data points is given by the solid line.

To compare the relation between PCF and the PEF of the 3 species we have plotted the linear range of PCF as a function of PEF of these 3 species in Figure 5.4. It should be noted that PCF and PEF are photosynthetic outputs per m^3 sample and therefore dependent on the amount of algae in the sample. The photon flux density range over which linearity was found (as was deduced from Fig. 5.3, not shown here) is different for all 3 species: *Isochrysis*: linear until about $650 \mu\text{mol m}^{-2} \text{s}^{-1}$; *S. Costatum*: linear until about $280 \mu\text{mol m}^{-2} \text{s}^{-1}$; *Phaeocystis*: linear until about $140 \mu\text{mol m}^{-2} \text{s}^{-1}$. At comparable PEF values the fit of the data of *S. Costatum* shows somewhat higher PCF values than the fits of the data of *Isochrysis* and *Phaeocystis*.

We were interested in the degree of photoinhibition occurring after incubating the phytoplankton samples at $1528 \mu\text{mol m}^{-2} \text{s}^{-1}$. Table 5.1 shows both $\Phi_{\text{PS II}}$, F_v/F_m and F_0 for each species as a function of the incubation period. Both in *Isochrysis* and in *Phaeocystis* the efficiency of PS II electron flow in the light decreased rapidly to undetectable values. The maximal efficiency of PS II electron flow, measured after one hour dark incubation, is lowered by the incubation but much higher than the efficiency of PS II in the light, indicating that there are still active PS II reaction centres in these samples. *S. costatum* also showed a low $\Phi_{\text{PS II}}$ in the light, but the effect on F_v/F_m was not as large as for the other 2 species. In *Isochrysis* the minimal fluorescence starts to decrease after 1 hour incubation at the highest photon flux density to a level of 55 % of the initial F_0 after 4 hours. In *Phaeocystis* the minimal fluorescence increases from $t = 0$ to $t = 1.5$

hours and decreases afterwards to 75 % of the initial F_0 . In *S. costatum* the minimal fluorescence does not change due to the incubation in the light. The variable fluorescence measured after dark adaptation after 4 hr incubation in the light corresponds to respectively 5, 11 and 30 percent of the variable fluorescence measured at $t = 0$ for *Isochrysis*, *Phaeocystis* and *S. costatum* respectively (data not shown).

5.4 Discussion

With the 3 algal species used here (*Isochrysis*, *Phaeocystis* and *S. Costatum*) we found a fairly linear relation between the PCF and the PEF at low to medium photon flux densities (Fig. 5.2 and 5.3). Deviation from linearity occurred at high photon flux densities. Application of the photosynthesis model of Eilers and Peeters (1988) gives a satisfactory fit of both PEF and PCF as a function of the photon flux density. The relation between PCF and PEF is linear until about $140 \mu\text{mol m}^{-2} \text{s}^{-1}$ in *Phaeocystis*, until about $280 \mu\text{mol m}^{-2} \text{s}^{-1}$ in *S. Costatum* and until about $650 \mu\text{mol m}^{-2} \text{s}^{-1}$ in *Isochrysis*. For *Phaeocystis* and *S. Costatum* these photon flux densities are more or less equivalent to the irradiance where carbon fixation starts to saturate (I_k). For *Isochrysis* this photon flux density is somewhat higher than I_k . This range corresponds reasonably with the range of the typical mean photon flux densities in a seawater column (Kirk 1994). The linear range between PCF and PEF extends to a photon flux density which is 2 to 10 times higher than the photon flux density at which the species were grown. This covers a larger range as what was found for the linear relation between oxygen evolution and PSII electron flow in Chapter 3 (2 to 5 times the growth irradiance) and is much larger than reported by Rees et al (1992) who found non-linearity between the efficiency of oxygen evolution and the efficiency of PS II electron flow even at growth irradiances.

The difference in PCF versus photon flux density and PEF versus photon flux density results in a non-linearity between PCF and PEF. The non-linearity might be caused by several factors. Previous experiments with marine algae (Chapter 3) have shown that the non-linearity is not caused by photorespiration. Therefore we do not expect that in these experiments photorespiration is interfering either. Alternatively an increased activity of the Mehler-reaction at high photon flux densities might lead to a decrease in carbon fixation as less NADPH is formed, leading to a non-linearity in the relationship between carbon fixation and PSII electron flow. Results from Kana with plankton from estuarine surfaces waters and in cyanobacteria confirm the possibility of an increased Mehler-reaction at high irradiances (Kana 1990, 1992, 1993). Weger et al. (1989) found a higher mitochondrial respiration in the light than in the dark. This phenomenon is also suggested by the results of Beardal et al (1994) who found an increased oxygen consumption directly after a light incubation. When carbon fixation measurements give net photosynthesis data (Williams et al 1996) the non-linearity between PEF and PCF in our experiments might be caused by an increased mitochondrial respiration at high photon flux densities. On the other hand in experiments of Xue et al (1996) the increase in oxygen consumption in the light compared to the dark was accompanied by a decrease in carbon dioxide release. According to these results we should not necessarily expect the same relation for carbon

dioxide fixation as for oxygen evolution. We are not able to compare the PEF values of the oxygen evolution measurements as shown in Chapter 4 with the carbon fixation measurements of this Chapter as the fluorescence measurements were not done under the same conditions.

Table 5.1. Actual and maximal PS II efficiency ($\Phi_{PS II}$ and F_v/F_m respectively) after varying incubation periods at $1528 \mu\text{mol m}^{-2} \text{s}^{-1}$. F_v/F_m was measured after 1 hour dark adaptation at 18°C . n.d stands for not detectable which means that $\Phi_{PS II}$ was lower than 0.1. F_0 is given as % of the F_0 level at $t = 0$.

Time (min)	<i>Isochrysis</i>			<i>Phaeocystis</i>			<i>S. costatum</i>		
	$\Phi_{PS II}$	F_v/F_m	F_0	$\Phi_{PS II}$	F_v/F_m	F_0	$\Phi_{PS II}$	F_v/F_m	F_0
0	-	0.694	100	-	0.651	100	-	0.690	100
10	0.180	0.683	107	n.d.	0.440	108	0.178	-	-
30	0.148	0.434	107	n.d.	0.324	120	0.124	0.449	103
60	n.d.	0.345	105	n.d.	0.296	125	0.104	0.412	94
90	n.d.	0.570	91	n.d.	0.284	115	0.132	0.402	104
120	n.d.	0.283	66	n.d.	0.267	99	0.138	0.416	110
150	n.d.	0.138	68	n.d.	0.291	92	0.150	0.434	98
180	n.d.	0.135	76	n.d.	0.256	91	0.163	0.467	106
240	n.d.	0.144	55	n.d.	0.219	75	0.143	0.397	102

Another cause of the non-linearity at high photon flux densities might be a shift in the metabolic pathways from carbon fixation to more nitrogen reduction (Huppe and Turpin 1994). Nitrate reduction was found to increase with increasing photon flux densities (Weger and Turpin 1989), though it is not clear whether the increase in nitrate reduction is comparable to, or larger or smaller than the increase in carbon fixation with increasing photon flux densities. The nitrogen source (ammonium or nitrate) was found to have a large effect on the amount of fixed carbon (Williams et al 1979).

All 3 species suffered from a high amount of photoinhibition when incubated at the highest photon flux density as can be concluded from the decrease in the maximal efficiency of PS II electron flow (Table 5.1). After 4 hr of incubation F_v/F_m is 0.144, 0.219 and 0.397 in respectively *Isochrysis*, *Phaeocystis* and *S. costatum*. In *Isochrysis* the F_0 has decreased to 55 % of the initial level after 4 hr of incubation. In *Phaeocystis* the minimal fluorescence increases during the first 1.5 hr and decreases somewhat afterwards. In *S. costatum* the decrease in F_v/F_m is caused by a decrease in the maximal fluorescence. Schansker (1996) found a maximal efficiency of PS II electron flow measured with fluorescence of 0.44 in samples where oxygen evolution was inhibited completely. The variable fluorescence of these samples was equal to about 12% of the variable

fluorescence in control leaves. He attributed this variable fluorescence to PS II reaction centres with an inactive oxygen evolution system according to the results of Giersch and Krause (1991) and of Van Wijk and Krause (1991). In our experiments with *Isochrysis*, *Phaeocystis* and *S. costatum* the variable fluorescence after four hours of photoinhibition corresponds to 5, 11 and 30 % respectively of the initial variable fluorescence. According to the interpretation of Schansker (1996) the number of reaction centres, which are inactive in oxygen evolution, is not larger than respectively 5, 11 and 30 %. However, as the PCF data have not decreased markedly during 4 hours of photoinhibition, we suggest that there are no reaction centres inactive in carbon fixation at all in these algal species. This is a striking difference with pea leaves, spinach thylakoids and *Valerianella locusta* protoplasts examined by Schansker (1996), Krause et al (1990) and Van Wijk and Krause (1991) respectively.

In Chapter 3 we compared electron flow calculated as the product of Φ_{PSII} and the irradiance with oxygen evolution calculated on a chlorophyll *a* basis. In this case chlorophyll *a* is the major photosynthetic pigment. This oxygen evolution rates can be used as a measure for electron flow per 'photosynthetic unit'. However, most algal species contain more photosynthetic pigments and the ratio of chlorophyll to the other photosynthetic pigments is variable (Falkowski and Kiefer 1985, Kirk 1994). Therefore we have suggested that chlorophyll *a* is not a unique measure of a 'photosynthetic unit'. This comparison in fact resulted in different slopes of the relation between oxygen evolution and PSII electron flow for the different species we examined. In Chapter 4 we proposed that the PEF can be estimated from the minimal fluorescence, the efficiency of PS II electron flow and the photon flux density. Indeed we found a similar relation between the PEF and the phytoplankton oxygen flux (POF) for *D. tertiolecta* and *P. tricornutum*. In this Chapter we applied this method to the comparison of PEF and PCF with 3 different algal species. All 3 algal species show more or less the same relation for PCF as a function of PEF (Fig. 5.4) but some variation in this relationship is left. This variation in the relation between PCF and PEF is somewhat smaller than the variation found in the ratio of carbon fixation and PSII electron flow in the data of Falkowski and Kolber (1990) and Kolber and Falkowski (1993) who used the pump and probe method to calculate PS II electron flow.

We used the minimal fluorescence at the beginning of the experiment to calculate the PEF during the complete experiment. However, as the experiment lasted 4 hours, the minimal fluorescence might have changed during the experiment, due to growth or photoinhibition (at the high photon flux densities). For the incubations at the highest photon flux density F_0 has been determined (Table 5.1). For *Isochrysis* and *Phaeocystis* a decrease of the minimal fluorescence was found of 55 and 75 % respectively after 4 hr of incubation. However, Φ_{PSII} was not detectably for these data points and we can not calculate the effect of the decrease of F_0 on the PEF. In *S. costatum* the minimal fluorescence did not decrease compared to the value at $t = 0$. Therefore the PEF in *S. costatum* calculated for the highest photon flux density is not changed by photoinhibition or growth. The effects of growth and photoinhibition on the minimal fluorescence should also be reflected in the PCF data. However, as already concluded before, the variation in the PCF data could not be assigned to the length of the total incubation time. Therefore we suggest that there is no effect of growth or photoinhibition on the PEF data in this experiment.

The use of the minimal fluorescence as a measure for the product of the number of PS II

reaction centre and the absorption cross-section suffers from one limitation: the minimal fluorescence measured in the dark does not account for light induced changes in the absorption cross-section. These light induced changes in the absorption cross-section are important in cyanobacteria (Williams and Allen 1987, Geel et al 1994) but much less is known about the occurrence in the eukaryotic algae.

5.5 Conclusions

The relation between carbon fixation and PSII electron flow is shown to be almost linear at low and medium photon flux densities in several marine algae. At high photon flux densities the relationship is non-linear. The minimal fluorescence seems to be a reasonable tool in estimating the product of the number of PS II reaction centres and the absorption cross-section which is necessary to calculate the PEF. When electron sinks other than carbon fixation (for example nitrate reduction) are involved this will influence the relation between PEF and PCF. The variation in the relation between PCF and PEF is somewhat smaller than the variation found in the ratio of carbon fixation and PSII electron flow in the data of Falkowski and Kolber (1990) and Kolber and Falkowski (1993) who used the pump and probe method to calculate PS II electron flow.

6 ESTIMATION OF PHOTOSYNTHETIC PERFORMANCE OF MARINE PHYTOPLANKTON IN A MODEL ECOSYSTEM BY MEANS OF CHLOROPHYLL FLUORESCENCE

6.1 Introduction

In marine ecosystems solar energy is photosynthetically converted into chemical energy by its phytoplankton. This chemical energy in the form of organic matter is the basis of the food web and the rest of the community is using the energy by respiration. The ratio of photosynthesis and respiration (P/R-ratio) is an important parameter. In many aquatic ecosystems this P/R-ratio can be calculated by measuring oxygen production as well as oxygen consumption. In the marine environment, with its low chlorophyll content, however, these measurements are not feasible as the sensitivity of the oxygen measuring method is too low to detect the small changes in oxygen concentration. Measurement of photosynthetic carbon fixation by ^{14}C incorporation and respiration by ^{14}C release is a more sensitive method, but can only be applied in bottle enclosures in the natural environment or in an incubator simulating this environment. In recent years chlorophyll fluorescence has emerged as a method to estimate phytoplankton photosynthesis. Photosynthetic electron flow, which is the basis for carbon fixation and oxygen production, can be determined measuring the efficiency of PSII electron transport, Φ_{PSII} , and the absorption cross-section, σ_{PSII} , by means of fluorescence using the pump and probe method (Falkowski and Kiefer, 1985). The rate of PSII electron flow is then calculated as the product of Φ_{PSII} , σ_{PSII} , and the ambient photon flux density, PFD. Falkowski and Kolber (1990) found a good correlation between the rate of PSII electron flow and carbon fixation in marine phytoplankton.

Schreiber et al (1986) introduced the saturating pulse method to measure the efficiency of PSII electron flow. The saturating pulse method normally uses a multiple-turnover saturating flash, which reduces the plastoquinone pool. In the pump and probe method a short saturating flash is used which leads a single turnover in the PSII reaction centre resulting in the temporary reduction of Q_A . Due to fluorescence quenching by the oxidized plastoquinone pool, the maximal fluorescence level measured with the pump and probe method will be lower than the level measured with the saturating pulse method (Schreiber et al 1995b). Therefore the efficiency of PSII calculated from the pump and probe data will generally be lower than the efficiency of PSII measured with the saturating pulse method.

In higher plants and green algae the relationship between the efficiency of PSII electron flow, determined by the saturating pulse method, and the efficiency of carbon fixation or oxygen evolution has been examined under a variety of conditions. In general a linear relationship was found although the relationship is influenced by processes like photorespiration (Genty et al 1992), Mehler reaction (Öquist and Chow 1992), cyclic electron flow around PSII (Falkowski et al 1986, Rees et al 1992) and by the presence of inactive PSII centres (Hormann et al 1994). For a more precise description of recent results see Chapter 3.

Under several growing and preillumination conditions Heinze et al (1996) found a linear

relation between the efficiency of PSII electron flow and the efficiency of oxygen production in the green alga *Scenedesmus obliquus*. In a number of marine algae we found a linear relation between PSII electron flow determined with the saturating pulse method and oxygen evolution at low to intermediate irradiances (Chapter 3). At higher irradiances they found electron flow which is not connected with parallel oxygen evolution.

In addition to its use to determine the phytoplankton photosynthetic activity fluorescence is also used to estimate phytoplankton biomass which is usually approximated by the total amount of chlorophyll *a* (Heany 1978, Butterwick et al 1982, Falkowski and Kiefer 1985). The relation between fluorescence and the chlorophyll *a* concentration, however, is dependent on the species composition, the growing conditions of the sample and the photosynthetic processes. The minimal fluorescence measured in the dark, F_0 , is not dependent on photosynthetic processes and therefore will give the best possible correlation with chlorophyll *a* concentration.

Here we present a method based on *in situ* chlorophyll fluorescence measurements to estimate primary production in a model ecosystem. We have measured PSII electron flow by means of fluorescence, carbon fixation and oxygen evolution in an artificial ecosystem in a mesocosm container and examined their relationships. Due to the relatively high phytoplankton concentration in the mesocosm the oxygen determination was sensitive enough to calculate the daily oxygen production. The irradiance dependency of carbon fixation was measured. We also measured the irradiance dependency of PSII electron flow, J_E , determined as the product of the efficiency of PSII electron flow and the photon flux density, $J_E = \phi_{PSII} \cdot PFD$, in the mesocosm and in the laboratory. Phytoplankton electron flux, PEF, was estimated by the product of J_E and the minimal fluorescence which was measured in the mesocosm. The minimal fluorescence was used as a measure of both biomass and PSII absorption cross section. Photosynthesis versus irradiance curves of PSII electron flow and carbon fixation were fitted to the model of Eilers and Peeters (1988) resulting in 3 parameters A, B and C. These parameters were used to integrate the primary production over the water column and over the day.

Daily primary production calculated from PSII electron flow showed reasonable correlation with carbon fixation. The correlation with oxygen evolution is highest in the peak of the algal blooms. *In situ* measurements done in the mesocosm container result in the same primary production as the laboratory measurements for PSII electron flow.

6.2 Materials and methods

Mesocosm

The experiments were carried out from May 19 to June 13 1994 in a mesocosm consisting of a 3000 l black polyethylene tank (height 3 m, ϕ 1.2 m) (Fig. 6.1). At the bottom a sediment container of 150 l was placed. The water was mixed with a rotating mixer (mixing time *ca* 10 min). The container was covered with a diffusor screen leading to a more homogeneous light gradient in the water column, with an intensity at the surface of 74 % of the available sunlight and an increased apparent light attenuation. The mixing and the light conditions in the mesocosm reproduced the conditions of a 10 m water column in the Dutch coastal waters (Peeters et al

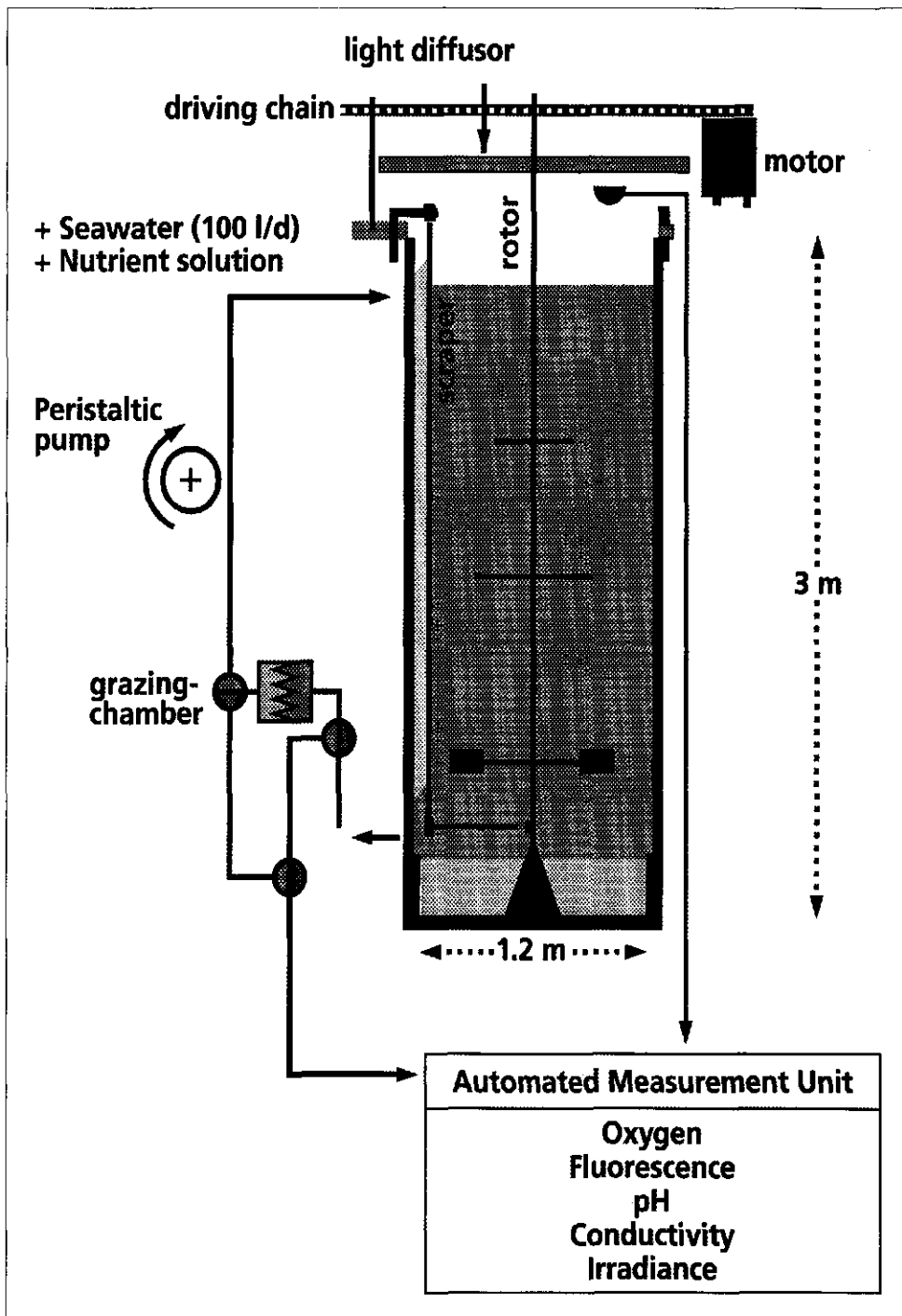


Figure 6.1. Schematic view of the mesocosm container

1993). On the first day of the experiment the container was filled with seawater. Subsequently the container was continuously refreshed with seawater at a flushing rate of 100 l day^{-1} , resulting in a dilution rate of 0.033 day^{-1} . Inorganic nutrients were added continuously from stock solutions to the container: $7.68 \text{ mmol day}^{-1}$ dissolved inorganic nitrogen (NO_3^-), $0.63 \text{ mmol day}^{-1}$ dissolved inorganic phosphate and $4.71 \text{ mmol day}^{-1}$ silicate. The water from the container was flowed through a benthos chamber at a rate of 100 l day^{-1} , where the algae were grazed by 16 mussels. Fluorescence, oxygen, temperature, conductivity, and pH were continuously monitored via a bypass. The container was cooled by spraying seawater on the outer wall of the tank. For a more precise description see Escaravage et al (1996).

Irradiance

Photon flux density (PFD) was measured continuously with a Kipp and Zonen Solar integrator in combination with a light sensor and averaged per hour. Light attenuation in the water column was measured 3 times a week with a LiCor datalogger LI-1000 connected with a LiCor SPA-QUANTUM spherical sensor. The apparent attenuation coefficient (K_d in m^{-1}) was calculated from $\ln(I_z/I_0) = -K_d \cdot z$ using linear regression. I_0 is the daily irradiance at the surface and I_z is the incident irradiance at z meters.

Chlorophyll

Chlorophyll *a* (in mg m^{-3}) was analysed three times a week by reversed phase HPLC method (Escaravage et al 1996) after extraction according to Gieskes and Kraay (1984). The continuously measured fluorescence data which were measured in the bypass of the mesocosm container were scaled with the estimated chlorophyll *a* concentration (chl). On the intermediate days chlorophyll *a* was calculated from the fluorescence data and the calibration to chlorophyll *a*.

Carbon fixation

The irradiance dependence of the phytoplankton carbon flux, PCF, in $\mu\text{mol m}^{-3} \text{ s}^{-1}$, was measured (by ^{14}C -incubations) twice a week. Samples of the mesocosm were taken at 7 a.m. and the incubation for carbon fixation started at 8 a.m.. The samples were incubated for 2 hours with $185 \text{ kBq } ^{14}\text{C}$ -bicarbonate in 120 ml at 8 discrete PFD values in the range from 0 - $1628 \mu\text{mol m}^{-2} \text{ s}^{-1}$ in a thermostated incubator. The temperature was adapted to the mesocosm temperature. After incubation the reaction was stopped by addition of lugol. Carbon incorporation in organic substances was measured after inorganic carbon was removed by acidification (Escaravage et al 1996). The normalized rate of carbon fixation, I_c , was calculated as PCF/chl .

Oxygen production

The oxygen level of the mesocosm water and of the water that leaving the benthos chamber was measured automatically at regular intervals. The increase in oxygen measured in the mesocosm from sunrise until sunset is called the net system daily (oxygen) production NSDP. It is determined by photosynthesis and respiration from phytoplankton and heterotrophic organisms in the mesocosm, mussel respiration in the benthos chamber and diffusion of oxygen from and to the atmosphere. The decrease in oxygen from sunset until sunrise is called the

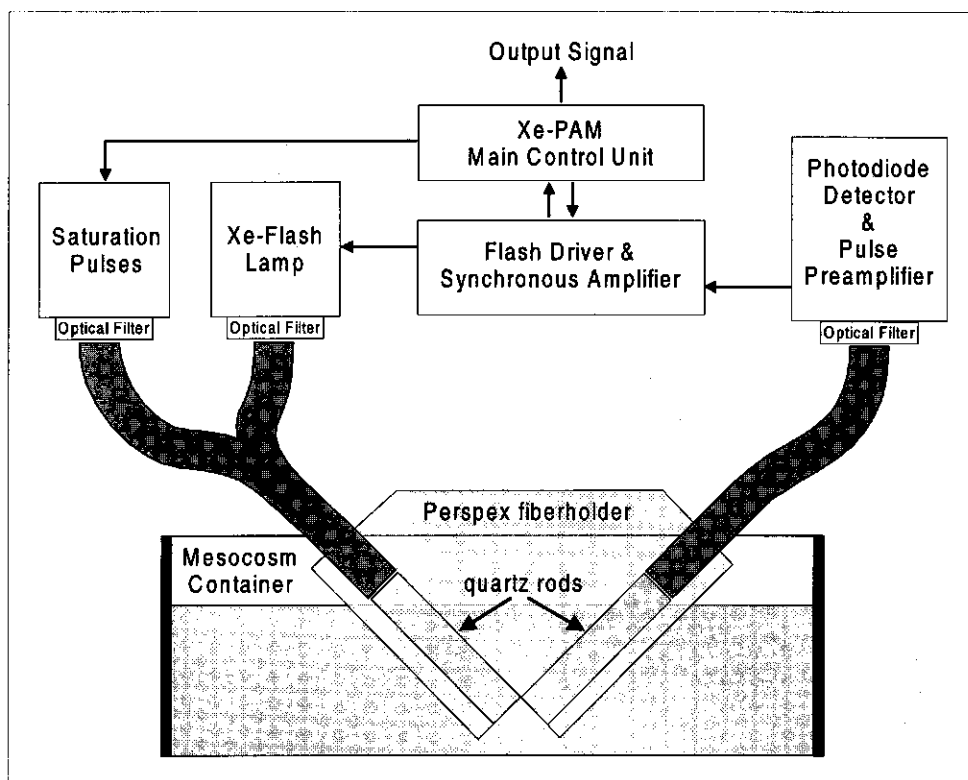


Figure 6.2. The measuring scheme and set-up of the Xe-PAM fluorometer.

system night respiration. It is determined by the respiration of all organisms and diffusion from and to the atmosphere. Assuming that respiration during the night is equal to respiration during the day the system day respiration (SDR) is calculated. Daily primary oxygen production (PPO) is calculated as NSDP + SDR + diffused oxygen (Prins et al 1995).

Fluorescence

Fluorescence measurements were done with a Xe-PAM fluorometer. The Xe-PAM fluorometer (Walz, Effeltrich) uses excitation pulses to discriminate the fluorescence generated by the measuring light from the fluorescence generated by the background light (Schreiber et al 1993). A Xenon-flash lamp, filtered through a blue green filter (6 mm BG39) was used for excitation, and a photodiode detector placed behind two long-pass filters (dichroic filter R65, Balzers and RG645, Schott) was used for detection. Saturating light pulses of 1 second duration and a photon flux density of $\pm 6000 \mu\text{mol m}^{-2} \text{s}^{-1}$ PAR were given with a halogen lamp. The saturating light pulses were filtered through a 650 nm short-pass filter (Balzers DT Cyan special). The measurements were carried out at a modulation frequency of 16 Hz. The Xe-PAM fluorometer was used in combination with a PC equipped with a data logger (Keithley model 576). A dedicated program PPMON (Phytoplankton Photosynthesis MONitor, Lovoan Software and

Education, Wageningen, The Netherlands) controlled the operation of the data logger and the analysis of the output-data. Fluorescence nomenclature was according to Van Kooten and Snel (1990). The efficiency of PSII electron flow was determined as $(F_M' - F)/F_M'$.

For the comparison of fluorescence data obtained in laboratory experiments with data obtained *in situ*, mesocosm samples were incubated in the laboratory under the same conditions as for carbon fixation. The efficiency of PSII electron flow was measured in subsamples of 1 ml in the Xe-PAM cuvette after 10 minutes, 1 hour and 2 hours incubation (on day 11 and 29). The efficiency of PSII electron flow after 1 and 2 hours was almost the same as after 10 minutes. On day 18 and 24 the efficiency of PSII electron flow was measured after 10 minutes incubation in the cuvette, at the same 8 irradiances. PSII electron flow, J_E^L , was estimated as the product of Φ_{PSII} and the imposed PFD. Phytoplankton electron flux, PEF^L , was estimated by the product of Φ_{PSII} , PFD and F_0 (see Chapter 4).

In the mesocosm container the fluorescence measurements were done 2 cm below the water surface. Fibre optics and quartz rods were used to conduct the light from the Xe-PAM fluorometer to the water sample in the container and back (Fig. 6.2). The perspex fibre holder was situated on the north side of the container to minimize light attenuation. Simultaneous measurements of the efficiency of PSII electron flow and photon flux density were performed every 30 minutes in the mesocosm under the prevailing light conditions. The photon flux density was measured above the water surface under the diffusor screen with a modified Hansatech fluorescence detector probe (FDP/2) equipped a neutral density filter and a PAR filter (transmission from 400 to 700 nm). The output was amplified by a fluorescence detector control box (FDC) and digitized by the data logger. The photodiode data were calibrated using the global irradiance data. The minimal fluorescence, F_0 was determined by averaging measurements from 0 a.m. to 4 a.m. PSII electron flow, J_E^M , was estimated as the product of Φ_{PSII} and the ambient PFD at the time of the measurement. Phytoplankton electron flux, PEF^M , was estimated by the product of Φ_{PSII} , PFD and F_0 (see Chapter 4).

Modelling

The photosynthesis model of Eilers and Peeters (1988) describes the photosynthesis process with photosynthetic factories which can exist in an open, a closed or an inhibited state. This model results in a steady state solution for the rate of photosynthetic production (P):

$$P = \frac{I}{(AI^2 + BI + C)} \quad (6.1)$$

where I is the photon flux density and A , B and C are constants.

Parameters characteristic for the photosynthesis irradiance curve can be derived from A , B and C : the initial slope $\alpha = C^L$; the maximum production $P_m = (B + 2(AC)^{1/2})^{-1}$; the irradiance at which α and P_m intersect $I_k = C/(B + 2(AC)^{1/2})$.

For a derivation and explanation of this formula see Eilers and Peeters (1988) and Chapter 3. The fitting procedure was performed in MathCad 5.0+ (MathSoft, Cambridge, Massachusetts, USA) using a least squares method.

Fitting the carbon fixation, $J_{c,n}$ (the carbon fixation per mg chlorophyll for each day n on which

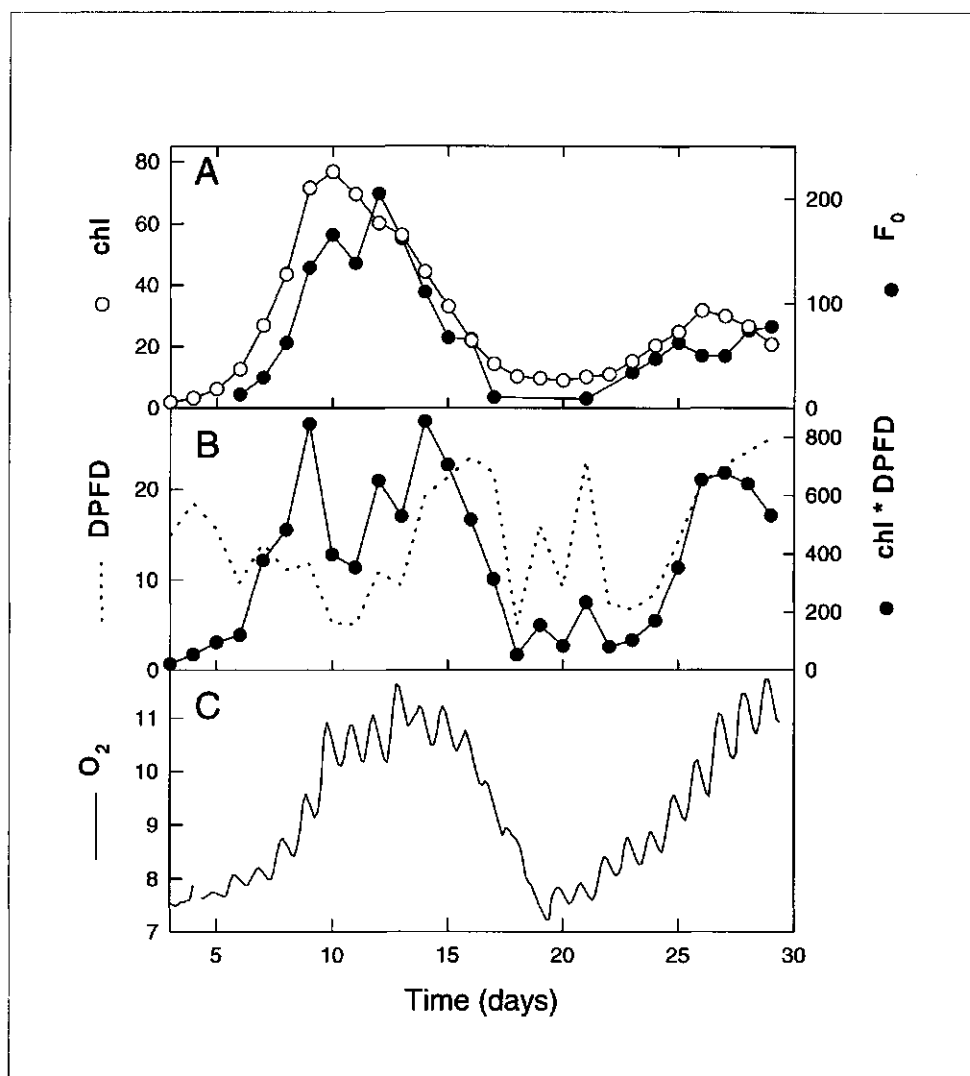


Figure 6.3. A: chlorophyll (mg m^{-3}): ○; the minimal fluorescence (r.u.): ●; B: daily photon flux density ($\text{mol m}^{-2} \text{d}^{-1}$): ----; the product of chlorophyll content and irradiance: ●; C: oxygen concentration (mg l^{-1}): solid line.

carbon fixation was measured), to Eqn. 1 led to the optimized model parameters $A_{C,n}$, $B_{C,n}$ and $C_{C,n}$. For each hour carbon fixation in the water column was estimated by combining the hourly averaged photon flux density at the surface, the light attenuation in the water column, K_d , and chl with the model parameters $A_{C,n}$, $B_{C,n}$ and $C_{C,n}$, as described in Eilers and Peeters (1988). Daily primary production in carbon fixation, PPC, was estimated by summation of the carbon fixation data of each hour of the day. As ^{14}C -incubations were carried out only twice a week on

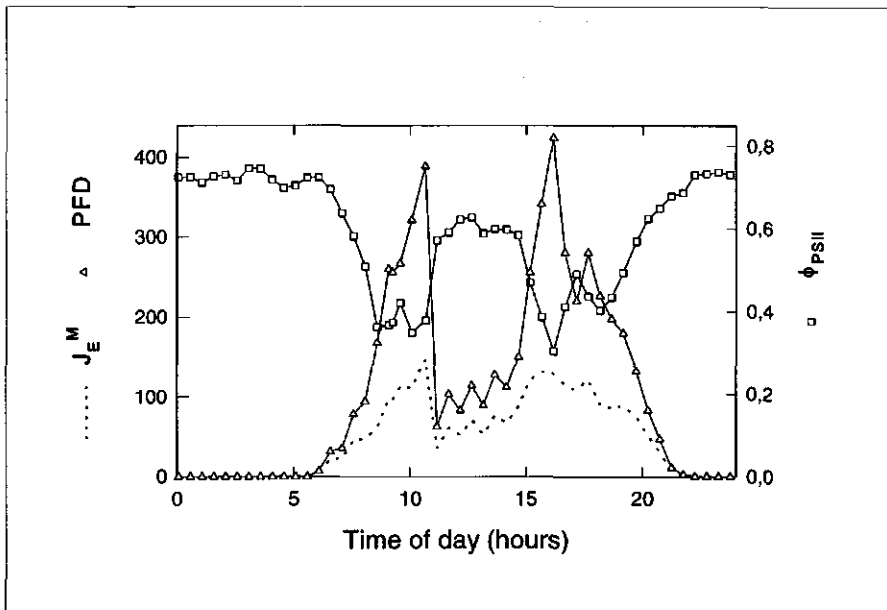


Figure 6.4. Example of one day of measurements in the mesocosm: the efficiency of PSII electron flow: \square ; the photon flux density ($\mu\text{mol m}^{-2} \text{s}^{-1}$): Δ ; the estimated rate of PSII electron flow: —, data of day 13.

intermediate days the fit parameters A, B and C of the nearest day were taken for calculation of the daily primary production.

PS II electron flow data from the mesocosm, J_E^M , and the PS II electron flow data from the laboratory, J_E^L , were also fitted to Eqn. 1 leading to model parameters $A_{E,n}^M$, $B_{E,n}^M$ and $C_{E,n}^M$ and $A_{E,n}^L$, $B_{E,n}^L$ and $C_{E,n}^L$ respectively. For each hour PSII electron transport in the water column was estimated by combining the hourly averaged photon flux density at the surface, the light attenuation in the water column, K_d and F_0 values with the model parameters. Daily primary production in PSII electron flow, PPE^M and PPE^L respectively, was estimated by summation of the PSII electron flow data of each hour of the day. As PSII electron flow laboratory measurements were not carried out every day on intermediate days the fit parameters A, B and C of the nearest day were taken for calculation of the daily primary production.

6.3 Results

Figure 6.3 illustrates the results of the experiment. The chlorophyll *a* concentration, chl, displays a pattern associated with two algal blooms. The first maximum occurred around day 10 and the second maximum around day 26 (Fig. 6.3A). Both blooms mainly consisted of diatoms: *Nitzschia delicatissima* and *Chaetoceros sp.* in the first bloom; *Rhizosolenia sp.*, *Eucampia zoodiacus*, *Nitzschia seratia* and the flagellate *Phaeocystis sp.* in the second bloom. The minimal

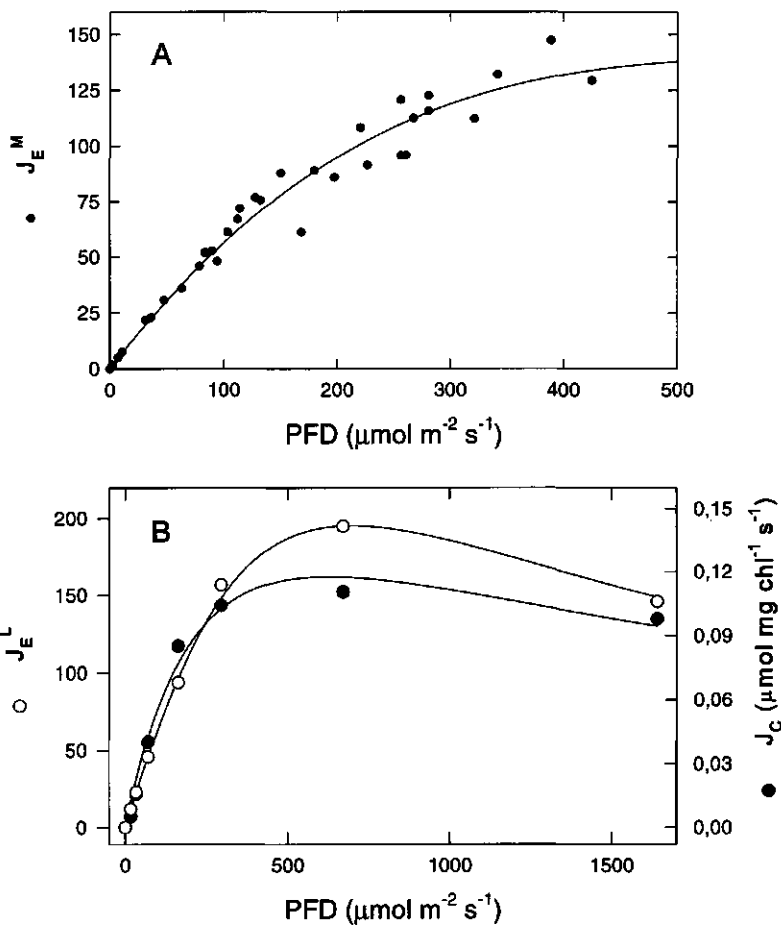


Figure 6.5. A: The estimated rate of PSII electron flow as a function of the irradiance, data of Figure 6.4. The solid line represents the fits according to the model of Eilers and Peeters (1988) ($A_{E,13}^M = 4.3 \cdot 10^{-6}$, $B_{E,13}^M = 2.0 \cdot 10^{-3}$, $C_{E,13}^M = 1.53$). B: the estimated rate of PSII electron flow (\circ) and the rate of carbon fixation, J_C (\bullet) ($\mu\text{mol mg chl}^{-1} \text{s}^{-1}$) as a function of the irradiance, determined in the laboratory, data from day 11 ($A_{E,11}^L = 2.96 \cdot 10^{-5}$, $B_{E,11}^L = 9.98 \cdot 10^{-4}$, $C_{E,11}^L = 1.44$, $A_{C,11} = 3.34 \cdot 10^{-3}$, $B_{C,11} = 4.33$, $C_{C,11} = 1304$).

fluorescence, F_0 , displays a similar pattern as the chlorophyll a concentration. The proportionality between F_0 and chl indicates that, under our conditions, F_0 is a reasonable measure for the chlorophyll content.

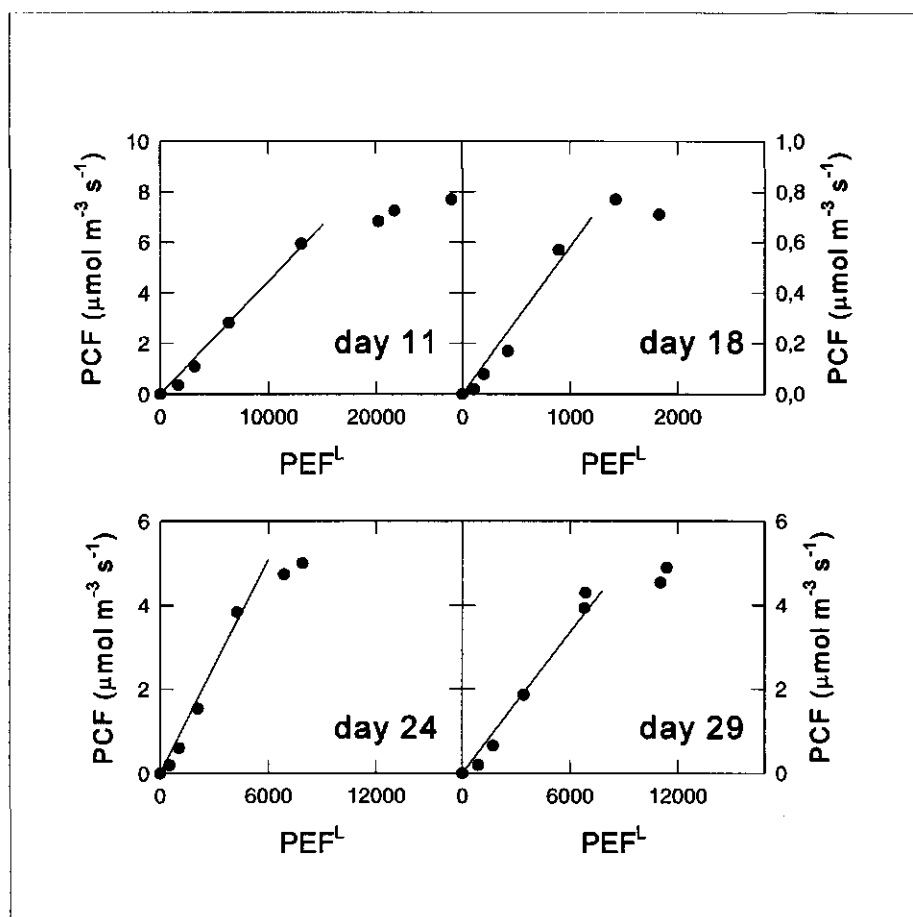


Figure 6.6. Phytoplankton carbon flux, PCF, ($\mu\text{mol m}^{-3} \text{s}^{-1}$) as a function of the phytoplankton electron flux (PEF^L) (both measured in the laboratory), data of resp day 11, 18, 24 and 29. The solid lines, D, represent the initial slopes determined from the first 5 Data points in each graph. Value of D: day 11: $4.5 \cdot 10^{-4}$; day 18: $5.8 \cdot 10^{-4}$; day 24: $8.5 \cdot 10^{-4}$; day 29: $5.6 \cdot 10^{-4}$.

Figure 6.3B shows the daily photon flux density, DPF_D, and the "primary production" approximated here (but see later) as the product of chlorophyll concentration and photon flux density. This primary production shows relation with the two algal blooms which were found in the chlorophyll and fluorescence data (Fig. 6.3A)

Figure 6.3C shows the changes in the oxygen concentration of the mesocosm. The oxygen concentration increases during both algal blooms. The increase is about the same for both blooms.

Figure 6.4 shows the time course of the photon flux density and the efficiency of PSII electron flow measured just below the water surface in the mesocosm at day 13. During the two periods of high irradiance the efficiency of PSII electron flow dropped below 0.4. The variation in the Φ_{PSII}

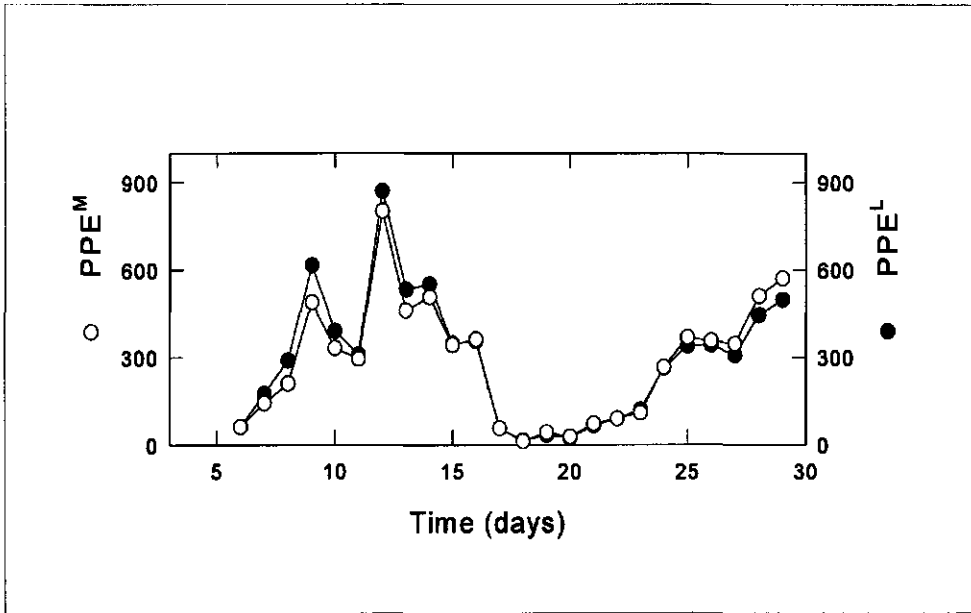


Figure 6.7. Primary production in the mesocosm integrated over depth and time calculated from electron flow data: using the fits of the mesocosm (○) and laboratory (●).

values measured during the night give an idea on the accuracy (approximately 5 %) of the applied method. The rate of PSII electron flow in the upper water layer was calculated ($J_E^M = \text{PFD} * \Phi_{\text{PSII}}$) and shows that in the high irradiance periods PSII electron flow is somewhat higher but disproportional with that in the low irradiance periods.

From the PFD and J_E^M time series the light dependence of PSII electron flow was modelled (figure 6.5A) to estimate the parameters $A_{E,13}^M$, $B_{E,13}^M$ and $C_{E,13}^M$ using the Eilers and Peeters photosynthesis model. Figure 6.5A shows that the data are satisfactorily described by the model although each data point represents another time of the day. Therefore changes in the light dependence of photosynthesis due to light adaptation did not occur on a timescale of 15 hour.

An example of the light response of carbon fixation, J_C , and PSII electron flow as measured in the laboratory, J_E^L , is shown in Figure 6.5A (data of day 11). The carbon fixation data and the PSII electron flow data were fitted separately yielding $A_{C,11}$, $B_{C,11}$, $C_{C,11}$ for carbon fixation and $A_{E,11}^L$, $B_{E,11}^L$, $C_{E,11}^L$ for PSII electron flow on day 11.

The distribution of data points around the fit as shown in Figure 6.5A and in Figure 6.5B is representative for the mesocosm experiment. The irradiance range in the mesocosm experiments is smaller than in the laboratory experiments. On some days this irradiance range covers only the irradiance dependent part of the photosynthesis irradiance curve. The determination of C which describes the initial slope, $C = \alpha^{-1}$ is not disturbed. However, mistakes might be made in the determination of A and B values, which are necessary for a correct determination of I_k and P_m . The irradiance dependency for the irradiance which is experienced on that day can be described anyhow with the model. Therefore also the daily primary production can be calculated. In the

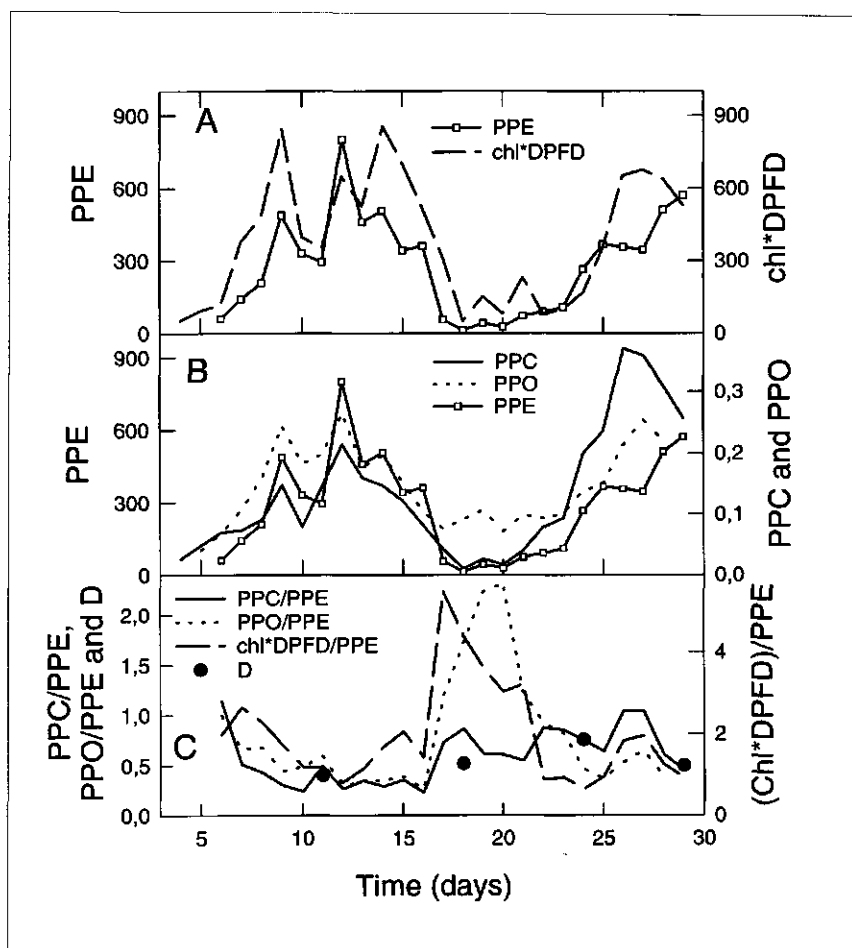


Figure 6.8. A: primary production in the mesocosm calculated from electron flow data, using the fits of the mesocosm (PPE^M): \square —; primary production estimated as the product of chl and PFD: \cdots . B: PPE^M as in Figure 6.8A: \square —; primary production in carbon fixed, PPC, ($\text{mol m}^{-2} \text{d}^{-1}$): —; primary oxygen production in the mesocosm, PPO, ($\text{mol m}^{-2} \text{d}^{-1}$): \cdots . C: $PPC/PPE^M \cdot 10^3$: —; $PPO/PPE^M \cdot 10^3$: \cdots ; $chl*DPFD/PPE^M$: \cdots . The initial slopes of four experiments on the relation between PSII electron flow and carbon fixation at the indicated days as shown in Figure 6.6, $D \cdot 10^3$: \bullet .

laboratory experiments the irradiance range is high enough to guarantee correct determination of all fit parameters.

Data points of phytoplankton carbon flux, PCF, and associated phytoplankton electron flux, PEF^L measured on day 11, 18, 24 and 29 are shown in Figure 6.6. For low PEF^L values there appears to be a linear relationship. Its slope, called D, can be considered as a calibration parameter related to the yield of carbon flux per PSII electron flux.

In Figure 6.7 the daily amount of PSII electron flow as determined both from the mesocosm measurements and from the laboratory measurements is shown. Several peaks are found, the first two (day 9 and 12) during the first algal bloom, the last one (day 29) in the second algal bloom. The data of PSII electron transport derived from mesocosm and laboratory measurements show close similarity. Therefore we come to the conclusion that under these modelling conditions the *in situ* fluorescence measurements in the mesocosm container give a good alternative to the incubator measurements.

In Figure 6.8A PPE and chl*DPFD are compared. Figure 6.8B shows the daily amounts of fixed carbon, PPC, and the daily amounts of oxygen production, PPO. Both show 3 maxima, 2 in the first algal bloom, (day 9, 12) and 1 in the second, (26/27). In the first bloom oxygen production values are a bit higher than carbon fixation values. In the second bloom carbon fixation values are a bit higher than oxygen production values. During the blooms PPE (Fig. 6.8B) shows best similarity with the PPO data, as both show 2 maxima of about the same height. Between the 2 blooms however PPO stays relatively high and PPE decreases to almost zero. This is more in agreement with the PPC data.

Figure 6.8C shows the ratio of PPC and PPE during the experiment. The ratio varies from 0.2 to 1. During the second bloom somewhat higher PPC/PPE values are found than during the first bloom. The values of the ratio $D (PCF/PEF^L)$ at limiting light, as determined from the data in Figure 6.6, are in good agreement with the ratios PPC/PPE observed in the mesocosm (Fig. 6.8C). Figure 6.8C also shows the ratio of PPO and PPE during the experiment. This ratio varies from 0.3 to 2.6 during the blooms. In between the 2 blooms PPO/PPE is higher, due to the high PPO values in this period. The ratio of chl*DPFD and PPE shows a relatively constant value during the 2 blooms and higher values in between the 2 blooms.

6.4 Discussion

Laboratory measurements

Phytoplankton electron flux, PEF, determined from fluorescence measurements gives a reasonable measure of phytoplankton carbon flux, PCF, (Fig 6.6). Therefore we conclude that fluorescence measurements give a manageable alternative to the carbon fixation measurements, with the advantage that a higher time-resolution can be reached. In Chapter 3 the relation between the estimated rate of PSII electron flow, J_{E^L} and the rate of oxygen evolution, J_{O_2} , in a series of single species experiments was compared and we found that the relationship was species dependent. We suggested that this was partly due to differences in light absorption and that measurement of the PSII absorption cross section might overcome this problem. Here we estimated the light intercepted by PSII, i.e., the product of the number of PSII reaction centra, n_{PSII} , and the PSII absorption cross section, σ_{PSII} , by F_0 (see Chapter 4). As we found a good correlation between phytoplankton electron flux and phytoplankton carbon flux (Fig. 6.6), we conclude that this estimation which is based on the assumption that F_0 is proportional to the product of the number of PSII reaction centra and the PSII absorption cross section, is justified. Because of the resemblance of results on PPE^M and PPE^L (Fig. 6.7) we conclude that the

incubation method and the *in situ* method give comparable results for the long timescale measurements as used here.

Correlation of chlorophyll *a* concentration and minimal fluorescence

The relation between the minimal fluorescence and the chlorophyll concentration (Fig. 6.3A) changes during the experiment, especially during the rise and decrease of the first algal bloom. This change is probably caused by accessory photosynthetic pigments other than chlorophyll which affect the absorption cross-section and contribute more to the minimal fluorescence in the decline of the first bloom than in the rise of this bloom. The main accessory photosynthetic pigment will have been fucoxanthin as it is the most important accessory photosynthetic pigment of the diatoms which were dominating the ecosystem during the entire experiment. Therefore the variation in the relation between minimal fluorescence and chlorophyll concentration is probably not attributable to a change in the presence of algae of different pigment classes. A comparable variation in the relation between chlorophyll fluorescence and the amount of extracted chlorophyll has been found previously (Heany 1978, Butterwick et al 1982, Falkowski and Kiefer 1985).

Estimation of primary production from chlorophyll *a* concentration and irradiance

The ratio between the product of chl and DPFD and PPE is relatively constant during the blooms but increases substantially in the period between the two blooms (days 17-21)(Fig. 6.8C). Due to cell degradation the amount of inactive chlorophyll is expected to be higher in this period. The product of chl and DPFD therefore overestimates primary production in this period.

PSII electron flow as a measure for carbon fixation

The daily amounts of fixed carbon in the second bloom are higher than the first one (Fig. 6.8B), even though the amount of chlorophyll is lower in this period (see Fig. 6.3A). The high carbon fixation in the second bloom might be explained by the presence of more accessory pigments other than chlorophyll (e.g. fucoxanthin) in the second bloom compared to the first bloom. As these photosynthetically active pigments will contribute to F_0 , then also a higher phytoplankton electron flux in the second bloom compared to the first one is expected. Phytoplankton electron flux, however, reaches roughly the same maxima during the two blooms (Fig. 6.8B) and therefore the high carbon fixation in the second bloom is not due to more accessory pigments. This variation in PPC/PPE during the growth period (Fig. 6.8C) is comparable to the variation found in the ratio of carbon fixation and PSII electron flow in the data of Falkowski (1990). Baker et al (1995) found that the ratio of PSII efficiency and the quantum yield of carbon fixation in maize is higher under suboptimal growing conditions than under optimal growing conditions. They suggest that another, yet unknown, electron sink might be involved under suboptimal growing conditions. Other studies on higher plants (Öquist and Chow 1992, Genty et al 1992) show less variation in the ratio of PSII quantum yield and the quantum yield of oxygen evolution.

The high PPC/PPE ratio in the second bloom compared to that in the first one would suggest that oxygen consuming (i.e. photorespiratory and Mehler) reactions or electron consuming reactions (i.e. the conversion of NO_3^- to NH_4^+) are impaired in the second bloom.

Photorespiration and Mehler reaction are probably also responsible for the deviation from linearity in the relation between carbon fixation and PSII electron flow which is found at higher irradiances (Fig. 6.6). The daily irradiance (Fig. 6.3B) and the hourly averaged photon flux densities (data not shown) give us no reason to suggest that these reactions would be more probable in the first bloom than in the second.

The ratio D , i.e. PCF/PEF^I at limiting light as determined under laboratory conditions, represents the maximal efficiency of carbon fixed per PSII electron transported. At this maximal efficiency processes like photorespiration and Mehler reaction play a minor, or at least constant role. The ratios D determined at the indicated days (Fig. 6.6) compare well with PPC/PPE (Fig. 6.8C). In view of these results we conclude that photorespiration and Mehler reaction are of little consequence to the variation in the ratio of PPC and PPE in this experiment. Therefore we join the suggestion of Baker et al (1995) that another, yet unknown, electron acceptor might be involved in the variation of PPC/PPE. A possible candidate for electron consumption is the conversion of nitrate to ammonium (Huppe and Turpin, 1994). In this experiment, however, we have no data on nitrate conversion and its effect on the PPC/PPE ratio.

Estimation of primary production from *in situ* oxygen measurements

The oxygen production is higher than the carbon fixation in the first bloom but lower in the second (Fig. 6.8B). In the absence of non-assimilatory pathways carbon dioxide fixation is coupled with PSII oxygen production in a one to one ratio. This ratio decreases when NADPH is used for the conversion of ammonium to nitrate instead of for carbon fixation. Therefore we would expect that oxygen production is as large as, or larger than carbon fixation and we conclude that during the second bloom (after day 23) either an overestimation of carbon fixation or an underestimation of oxygen production has occurred. The oxygen method is restricted by its sensitivity and by the corrections one has to make to calculate gross oxygen production. We assumed that the respiration during the day is identical to the night respiration. However Weger et al (1989) and Beardall et al (1994) found enhanced respiration in the light. The uncertainty in the oxygen data is reflected by the unexpectedly high oxygen evolution levels which are found between the 2 algal blooms (day 17-21). These relatively high oxygen evolution levels are not consistent with the PSII electron flow data and the carbon fixation data (Fig 6.8B). The chlorophyll data (Fig. 6.3A) and the amount of algal cells (data not shown) in this period also predict low photosynthesis levels. During the algal blooms the changes in oxygen concentrations are larger and the calculations will be less sensitive to errors in the estimation of respiration and diffusion.

Concluding remarks

Measurement of chlorophyll fluorescence is easy and can be done *in situ*. The advantage is that one can measure under prevailing conditions, in our case nutrient limitation. The time resolution is rather high as one measurement only lasts a few seconds. This is contrary to the carbon fixation measurements which last relatively long and must be done in closed containers. Both methods, however, need an independent measurement of light dependence and light environment for the extrapolation to the ecosystem level. The product of chl and DPFD is also

easily done but in periods with relatively high amounts of inactive chl the primary production is overestimated. The oxygen method has the advantage that it yields an ecosystem parameter, but it is not very sensitive and especially in periods with low production rates small errors in the correction for diffusion and respiration have a significant effect on the result.

7 THE MINIMAL FLUORESCENCE IN THE DARK AS A MEASURE FOR PHOTOSYSTEM II EXCITATION IN THE LIGHT:

Effects of chlororespiration and state transitions

7.1 Introduction

In Chapter 4 we have shown that under certain conditions the minimal fluorescence (F_0) can be used to estimate the product of the number of photosystem II (PS II) reaction centres and the absorption cross-section. From the ambient PFD and this product PS II excitation can be estimated. As F_0 cannot be measured in the light, we used F_0 in the dark to estimate PS II excitation in the light. This method gave a good relationship between the phytoplankton electron flux and the phytoplankton carbon flux at low and medium irradiances as was shown in Chapters 4-6. In Chapter 3 it was also shown that the maximal value of F_m in *Phaeodactylum tricornutum* was observed in low light instead of in the dark. This increase in F_m in low light compared to the dark was also found for the other species described in this thesis (data not shown) and is about 10 % in our conditions. This increase in F_m might be explained either by a state transition from state II to state I, or by changes in spill-over from PS II to PS I, or by energy dependent fluorescence quenching in the dark which is inhibited in low light. A significant state transition during light adaptation would imply that the minimal fluorescence, F_0 , is lower than the minimal fluorescence in the light adapted state, F_0' . In case of energy dependent quenching caused by chlororespiration, as suggested by Ting and Owens (1993), F_0' is observed which is lower than the F_0 under non-energized conditions, but this effect might be masked due to reduction of Q_A by chlororespiration. In this chapter we looked at the effect of conditions which modulate chlororespiration and state transitions on the apparent F_0 in *P. tricornutum*, a species relatively well examined with respect to regulation of light harvesting and chlororespiration, to see if the assumption is correct that F_0 measured in the dark is a good measure for the minimal fluorescence in the light.

7.2 Materials and Methods

Growth of *Phaeodactylum tricornutum*, oxygen evolution, fluorescence measurements and the determination of fluorescence parameters were done as described in Chapter 3. Fluorescence measurements were done with the Xe-PAM fluorometer. F_0 is defined as the minimal fluorescence observed in darkness in the presence of only measuring light. F_0' is the minimal fluorescence observed in any light adapted state. Experiments were done at 20 °C and oxygen saturation unless indicated otherwise.

The oxygen content of the samples was lowered with glucose/glucose oxidase. Inhibitors of chlororespiration (antimycin A, CCCP and nigericin, dissolved in ethanol) were added to the

samples 5 minutes before the start of the measurement. Final concentrations (in μM) were: antimycin A: 50; CCCP: 5; nigericin: 5. The final ethanol concentration never exceeded 1 %. Samples measured at 5 and 10 °C were adapted to that temperature for 30 minutes in the dark prior to measurement. Far red light intensity was measured in W m^{-2} and converted to photon flux density by calculation.

Table 7.1. Effects of temperature, oxygen concentration, antimycin A, CCCP and nigericin on the minimal (F_0) and the maximal (F_M) fluorescence and on the maximal efficiency of PS II electron flow (F_V/F_M) of *P. tricornutum*. All data are expressed relative to the control measurements at 20 °C and an oxygen content of 100 % of air saturation without further additions. The oxygen data were determined from the experiment presented in Figure 7.1. The F_V/F_M of the control samples was between 0.64 and 0.70.

condition (number of experiments)	F_0 (\pm std) (r.u.)	F_M (\pm std) (r.u.)	F_V/F_M (\pm std)
control	100	100	100
10 °C (10)	1.02 ± 0.03	1.14 ± 0.03	1.06 ± 0.01
5 °C (10)	1.09 ± 0.04	1.21 ± 0.04	1.06 ± 0.01
22 % O_2 (4)	0.94 ± 0.01	1.02 ± 0.01	1.05 ± 0.01
4 % O_2 (3)	0.89 ± 0.01	0.91 ± 0.02	1.01 ± 0.01
back to 20 % O_2 (1)	92	88	97
+ antimycin A (16)	1.08 ± 0.18	1.04 ± 0.09	0.98 ± 0.06
+ CCCP (15)	0.95 ± 0.13	1.05 ± 0.11	1.04 ± 0.03
+Nigericin (11)	1.05 ± 0.16	1.08 ± 0.13	1.01 ± 0.02

7.3 Results

In Chapter 3 it was shown that F_V/F_M in *P. tricornutum* increased with decreasing temperature and we suggested that this phenomenon might be interpreted as the inhibition of chlororespiration at low temperatures. Table 7.1 shows that lowering of the temperature from 20 to 10 °C leads to an increase of F_V/F_M , caused by an increase of F_M . This temperature effect might be explained by the removal of chlororespiration but as well by a change in energy distribution via spill-over. A further lowering of the temperature to 5 °C led to an increase of both F_0 and F_M , but the F_V/F_M did not increase any further (Table 7.1). The increase of F_0 and F_M can not be explained by the removal of energy dependent quenching as that should result in an increase of F_V/F_M as well. The observed congruent increase of both F_0 and F_M is better

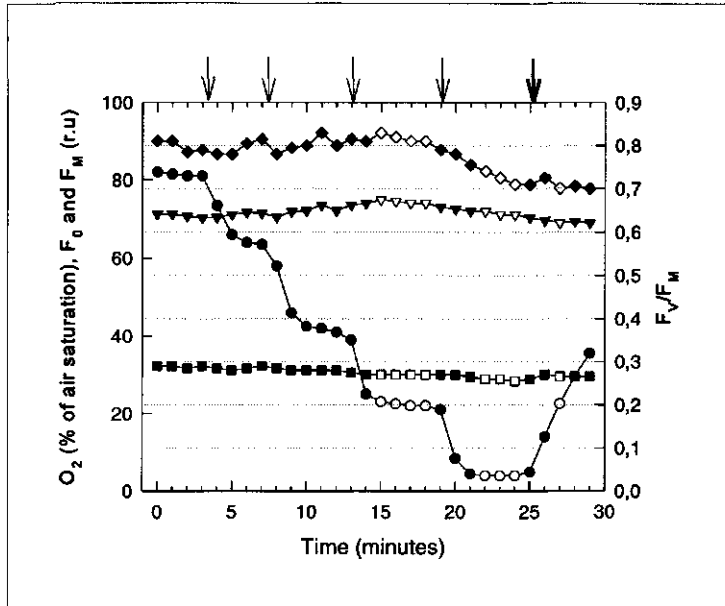


Figure 7.1. Effect of lowering the oxygen concentration (●, ○) on F_0 (□, ■), F_M (◆, ◇) and F_v/F_M (▼, ▽). The oxygen content was lowered with glucose/glucose oxidase; 20 units of glucose oxidase in 20 μ l were added to 2 ml algal suspension at time zero. Glucose was subsequently added in amounts of 0.125 μ mol in 2.5 μ l at the times indicated by the thin arrows. After 25 min, when an oxygen concentration of 4 % of air saturation was reached, the cuvette was opened to let the oxygen content increase again (heavy arrow). The open symbols represent the data points used in Table 7.1.

explained by a state transition from state I to state II.

A possible involvement of chlororespiration and its effect on both F_0 , F_M and F_v/F_M in the temperature experiments was examined by using known inhibitors of chlororespiration. As oxygen is a substrate, lowering the oxygen content of the samples should diminish chlororespiration (Bennoun 1982). The oxygen concentration in the algal samples was lowered using the glucose/glucose oxidase system. The reaction was started by the injection of small amounts of glucose into the cuvette. F_0 slightly decreased and F_M showed a very small increase by lowering the oxygen content from 100 % to 22 % of air saturation, leading to a small increase of F_v/F_M (Fig. 7.1, Table 7.1). Below an oxygen content equivalent to 22 % of air saturation F_M decreased. At an oxygen content of 4 % of air saturation both F_0 and F_M were smaller than at 100 % of air saturation, but F_v/F_M was about the same as at 100 % of air saturation (Fig. 7.1, Table 7.1). The decrease of F_M was not readily reversible upon the readdition of oxygen and the decrease of F_0 appears to relax (Fig. 7.1, Table 7.1). The effects on F_0 and F_M led to an F_v/F_M which was slightly lower than at the beginning of the experiment (Fig. 7.1, Table 7.1). The absence of recovery of both F_M and F_v/F_M upon increasing the oxygen

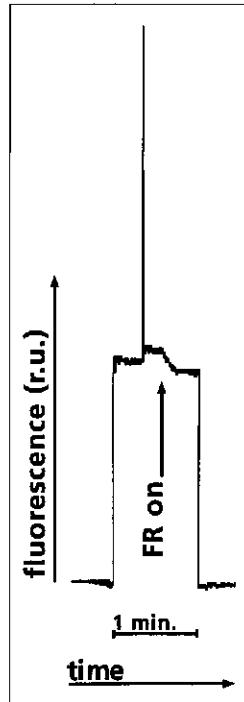


Figure 7.2. The effect of far red light on the steady state and maximal fluorescence yield of *P. tricornutum*. The farred light was obtained from a halogen lamp shielded by a 715 nm longpass filter resulting in a photon flux density of $6 \mu\text{mol m}^{-2} \text{s}^{-1}$. Integrated measuring light intensity $3.5 \text{ nmol m}^{-2} \text{s}^{-1}$. Flash frequency 8 Hz. Abbreviation: FR: far red light.

concentration is not well understood yet. At 10°C a lowering of the oxygen content did not cause an effect on F_v/F_m (data not shown). This suggests that, if chlororespiration is present, the effect of chlororespiration on fluorescence is absent at 10°C .

To modulate a possible proton gradient in the dark we added the inhibitor of chlororespiration, antimycin A, and the uncouplers CCCP and nigericin to dark adapted samples of *P. tricornutum*. Antimycin A, CCCP and nigericin gave only small effects on F_0 , F_m and F_v/F_m (Table 7.1), which in view of the relatively large standard deviation (Table 7.1), can hardly be considered to be significant. A small increase of F_0 is found for antimycin A and nigericin, whereas CCCP decreases F_0 . The F_m increases for all additions, leading to a small decrease of F_v/F_m in the case of antimycin A, a small increase of F_v/F_m in the case of CCCP and almost no effect on F_v/F_m in the case of nigericin. We did not find energy dependent fluorescence quenching in the dark. Therefore we conclude that in the dark adapted state the proton gradient, if present at all, is not large enough to induce energy dependent quenching. Our results are different from the results of Ting and Owens (1993). They found a small but significant increase of both F_0 and F_m using antimycin A, CCCP, nigericin and anaerobiosis. However, they did their experiments after a preillumination with of far red light of 10 Watt m^{-2} of 704 nm. Therefore we examined the effect of far red light on steady state fluorescence F , F_m' and Φ_{PSII} . In Figure 7.2 it can be seen that the fluorescence in low far red light ($6 \mu\text{mol m}^{-2} \text{s}^{-1}$) is lower than in darkness (in general about 3 %). The decrease of the minimal fluorescence in the presence of farred light suggests that in the dark the PQ-pool is somewhat reduced. Figure 7.3 shows the dependency of F_0 , F_m' and Φ_{PSII} on

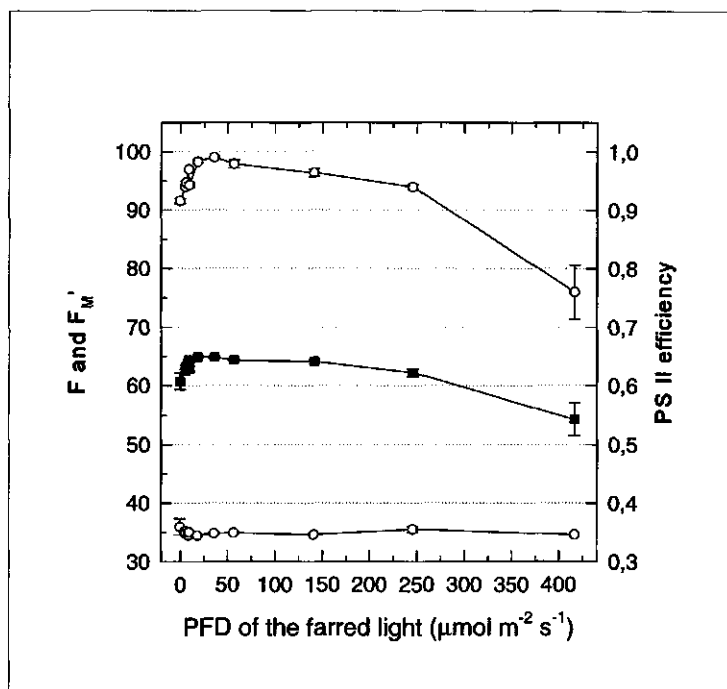


Figure 7.3. The steady state fluorescence F (○), maximal fluorescence F_M' (○) and the efficiency of PS II electron flow (■) as a function of the photon flux density of the far red light. Datapoints are the average of 2 measurements. One series of photon flux densities was measured using a single sample. F and F_M' were determined after 3 min light adaptation after which the photon flux density was increased. The farred light and measuring light were supplied as in Figure 7.2.

the photon flux density of the farred light. Conclusive with Figure 7.2 F_0 slightly decreased in low farred light and remains constant at higher photon flux densities. F_M' and Φ_{PSII} both show an increase at low photon flux densities and a decrease at higher photon flux densities. The maximum of F_M' was found at about $35 \mu\text{mol m}^{-2} \text{s}^{-1}$ far red light. This increase of F_M' might be explained both by a state II to state I transition or by the elimination of energy dependent fluorescence quenching between darkness and $35 \mu\text{mol m}^{-2} \text{s}^{-1}$. At $65 \mu\text{mol m}^{-2} \text{s}^{-1}$ of farred light, which is approximately the photon flux density used by Ting and Owens (1993), we found a higher value of both F_M' and Φ_{PSII} compared to the value measured in darkness. The decrease of F_M' at higher photon flux densities is probably due to energy dependent fluorescence quenching. The responsible proton gradient might be caused by PS I driven cyclic electron flow, or by linear electron flow driven by farred light delivered to the PS II reaction center as well.

Figure 7.4 shows the fluorescence transients of a dark adapted *P. tricornutum* sample illuminated with farred light ($245 \mu\text{mol m}^{-2} \text{s}^{-1}$). In contrast to the steady state results shown in Figure 7.2 where the photon flux density was increased stepwise without dark adaptation

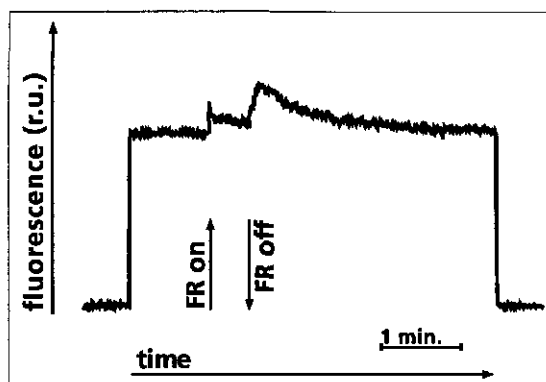


Figure 7.4. The effects of farred light on the minimal fluorescence of *P. tricornutum*. The farred light ($245 \mu\text{mol m}^{-2} \text{s}^{-1}$) was supplied as in Figure 7.3. Integrated measuring light intensity $4.3 \text{ nmol m}^{-2} \text{s}^{-1}$. Flash frequency 4 Hz. Abbreviation: FR: far red light.

between 2 succeeding photon flux densities, the farred light led to an immediate increase of fluorescence. This increase might be explained by a transition from state II to state I, although a state transition in terms of phosphorylation is not very likely as the fluorescence rise is almost instantaneous. When the farred light is turned off the fluorescence yield shows a transient increase followed by a slower decrease to the fluorescence level at the beginning of the experiment. This phenomenon might be explained by a temporary overreduction of the PQ-pool caused by an unequal distribution of excitons just after the farred light was put off. However, this would implicate that the very low intensity of measuring light (in this experiment the photon flux density of the measuring light was $4.3 \text{ nmol m}^{-2} \text{s}^{-1}$) is able to induce reduction of the PQ-pool in *P. tricornutum*. The suggestion that even measuring light of such low photon flux densities might influence the measurement is confirmed by the results shown in Table 7.2. This table shows that even at very low photon flux densities the F_v/F_m is dependent on the measuring light.

7.4 Discussion

7.4.1 Effects of chlororespiration on the fluorescence yield

Our measurements indicate the absence of a proton gradient in the dark in *P. tricornutum* as the F_v/F_m in the presence of the uncouplers CCCP and nigericin is not different from the control (Table 7.1). Also antimycin A, suggested to be an inhibitor of chlororespiration (Ravenel and Peltier 1991) did not affect the minimal and maximal fluorescence in the dark (Table 7.1). Therefore we conclude that under our conditions F_o is not affected by energy dependent quenching in the dark. These results might at first glance seem to be in contradiction with the results of Ting and Owens (1993). Ting and Owens (1993) found fluorescence quenching in the dark, which could be inhibited by CCCP, nigericin, antimycin A and anaerobiosis. They concluded

Table 7.2. Maximal efficiency of PS II electron flow (F_v/F_m) of *P. tricornutum* as a function of the photon flux density of the measuring light. Results are the average of 10 measurements. Photon flux density (PFD) is given as the integrated measuring light intensity. Flash frequency was 16 Hz.

PFD ($\text{nmol m}^{-2} \text{s}^{-1}$)	F_v/F_m
17	0.65
6.9	0.66
3.6	0.67
2.0	0.70

that a proton gradient, caused by chlororespiration, was present in the dark. Our experiments with the sensitive Xe-PAM fluorometer indicate that the F_v/F_m of *P. tricornutum* is very sensitive for light as the F_v/F_m increased from 0.65 to 0.70 upon decreasing the measuring light from 17 $\text{nmol m}^{-2} \text{s}^{-1}$ to 2 $\text{nmol m}^{-2} \text{s}^{-1}$ (Table 7.2). It is very well possible therefore that the measuring light, or the farred light used to oxidize Q_A^- prior to the measurements, may have induced energy dependent quenching in the experiments of Ting and Owens (1993).

What is the evidence for chlororespiration driving energy dependent quenching? Fluorescence quenching in the light in the presence of DCMU was found by Owens (1986b) and Caron et al (1987) and the quenching was intensity dependent (Ting and Owens 1993). The quenching disappeared after addition of NH_4Cl (Caron et al 1987) and CCCP (Ting and Owens 1993) suggesting that energy dependent quenching is involved. The quenching was also inhibited by antimycin A which was attributed to the inhibition of a chlororespiratory pathway which involves the quinones of the PQ-pool but not the cytochrome b_6f complex (Ravenel and Peltier 1992). However, as noted by Ting and Owens (1993), a proton gradient in the light can also be induced by cyclic electron around PS I. Furthermore, Oxborough and Horton (1987) showed that antimycin A affects the relation between energy dependent quenching and the proton gradient. Such an effect of antimycin A might be involved in the removal of the fluorescence quenching as found by Caron et al (1987) and by Ting and Owens (1993). Relaxation of fluorescence quenching was also found under anaerobiosis (Ting and Owens 1993), but those results could not be confirmed here.

From the arguments above it seems obvious that a reevaluation of the contribution of chlororespiration to energy dependent quenching in the dark is necessary.

7.4.2 Effects of state transitions on the fluorescence yield

Far red light ($245 \mu\text{mol m}^{-2} \text{s}^{-1}$) immediately led to an increase of the fluorescence in a dark adapted sample of *P. tricornutum* (Figure 7.4). Turning off the far red light led to a temporary increase of the fluorescence, followed by a subsequent decrease. This transient at first sight resembles a state transition from state II to state I, involving movement of LHC II from PS I to PS II. The rate of these changes is, however, much faster than might be expected when the transition involves phosphorylation and dephosphorylation of LHC II. Half times for relaxation of fluorescence quenching due to state transitions of 5 to 8 minutes in barley were reported by Quick and Stitt (1989) and by Horton and Hague (1988), respectively. A mechanism involving regulation of energy distribution in *P. tricornutum* by ionic distributions independently of the redox state of the PQ-pool, as suggested by Owens (1986b), might seem more compatible with the rate of these changes. The immediate increase upon illumination with far red light probably is partially caused by reduction of Q_A by the far red light. The increase and subsequent decrease of the fluorescence yield when the far red light was turned off can be explained by a temporary overreduction of PSII, caused by the unequal energy distribution when the far red light is turned off. This implies that measuring light of $4.3 \text{ nmol m}^{-2} \text{s}^{-1}$ already is actinic. This is in agreement with the light dependence of F_v/F_m (Table 7.2). Accepting that the measuring light is somewhat actinic, is it easy to interpret the decrease of F_0 found in Figure 7.2 and 7.3 under weak far red light as an oxidation of Q_A .

A state transition from state II in the dark to state I in the light would implicate that in the dark the PQ-pool is more reduced than in the light. This might be caused by the fluorescence measuring light (see Table 7.2). A decrease of the amount of spill-over between darkness and low light would implicate that in the dark adapted state energy distribution towards PS I is favoured.

The increase in F_m' found with farred light (Fig. 7.3) and with white light (Chapter 3) also suggests a transition from state II in the dark to state I in the light or a decrease of the amount of spill-over from dark to low light. As the increase in F_m' with far red light is found at a lower photon flux density than with white light (about $35 \mu\text{mol m}^{-2} \text{s}^{-1}$ compared to about $100 \mu\text{mol m}^{-2} \text{s}^{-1}$) we suggest that the state transition or spill over in *P. tricornutum* is both intensity and wavelength dependent. This is different from the state transitions in *Pleurochloris meiringensis* which were shown to be only dependent on the intensity of the actinic light (Büchel and Wilhelm 1990).

7.4.3 How much does F_0' (the light adapted state) differ from F_0 (the dark adapted state)?

Figure 7.2 shows that far red light leads to a small decrease (about 3 %) of the apparent F_0 , probably due to oxidation of the PQ pool by PS I. When F_0 is measured in the dark only a small overestimation of the real F_0 in the dark is made. In the light adapted state a state transition or a change in spill-over might occur, leading to higher fluorescence levels in the light adapted state. Therefore an underestimation of the F_0 in the light might be made by using the F_0 measured in the dark. Based on our observations on the increase of the maximal fluorescence we think that the underestimation does not surpass 10 % in the case of state transition and even less in the case of spill-over. Furthermore one should note that the effect of reduction of the PQ pool and

the effect of state transitions work in the opposite direction so the overall effect is expected to be somewhat smaller than 10 %.

7.5 Conclusions

We were not able to demonstrate energy dependent quenching in the dark in *P. tricornutum* and the PQ-pool was largely oxidized. This suggests that chlororespiration was not active in our samples and therefore we can exclude any prominent effect of chlororespiration on the minimal fluorescence in the dark in our experiments.

The higher maximal fluorescence in medium white and in low far red light compared to the dark is suggested to be caused by a state transition involving a change in absorption cross-section of PS II from state II to state I or by a decrease in the amount of spill-over. The maximal underestimation of F_0' by using the F_0 is 10 %. The F_0 measured in the dark-adapted state is therefore a good estimate for the F_0 in the light adapted state.

8 GENERAL DISCUSSION

8.1 Introduction

Our goal was to explore the possibility of determining primary production in a marine ecosystem with chlorophyll fluorescence measurements instead of oxygen evolution or carbon fixation measurements. The first step was to overcome the methodological limitations in the determination of the rate of PS II electron flow in phytoplankton samples. This led to the development of the Xe-PAM and to the concept of phytoplankton electron flux (PEF) to describe PS II electron flow in phytoplankton samples. At the same time the relation between PS II electron flow and primary production determined as carbon fixation or oxygen evolution had to be described, first in single species experiments, but later also in natural phytoplankton samples. This thesis mainly describes the relation between PS II electron transport determined with fluorescence and photosynthetic oxygen evolution or carbon fixation. With this information on the relation between the phytoplankton electron flux and phytoplankton carbon flux (or phytoplankton oxygen flux) the prospects and limitations of each method can be outlined resulting in some recommendations for future research.

8.2 Fluorescence measurements on phytoplankton samples

In Chapter 2 a correlation was found between growth and the rate of PS II electron transport (determined as $\Phi_{PSII} \cdot PFD$) in *Dunaliella tertiolecta* grown in batch cultures at a number of light intensities using a PAM 101 fluorometer (Fig. 2.5). Both the actual and the maximal efficiency of PS II electron flow decreased at the end of the exponential growth phase (Fig. 2.4A and 2.6). This study also demonstrated the main shortcomings of the PAM 101 fluorometer for marine applications: i) lack of sensitivity; ii) unfavourable excitation and detection wavelength. Two research lines were followed: one was to compare PS II electron flow with other methods for determining photosynthesis like oxygen evolution and carbon dioxide fixation and to extend the research to algal groups with other light harvesting complexes (see next paragraph); the other was to develop a fluorometer with an increased sensitivity. The PAM 101 fluorometer, as applied in Chapter 2, can only be used with samples which have a high chlorophyll density.

In Chapter 4 we have described the Xe-PAM fluorometer which was developed for our purpose by Prof U. Schreiber and which has a manifold higher sensitivity and is much more versatile than the PAM 101 fluorometer (Schreiber et al 1993; Chapter 4). This was reached by a number of measures: i) use of a Xenon flash lamp as an excitation source, enabling excitation in the VIS-UV wavelength region; ii) improved detection range typically from 650 nm to 750 nm which covers most of the main chlorophyll fluorescence band; iii) improved optical efficiency through the use of quartz rods for light transmission; iv) rapid change of excitation and detection wavelengths by means of optical filters. The apparatus was most sensitive when excitation and detection were at a relative angle of 90 ° and light was conducted to the measuring cuvette with quartz rods. In

the mesocosm measurements described in Chapter 6 we had to deal with 2 problems: i) the timing of the Xenon flash lamp and the synchronous pulse amplifier was found to be temperature dependent. This led to the measurement of negative F_0 values in some nights; ii) incoming solar radiation at bright days was intense enough to saturate the sensitive detector. This did cause non-linear behaviour resulting in errors in the measurement of the efficiency of PS II electron flow, which were sometimes hard to discover or recognize. Therefore the detector preferentially had to be placed at a angle of 90° relative to incoming solar radiation to prevent saturation. The use of a filter which does not transmit far red light and heat radiation also might help. Beside the development of the fluorometer, the development of the process control and data acquisition program PPMON was important for accurate measurements at low chlorophyll concentrations. The PPMON program contains procedures for control and simultaneously registration of fluorescence and oxygen measurements, for averaging measurements and for semicontinuous monitoring of the efficiency of PS II electron flow. For this purpose a new cuvette for simultaneous oxygen and fluorescence measurements was developed. The monitoring procedure of the PPMON program proved to be very useful in the experiments of Chapter 6 where the efficiency of PS II electron flow was monitored in a mesocosm container for a period of 3 weeks. Furthermore the PPMON program could be used to average measurements and correct them with blank samples, which was very useful at low chlorophyll concentrations. The combination of the Xe-PAM fluorometer and the PPMON program was sensitive enough for monitoring phytoplankton electron flux in a mesocosm and therefore it appears to be sensitive enough for monitoring phytoplankton concentration and activity in coastal waters.

8.3 The relation between PS II electron flow, oxygen evolution and carbon fixation

8.3.1 Oxygen evolution and carbon fixation

Comparing the apparent PS II electron flow per photosystem II, J_E , with photosynthetic oxygen evolution per chlorophyll a , J_O , we found that the relation was nearly linear at low to medium irradiances for the species examined (Fig. 3.3, 3.4, 3.5 and 3.6B). The cells were grown at a photon flux density of $100 \mu\text{mol m}^{-2} \text{s}^{-1}$ and linearity between J_E and J_O was found below $400 \mu\text{mol m}^{-2} \text{s}^{-1}$. A similar relation was found comparing phytoplankton electron flux, PEF, with phytoplankton oxygen flux, POF, (Fig. 4.4) or with phytoplankton carbon flux, PCF, (Fig. 5.2, 5.3 and 6.6). In the experiments of Chapter 5 the linear relation between PEF and PCF was found at irradiances which were about 4 times larger than the growth irradiance (about 280 and $69 \mu\text{mol m}^{-2} \text{s}^{-1}$ respectively).

At higher irradiances non-linearity was found both in the relation between J_E and J_O (Chapter 3) and in the relation between PEF and POF (Chapter 4) or PCF (Chapters 5 and 6). In Chapter 3 the non-linearity between J_E and J_O was shown not to be caused by photorespiration and we suggested that a Mehler type of reaction or increased mitochondrial respiration at high irradiances as the most probable explanation. The non-linearity between PEF and PCF is also attributed to these processes as our carbon fixation measurements most probably give net photosynthesis data (see Williams et al 1996). A similar relation between J_E and J_O as found for these eukaryotic

species was found for the cyanobacterium *Synechocystis PCC6803* (Geel et al 1994).

Even in the linear part of the relation the ratio of J_0 and J_E was species dependent (Fig. 4.5). To account for differences in pigment composition and PS II absorption cross section we introduced the concept of the phytoplankton electron flux. In Chapter 4 it was shown that the comparison of PEF with POF yielded a similar ratio for both *Phaeodactylum tricornutum* and *Dunaliella tertiolecta* (Fig. 4.4). The ratio of PCF and PEF (Fig. 5.4) was about 1.5 times larger in *Skeletonema costatum* than in the other 2 species. This variation in the ratio of PCF and PEF is somewhat less than was found in the ratio of J_0 and J_E in the experiments of Chapter 3 (Fig. 3.5), though larger than the variation in the ratio of POF and PEF in Chapter 4 (Fig. 4.4). In all these experiments we worked with exponentially growing algae which all grew on nitrate. This is not the case in the experiments of Chapter 6. The mesocosm is continuously supplied with NO_3^- but as algal decomposition takes also place also NH_4^+ might be more or less available and degradation product of chlorophyll might be present. These phenomena might effect the ratio of PS II electron flow and carbon fixation. Two known effects are the nitrogen source used for metabolism and the contamination of F_0 (both: see later), but other yet unknown effect might also be important. Indeed, in Chapter 6 the variation in the ratio of the daily primary production measured as carbon fixation and the daily primary production measured as PS II electron flow was larger than in the laboratory experiments and was shown to vary by a factor 4 (Fig. 6.8C). The parameter D (the ratio of PCF and PEF, both measured in the laboratory) varied by a factor 2 (Fig. 6.8C), though the variation in the ratio of J_c and J_E determined from the same 4 experiments was twice as large (data not shown). Therefore we conclude that both for algae grown under controlled laboratory conditions and under uncontrolled outdoor conditions the F_0 concept yields somewhat better results than the comparison of J_0 or J_c and J_E . However, under uncontrolled outdoor conditions the variation in the comparison of PS II electron flow and carbon fixation is expected to be larger, though this is not caused by the measuring method but by the physiological state of the algae.

Comparison of carbon fixation with PS II electron flow should take into account that NADPH is not only used in carbon reduction but also for sulfate and nitrogen reduction. Therefore the relation between PEF and PCF also depends on the rate of this pathway relative to the rate of carbon assimilation. Assuming that the average elemental composition of the phytoplankton is constant and equals the Redfield ratio (Geider and Osborne 1992), it can be calculated that reduction of NO_3^- to NH_4^+ requires about 25 % of the NADPH generated by PS II electron transport (Lindblad and Guerrero 1993). When both NO_3^- and NH_4^+ are present, normally NH_4^+ is preferentially metabolized. When the conversion of NO_3^- to NH_4^+ is assumed to be independent of the NADPH supply by the light reactions, and therefore independent of the irradiance, a change in the ratio of PCF and PEF might be expected due to changes in the availability of NO_3^- and NH_4^+ . This, however, can only explain a small part of the variations in the ratio of PCF and PEF.

Another cause for the variation in the ratio of PCF and PEF might result from the contamination of F_0 by non-photosynthetic fluorescing substances. Non-photosynthetic fluorescing substances will result in an apparent increase of F_0 . However, the apparent increase in F_0 is accompanied by an apparent increase of F and F_M' , which leads to a decrease of the apparent $\Phi_{\text{PS II}}$. The effect of the decrease of $\Phi_{\text{PS II}}$ counteracts the increase in F_0 in the calculation of the PEF, but does not

cancel it completely. The use of phytoplankton electron flux as a measure for carbon fixation requires a frequent calibration of both the F_0 measurement and the ratio of PCF and PEF.

To model our data on PS II electron flow and oxygen evolution we extended the photosynthesis model of Eilers and Peeters (1988) with an extra oxygen uptake component which was assumed to be proportional to the proportion of reduced ferredoxin, a substrate of oxygen reduction. The model gives a satisfactory description of the relation between J_e and J_o at the cost of an increased number of parameters. This proved to be a problem in the PEF and PCF measurements of Chapter 5 and 6. The modified model with its 5 independent parameters could not be applied because the incubator did not allow more than 7 light intensities. Furthermore the PS II electron flow data which were obtained in the mesocosm could not be compared with the carbon fixation data obtained in the laboratory as the irradiances were not the same. Instead the data were analysed separately with the unchanged model of Eilers and Peeters (1988) which uses only 3 parameters. For a better fitting procedure, or when more information about kinetics is needed, PEF and/or PCF should be measured at more light intensities.

Both models are less suited to gain more information on the physiological state of the phytoplankton. The models treat the PS I and PS II reaction centre as one entity, but for analysis of phytoplankton electron flux it is more interesting to describe events occurring at the PS II reaction centre. The main problem of the model is that PS II efficiency is not regulated by heat dissipation in the antenna, as reflected in energy dependent quenching but only by PS II closure and photoinhibition. Incorporation of regulation of PS II efficiency by making PS II excitation ($\alpha \cdot I$) dependent on heat dissipation will make this model much more complex.

8.3.2 Minimal fluorescence, F_0

In Chapter 4 it was shown that the relation between PEF and POF was the same for *P. tricornutum* and *D. tertiolecta* (Fig. 4.4). The use of F_0 as an estimate of PS II excitation was shown to be correct when certain conditions are met: the spectral distribution of the measuring light and the actinic light should be identical and the measuring light photon flux density and all other optical properties should be kept constant in one series of measurements. When this is not possible it is recommended to measure the spectrum and the PFD, so that different measurements can be calibrated to each other.

Thus far PEF was calculated using F_0 , the minimal fluorescence in the dark adapted state instead of F_0' , the minimal fluorescence in the light adapted state. The reason for this is that F_0' is extremely difficult to measure. The fact that the maximal fluorescence in low light is higher than in the dark (Fig. 3.2A) and the increase of F_v/F_m when the temperature decreases (Table 3.2) gave us reason to assume that F_0 might be influenced by chlororespiration or state transitions which could lead to an error in the estimation of F_0' . Chlororespiration has been suggested to lead to a proton gradient (Ting and Owens 1993), resulting in a quenching of F_0 , but it also leads to a reduction of Q_A resulting in an increase of apparent F_0 . Chlororespiration might thus either increase the apparent F_0 or decrease the apparent F_0 , depending on the redox state of Q_A and the proton gradient in the dark respectively. Energy dependent fluorescence quenching, which might have been induced by chlororespiration was not found (Table 7.1), but the induction of a state transition or a change in spill over between darkness and low light is quite likely (Fig.

7.3 and 7.4).

A state transition will lead to an increase of F_0' compared to F_0 , which in case of *P. tricornutum* would lead to an underestimation of F_0' of about 10 %. When spill-over is responsible for the increase in F_M the underestimation of F_0' will be smaller than 10 %.

In the prokaryotic cyanobacteria a reduction of the PQ-pool in the dark and a dark to light state transition is found which is related to respiratory electron flow across the thylakoid membrane in the dark (Scherer et al 1988). State transitions in cyanobacteria are found to be quite large: an increase of the maximal fluorescence of about 85 % was found in *Anacystis* by Dominy and Williams (1987), a similar effect can be seen in fluorescence traces of *Synechococcus* in Schreiber et al (1993) and in *Synechocystis* PCC 6803 in Geel et al (1994). The effect of the state transition on the relation between PS II electron flow and oxygen evolution or carbon fixation might therefore be expected to be large. The results of Geel et al (1994), however, showed a similar relation between J_e and J_0 for *Synechocystis* PCC 6803 as for the eucaryotic algae described in Chapter 3. In the ecosystem of the North Sea cyanobacteria normally hardly contribute to primary production. Therefore the variation in PEF determined on North Sea phytoplankton samples is expected to be not more than about 10 %.

It was found in Chapter 7 that in *P. tricornutum* in the dark even the very low intensity of the measuring light of the Xe-PAM might cause a small reduction of Q_A (Fig. 7.2 and 7.3). The reduction of Q_A leads to a small overestimation of F_0' (about 3 %).

We have not determined these effects on F_0 for other species. Though we expect that for the species described in this thesis the effect will be of the same size as found for *P. tricornutum* as they all contain a more or less similarly organized photosynthetic system (see Chapter 1).

Thus far we treated the algal samples as if all cells behave the same. However, in case that a sample contains both a small population of algae with a high F_v/F_m ($F_0 = 10$, $F_M = 33$, $F_v/F_M = 0.70$) and a dominant species with a low F_v/F_m ($F_0 = 90$, $F_M = 150$, $F_v/F_M = 0.40$) it can be calculated that the measured F_v/F_m of the mixture of both ($F_0 = 100$, $F_M = 183$, $F_v/F_M = 0.45$) is higher than the weighted mean ($F_v/F_M = 0.1 \cdot 0.70 + 0.9 \cdot 0.40 = 0.43$). This effect is only important in extreme cases as described here. In general only a minor influence of this effect on the calculated PEF is expected.

8.4 Phytoplankton electron flux or phytoplankton carbon flux?

The scientific choice between measurements of primary production based on measurements of PEF or PCF in my opinion should be a choice on a physiological basis. Both methods have shown to have their own limitations in the prediction of primary production. Though it can be concluded that the variation in PEF measurements is smaller than the variation in PCF measurements (Fig. 5.3).

PS II activity can be determined *in situ* with chlorophyll fluorescence measurements. The fluorescence measurements can also be done simultaneously with ^{14}C incubations in carbon fixation measurements allowing the measurements to be carried out under identical conditions. The PEF is a measure of PS II activity in a sample but the PEF gives no information about the

nature of the electron sinks. Part of the reducing equivalents will be utilised in assimilatory processes, e.g., carbon fixation or nitrogen assimilation and a part will drive dissipative reactions like photorespiration and Mehler-reaction.

For carbon fixation measurements samples have to be taken out of the phytoplankton system for a relatively long incubation (in this thesis carbon fixation measurements on natural phytoplankton samples lasted 2 hours, Chapter 6) to reach sufficient sensitivity. Measurements of this length are found to give mostly net carbon fixation (see Williams et al 1996). Carbon fixation measurements do not give information on dissipative reactions like photorespiration and Mehler-reaction but are a measure of the increase of the phytoplankton biomass during the light period.

At low to medium irradiances, where the dissipative reactions only play a minor role, a good correlation between PEF and net photosynthesis determined as PCF was found and fluorescence measurements might be used to predict carbon fixation.

Independent of the relation between PEF and PCF, Φ_{PSII} is a good parameter for determining effects of environmental conditions, e.g. toxic substances (herbicides), excessive light (photoinhibition) on the phytoplankton and F_0 is a good parameter for estimation chlorophyll of phytoplankton.

8.5 Recommendations for future research

- * In our experiments we were not able to identify the cause of the non-linearity which was found at high irradiances in the relation between PS II electron flow and carbon fixation or oxygen evolution. It is very interesting, though, to identify the processes that are involved in the dissipation of excess excitation energy at high irradiances, and their role in the functioning of algae. Furthermore a good description of this non-linear relation is essential for the calculation of primary production. The model of Eilers and Peeters (1988), used in this thesis, is not easily modified into a simple model that incorporates fluorescence quenching to model the relation between PS II electron flow and oxygen evolution or carbon fixation. For that purpose a new model will have to be developed.
- * In the calculation of the phytoplankton electron flux F_0 is an essential parameter. Therefore more research on the effects of state transitions or a changes in spill-over on F_0 is needed.
- * Phytoplankton photosynthesis is the output of many individuals. Thus far we have regarded phytoplankton samples as if the individuals have identical properties. However, this is not the case. The importance of this phenomenon in natural phytoplankton samples is worth examining. It might be examined with the PHYTO-PAM fluorometer which is developed by Kolbowski and Schreiber (1995). The PHYTO-PAM fluorometer uses different light emitting diodes for excitation and makes it possible to distinguish between algal groups with different light harvesting pigments. The method might be promising for measurement of the contribution of green algae, cyanobacteria and diatoms to phytoplankton electron flux and, perhaps, in the separation of periphyton and macrophyte PS II activity *in situ*.
- * The current equipment can measure variable fluorescence on laboratory samples with a chlorophyll concentration as low as $0.02 \mu\text{g l}^{-1}$ (Schreiber et al 1993). At these low concentra-

tions than a calibration with a reference sample is required to subtract background signals for accurate determination of F and F_M' . In experiments with dilute suspensions it was difficult to obtain a reliable reference sample. Thus when wants to increase the sensitivity, the availability of a good reference system is required.

- * When outdoor measurements have to be done with an apparatus based on the Xe-PAM fluorometer the following should be considered: i) thermostating the equipment because the synchronization of the Xenon flashlamp and the synchronous pulse amplifier was temperature dependent; ii) optimal location of emitter and detector with respect to each other and with respect to the ambient light; iii) need for an accurate determination of F_0 in outdoors measurements; iv) provisions to account for automated measurements; v) Finally one should consider the use of combined spectral absorption and fluorescence. With such an apparatus it might be possible to measure the light environment, determine the composition of the phytoplankton sample and measure the photosynthetic activity.

SUMMARY

Saturating pulse fluorescence measurements, well known from studies of higher plants for determination of photosystem II (PS II) characteristics, were applied to cultures of the green alga *Dunaliella tertiolecta* (Chapter 2). The actual efficiency of PS II (Φ_{PSII}), the maximal efficiency of PS II (F_v/F_m), and both photochemical and non-photochemical fluorescence quenching were determined for cultures of *D. tertiolecta* growing under varying light intensities. The rate of PS II electron flow (J_E), estimated as the product of Φ_{PSII} and the photon flux density (PFD), appeared to correlate well with growth rates determined for the *D. tertiolecta* cultures. The results indicated that the saturating pulse fluorescence method may be successfully used to determine photosynthetic characteristics of phytoplankton. However, an increase of sensitivity by a factor 1000 was found to be needed for the application of this technique to *in situ* measurements. Conditions were outlined which have led to the development of the Xe-PAM fluorometer with a manyfold higher sensitivity.

The relation between photosynthetic oxygen evolution (J_O , expressed as oxygen production per chlorophyll *a*) and J_E was investigated for the marine algae *Phaeodactylum tricornutum*, *D. tertiolecta*, *Tetraselmis* sp., *Isochrysis* sp. and *Rhodomonas* sp. by varying the ambient PFD (Chapter 3). At limiting light a linear relation was found in all species. At PFD's approaching light saturation linearity was lost. The observed non-linearity at high PFD's is most probably not caused by photorespiration but by a Mehler-type of oxygen reduction. The relationship could be modelled by including a redox-state dependent oxygen uptake. The linear range between J_E and J_O extends to a PFD which is 2 to 10 times higher than the PFD at which the species were grown. The ratio of J_E and J_O in the light-limited range is species dependent and related to differences in absorption cross-section of PS II (σ_{PSII}). The ratio of J_E and J_O in the light-limited range is not dependent on temperature. F_v/F_m was found to be temperature dependent with an optimum near 10 °C in the diatom *P. tricornutum*.

The photosynthetic electron flux in a phytoplankton sample (PEF) was shown to depend on the product of J_E ($= \Phi_{PSII} \cdot \text{PFD}$), σ_{PSII} and the number of PS II (n_{PSII}) in the sample (Chapter 4). A mathematical expression was derived which relates the minimal fluorescence (F_0) to n_{PSII} and σ_{PSII} under the condition that the spectral distribution of the ambient light and the measuring light are identical. This condition can be approximated measuring F_0 with the Xe-PAM fluorometer. The experimental conditions under which the relationship between PEF, Φ_{PSII} and F_0 is valid, were examined. The maximal value of Φ_{PSII} (F_v/F_m) was shown to be independent on the wavelength under the measuring conditions. The apparent F_v/F_m depends on the intensity of the measuring light and the duration and intensity of the saturating light pulse. It is shown that, under certain conditions, the minimal fluorescence can be used as a measure of PS II excitation in the light. F_0 , obtained with the broad band excitation light of a filtered Xenon flash lamp, thus was used as a measure for the product of n_{PSII} and σ_{PSII} . The relationship between PEF calculated with this expression and net oxygen evolution (phytoplankton oxygen flux, POF, expressed as oxygen production per sample volume) was found to be similar in the diatom *P. tricornutum* and the green alga *D. tertiolecta*. Therefore we conclude that the use of PEF as a measure for POF yields

better results than the use of J_E for J_0 . The Xe-PAM fluorometer was found to be sensitive enough for coastal applications.

The relation between PEF and carbon fixation (phytoplankton carbon flux, PCF, expressed as the carbon dioxide fixed per sample volume) was examined in cultures of *Isochrysis sp.*, *Phaeocystis sp.* macroflagellates and *Skeletonema costatum* (Chapter 5). The F_0 used to calculate PEF was measured at the start of the experiments. Both the PFD and the duration of the incubation were varied. As found before for the relation between J_E and J_0 , the relation between PEF and PCF was also approximately linear at limiting light and deviated from linearity at saturating light. The linear range between PCF and PEF also extends to a PFD which is 2 to 10 times higher than the PFD at which the species were grown. The length of the incubation did not affect PEF and PCF except for the highest PFD ($1530 \mu\text{mol m}^{-2} \text{s}^{-1}$). The decline of F_v/F_m of the samples irradiated at the highest PFD showed a fast component within 30 minutes incubation and a minor slow component, indicating that photoinhibition was induced in the first 30 minutes.

PEF, PCF, oxygen production and their relationships were furthermore examined during phytoplankton development in a mesocosm at the field station (Chapter 6). PEF was calculated from F_0 , Φ_{PSII} and the PFD which were continuously monitored for three weeks in the upper water layer of the mesocosm. In addition PEF and PCF were estimated from laboratory measurements on samples taken from the mesocosms. Daily primary production in the mesocosm, measured as either PSII electron flow (PPE) or carbon fixation (PPC), was calculated using a photosynthesis model. Daily photosynthetic oxygen evolution (PPO) was calculated from changes in the oxygen concentration over the day. In the period between the 2 blooms the ratio of PPO and PPE was higher than during the peak of the blooms. The ratio of PPC and PPE was much more constant. In general PPE gave a reasonable measure of both PPC and PPO.

The effects of chlororespiration and state transitions on F_0 were determined in the diatom *P. tricornutum* (Chapter 7). Inhibition of chlororespiration by antimycin A or anaerobiosis did not affect F_v/F_m . The observed F_0 was insignificantly (8%) increased upon addition of antimycin A and slightly decreased upon illumination with farred light ($6 \mu\text{mol m}^{-2} \text{s}^{-1}$). These effects might be attributed to chlororespiratory activity, but could as well be caused by reduction of Q_A by the weak fluorescence measuring light. Addition of the uncouplers CCCP or nigericin did not increase the maximal fluorescence (F_m). The data show that under our conditions reduction of Q_A and energy dependent quenching in the dark by chlororespiration do not occur in *P. tricornutum*. Light-induced increases in F_m , therefore, are suggested to be caused by state transitions. Use of the F_0 to estimate photon capture in the light might lead to an underestimation of the PEF. The error is estimated to be not more than about 10 % as calculated from the increase in maximal fluorescence in the light.

The present work illustrates that the fluorescence pulse method is a reliable technique to get insight into the photosynthetic performance and gross primary production of the population of algal cells in a marine ecosystem.

SAMENVATTING

Fluorescentiemetingen met behulp van de verzadigende puls methode, een veel gebruikte methode voor de bestudering van de eigenschappen van fotosysteem II (PS II) bij hogere planten, zijn toegepast op culturen van de groene alg *Dunaliella tertiolecta* (Hoofdstuk 2). Zowel de actuele efficiëntie van PS II (Φ_{PSII}), de maximale efficiëntie van PS II (F_v/F_m), als de fotochemische en niet-fotochemische fluorescentie doving zijn bepaald aan culturen van *D. tertiolecta* die onder verschillende lichtcondities groeiden. De snelheid van elektronen transport door PS II (J_E), berekend als het produkt van Φ_{PSII} en de foton flux dichtheid (PFD), correleerde goed met de groeisnelheid van de culturen. De resultaten laten zien dat de verzadigende puls methode ook bij fytoplankton toegepast kan worden om fotosynthetische eigenschappen vast te stellen. De op dat moment beschikbare apparatuur was echter een factor 1000 te ongevoelig voor *in situ* metingen. Voorwaarden werden opgesteld die mede geleid hebben tot de ontwikkeling van een Xe-PAM fluorometer met een verhoogde gevoeligheid.

De relatie tussen fotosynthetische zuurstof productie (J_0 , uitgedrukt als zuurstof productie per hoeveelheid chlorofyl *a*) en J_E is onderzocht in de mariene algen *Phaeodactylum tricornutum*, *D. tertiolecta*, *Tetraselmis sp.*, *Isochrysis sp.* en *Rhodomonas sp.* door de lichtintensiteit te variëren (Hoofdstuk 3). Bij limiterend licht werd een lineaire relatie gevonden voor alle soorten. Bij verzadigend licht veranderde de relatie. Het gebied waarover lineariteit werd gevonden is 2 tot 10 maal groter dan de PFD waaronder de algen opgegroeid zijn. De verhouding tussen J_E en J_0 bij limiterend licht was afhankelijk van de soort en gerelateerd aan verschillen in de absorptie doorsnede van fotosysteem II (σ_{PSII}). De niet-lineariteit die bij hoge PFD's gevonden is wordt waarschijnlijk door een zuurstof reductie van het Mehler-type veroorzaakt en niet door fotorespiratie. De relatie tussen J_E en J_0 kan beschreven worden met een fotosynthesemodel waarin een zuurstof opname is opgenomen die afhankelijk is van de redox toestand van ferredoxine. In de diatomee *P. tricornutum* bleek dat F_v/F_m afhankelijk was van de temperatuur en optimaal bij 10 °C.

De fotosynthetische elektronen flux van een fytoplankton monster (PEF) is gedefinieerd als het produkt van J_E ($= \Phi_{PSII} \cdot \text{PFD}$), σ_{PSII} en het aantal aanwezige PS II reactie centra (n_{PSII}) (Hoofdstuk 4). Door een wiskundige afleiding blijkt het mogelijk om PEF te schatten met behulp van Φ_{PSII} en de minimale fluorescentie (F_0), die beiden met de Xe-PAM fluorimeter bepaald kunnen worden. De experimentele condities onder welke deze relatie geldig is zijn onderzocht. De maximale Φ_{PSII} (F_v/F_m) bleek onafhankelijk te zijn van de golflengte van het meetlicht. De schijnbare F_v/F_m hangt af van de intensiteit van het meetlicht en van de duur en intensiteit van de verzadigende lichtpuls. Onder bepaalde condities blijkt F_0 gebruikt te kunnen worden als een maat voor PS II excitatie in het licht. F_0 , verkregen met breedbandig excitatie licht van de Xenon-lamp werd gebruikt als een maat voor het produkt van σ_{PSII} en n_{PSII} . Er werd eenzelfde relatie tussen de uitgerekende PEF en de zuurstof productie van het sample (fytoplankton zuurstof flux, POF, uitgedrukt in zuurstof productie per volume) gevonden in de diatomee *P. tricornutum* en de groene alg *D. tertiolecta*. Daarom concluderen we dat PEF een betere schatting geeft van de POF dan J_E van J_0 .

PEF en koolstof fixatie (fytoplankton koolstof flux, PCF, uitgedrukt in kooldioxyde gefixeerd per volume) zijn bepaald in culturen van de flagellaat *Isochrysis sp.*, van de macroflagellaten van *Phaeocystis sp.* en van de diatomee *Skeletonema costatum* (Hoofdstuk 5). De PEF werd uitgerekend met behulp van F_0 die aan de start van de experimenten in iedere soort bepaald was. Zowel de licht intensiteit, als de duur van de belichting zijn gevarieerd. Zoals eerder beschreven voor de relatie tussen J_e en J_0 , bleek de relatie tussen PEF en PCF bij limiterend licht bij benadering lineair te zijn en bij verzadigend licht af te wijken van deze lineariteit. Het gebied waarover lineariteit werd gevonden was ook hier 2 tot 10 maal groter dan de PFD waarbij de algen zijn opgegroeid. De duur van de incubatie had weinig invloed op de relatie tussen PCF en PEF behalve bij de hoogste lichtintensiteiten waar met name in de eerste incubatie periode van 0 tot 0.5 uur hogere waarden voor zowel PCF als PEF werden gevonden dan in de latere incubaties. De afname van F_v/F_m van de samples die met $1530 \mu\text{mol m}^{-2} \text{s}^{-1}$ waren belicht vertoonde een snelle component in het eerste half uur van de incubatie en daarna een langzamere component. Dit duidt aan dat in de eerste 30 minuten fotoinhibitie geïnduceerd is.

PEF, PCF en zuurstof produktie zijn onderzocht in marien fytoplankton in een mesocosm (Hoofdstuk 6). PEF is zowel in laboratorium metingen als in *in situ* metingen in de mesocosm bepaald. PCF werd aan mesocosm monsters in het laboratorium bepaald. De dagelijkse primaire produktie uitgedrukt in zowel elektronen transport (PPE) als koolstof fixatie (PPC) werden uitgerekend met behulp van een fotosynthese model. Dagelijkse zuurstof produktie (PPO) werd uitgerekend aan de hand van de dagelijkse veranderingen in de zuurstof concentratie. Tussen de 2 bloei perioden van het fytoplankton was de verhouding tussen PPO en PPE hoger dan tijdens de piek van ieder bloei. De verhouding tussen PPC en PPE was constanter. In het algemeen geeft PPE een redelijke maat voor zowel PPC als PPO.

De effecten van chlororespiratie en "state transitie" op F_0 zijn onderzocht in de diatomee *P. tricornutum* (Hoofdstuk 7). Remming van chlororespiratie door antimycine A of door anaerobiose had geen effect op F_v/F_m . De waargenomen F_0 nam niet significant toe in aanwezigheid van antimycine A, en nam enigszins af tijdens belichting met verrood licht ($6 \mu\text{mol m}^{-2} \text{s}^{-1}$). Deze effecten zouden door chlororespiratie veroorzaakt kunnen worden, maar kunnen ook uitgelegd worden als reductie van Q_A door het fluorescentie meetlicht. Toevoeging van de ontkoppelaars CCCP en nigericine leidde niet tot een toename van F_m . Deze data laten zien dat in onze experimenten met *P. tricornutum* reductie van Q_A en fluorescentie diving door energetisatie van het thylakoid membraan in het donker, beiden veroorzaakt door chlororespiratie, niet voorkomen. De licht geïnduceerde toename van F_m wordt daarom verklaard door het optreden van een "state transitie". Het gebruik van F_0 om de excitatie van PS II in het licht te schatten kan leiden tot een onderschatting van PEF. De fout is niet groter dan 10 %, gebaseerd op de toename van de maximale fluorescentie in het licht.

Het onderzoek heeft laten zien dat de fluorescentie puls methode een goed instrument is voor de bepaling van de fotosynthese capaciteit en bruto primaire produktie van de algen in een mariene ecosysteem.

REFERENCES

- Allen JF (1992) Protein phosphorylation in regulation of photosynthesis. *Biochim Biophys Acta* 1098:275-335
- Asada K and Takahashi M (1987) Production and scavenging of active oxygen in photosynthesis. In: Kyle DJ, Osmond CB and Arntzen CJ (eds) *Photoinhibition*. Elsevier science publishers, the Netherlands: 227-287
- Baker NR, Oxborough K and Andrews JR (1995) Operation of an alternative electron acceptor to Q_c in maize crops during periods of low temperatures. In Mathis P (ed), *From light to biosphere*, Proceedings of the 10th International Conference on Photosynthesis, Kluwer, Dordrecht, The Netherlands Vol IV:771-776
- Beardall J, Burger-Wiersma T, Rijkeboer M, Susenik A, Lemoalle J, Dubinsky Z and Fontiella D (1994) Studies on enhanced post-illumination respiration in microalgae, *J Plankton Res* 16-10:1401-1410
- Bennoun P (1982) Evidence for a respiratory chain in the chloroplast. *Proc Natl Acad Sci USA* 72:4352-4356
- Bilger W and Björkman O (1994) Relationships among violaxanthin deepoxidation, thylakoid membrane conformation and non-photochemical fluorescence quenching in leaves of cotton (*Gossypium hirsutum* L.) *Planta* 193:238-246
- Björkman O (1987). Low temperature chlorophyll fluorescence in leaves and its relation to photon yield of photosynthesis in photoinhibition. In Kyle DJ, Osmond OB & Arntzen CJ (eds.) *Photoinhibition*. Elsevier Science Publishers, Amsterdam, p. 123-44
- Björkman O and Demmig-Adams B (1995) Regulation of photosynthetic light energy capture, conversion, and dissipation in leaves of higher plants. In: Schulze E-D and Caldwell MM (eds) *Ecophysiology of photosynthesis*. Springer-Verlag, Berlin Heidelberg, Germany: 17-47
- Briantais J-M, Verotte C, Krause GH, Weis E (1986) Chlorophyll a fluorescence of higher plants: chloroplast and leaves. In Govindjee, Ames J, Fork DC (eds) *Light Emission by Plants and Bacteria*. Academic Press, New York, p. 539
- Bryan, JR, Riley JP, Williams PLeB (1976). A Winkler procedure for making precise measurements of oxygen concentration for productivity and related studies. *J Exp Mar Biol Ecol* 21:191-197
- Butler WL (1978). Energy distribution in the photochemical apparatus of photosynthesis. *Ann Rev Plant Physiol* 29:345-78.
- Butterwick C, Heany SI, Talling JF (1982) A comparison of eight methods for estimating the biomass and growth of planktonic algae. *Br Phycol* 17:69-79
- Büchel C, Wilhelm C and Lenartz-Weiler I (1988) The molecular analysis of the light adaptation reaction in the yellow-green alga *Pleurochloris meiringensis*. *Bot Acta* 101:306-310
- Büchel C and Wilhelm C (1990) Wavelength independent state transitions and light regulated chlororespiration as mechanisms to control the energy status in the chloroplast of *Pleurochloris meiringensis*. *Plant Physiol Biochem* 28:307-314
- Caron L, Berkaloﬀ C Duval J-C and Jupin H (1987) Chlorophyll fluorescence transients from the diatom *Phaeodactylum tricornutum* relative rates of cyclic phosphorylation and chlororespiration. *Phot Res* 11:131-139
- Critchley C (1981) The molecular mechanism of photoinhibition - facts and fiction. *Austr J Plant Physiol* 15:27-41
- Cuello J Quile MJ Albacete MC and Sabater B (1995) Properties of a large complex with NADH

- dehydrogenase activity from barley thylakoids. *Plant Cell Physiol* 36:265-271
- Dau H (1994) Molecular mechanisms and quantitative models of variable Photosystem II fluorescence. *Photochem Photobiol* 60:1-23
- Dominy PJ and Williams WP (1987) The role of respiratory electron flow in the control of excitation energy distribution in blue-green algae. *Biochim Biophys Acta* 892:264-274
- Dring MJ, Jewson DH (1982) What does ^{14}C uptake by phytoplankton really measure? A theoretical modelling approach. *Proc R Soc Lond B* 214:351-68
- Eilers PHC and Peeters JHC (1988) A model for the relationship between light intensity and the rate of photosynthesis in phytoplankton. *Ecol Modell* 42:199-215
- Escaravage V, Prins TC, Smaal AC, Peeters, JHC (1996) The response of phytoplankton communities to phosphorus input reduction in mesocosms experiments, *J Exp Mar Biol Ecol* 198:550-579
- Falkowski PG and Kiefer DA (1985) Chlorophyll *a* fluorescence in phytoplankton: relationship to photosynthesis and biomass. *J Plankton Res* 7-5:715-731
- Falkowski PG, Wyman K, Ley AC and Mauzerall DC (1986) Relationship of steady state photosynthesis to fluorescence in eucaryotic algae. *Biochim Biophys Acta* 849:183-192
- Falkowski PG and Kolber Z (1990) Phytoplankton photosynthesis in the Atlantic ocean measured from a submersible pump and probe fluorometer *in situ*. in Baltscheffsky M (ed), *Current research in photosynthesis, Proceedings of the 8th International Conference on Photosynthesis*, Vol. 4, Kluwer, Dordrecht, The Netherlands: 923-926
- Fork DC, Herbert SK and Malkin S (1991) Light energy distribution in the brown alga *Macrocystis perifer*a (giant kelp). *Plant Physiol* 95:731-739
- Foyer CH and Lelandais M (1993) The roles of ascorbate in the regulation of photosynthesis. In Yamamoto HY and Smiths CM (eds) *Photosynthetic responses to the environment*. American society of plant physiologists vol 8:88-101
- Gallagher JC, Wood AM and Alberte RS (1984) Ecotypic differentiation in the marine diatom *S. costatum*. influence of light intensity on the photosynthetic apparatus. *Mar Biol* 82:121-134
- Geel C, Van Der Weijde M and Snel JFH (1994) Comparison of Photosystem II electron flow and oxygen evolution in *Synechocystis PCC6803*. *Proceedings on the BBSRC second Robert Hill symposium on photosynthesis*, 11-13 April 1994, Imperial college of science technology and medicine, London
- Geel C, Versluis W and Snel JFH (1997) Estimation of oxygen evolution by marine phytoplankton from measurement of the efficiency of Photosystem II electron flow. *Phot Res* 51:61-70
- Geider RJ and Osborne BA (1992) *Algal photosynthesis, the measurement of algal gas exchange*. Current phycology 2. Routledge, Chapman & Hall, New York, USA
- Genty B, Briantais J-M and Baker NR (1989) The relationship between the quantum yield of photosynthetic electron transport and quenching of chlorophyll fluorescence. *Biochim Biophys Acta* 990:87-92
- Genty B, Goulas Y, Dimon P, Peltier G, Briantais JM and Moya I (1992) Modulation of efficiency of primary conversion in leaves, mechanisms involved at PS2. in Murata N (ed), *Research in Photosynthesis*, Vol IV 603-610
- Genty B, Wonders J and Baker NR (1990) Non-photochemical quenching of F_0 in leaves is emission wavelength dependent: consequences for quenching analysis and its interpretation. *Phot Res* 26:133-139
- Giersch C and Krause GH (1991) A simple model relating photoinhibitory fluorescence quenching in chloroplasts to a population of altered Photosystem II reaction centres. *Photosynth Res* 30:115-121
- Gieskes WWC and Kraay GW (1984) Phytoplankton, its pigments, and primary production at a central

- North Sea station in May, July and September 1981. *Neth J Sea Res* 18:51-70
- Gimmler H (1977) Photo phosphorylation in vivo. In Trebst A and Avron M (eds) *Photosynthesis I: photosynthetic electron transport and Photo phosphorylation*. Springer-Verlag Berlin, Heidelberg, Germany. 448-472
- Goedheer JC (1970) On the pigment system of brown algae. *Biochim Biophys Acta* 314:191-201
- Goedheer JC (1973) Chlorophyll *a* forms in *Phaeodactylum tricornutum*: comparison with other diatoms and brown algae. *Biochim biophys Acta* 314:191-201
- Hall CAS and Moll R (1975) Methods of assessing aquatic primary productivity. in *Primary productivity of the biosphere*, ed Lieth H, Witthaker RH, 19-53
- Hall DO and Rao KK (1987) *Photosynthesis*, 4th edition, E Arnold, London, Great Britain
- Harbinson J, Genty B and Baker NR (1990) The relationship between CO₂ assimilation and electron transport in leaves. *Photosynth Res* 25: 213-224
- Haxo FT and Blinks R (1950) Photosynthetic action spectra of marine algae. *J Gen Physiol* 33:389-422
- Heany SI (1978) Some observations on the use of the in vivo fluorescence technique to determine chlorophyll *a* in natural populations and cultures of freshwater phytoplankton. *Freshwat Biol* 8:115-126
- Heinze I, Dau H and Senger H (1996) The relation between the photochemical yield and variable fluorescence of Photosystem II in the green alga *Scenedesmus obliquus*. *J Photochem Photobiol B: Biol* 26:89-95
- Hilton J, Rigg E, Jaworski G (1989) Algal identification using in vivo fluorescence spectra. *J Plankton Res* 11:65-74
- Hofstraat JW, Van Zeijl WJM, Peeters JCH, Peperzak L, Dubelaar GBJ (1990) Flow cytometry and other optical techniques for characterization and quantification of phytoplankton in seawater. In Nielsen HO (ed) *Environment and Pollution Measurement Sensors and Systems*. SPIE Proceedings 1269:116-33
- Hofstraat JW, Peeters JHC, Snel JFH, Geel C (1994a) simple determination of photosynthetic efficiency and photoinhibition of *Dunaliella tertiolecta* by saturating pulse fluorescence measurements. *Mar Ecol Prog Ser* 103:187-196
- Hofstraat JW, Van Zeijl WJM, De Vreeze MEJ, Peeters JHC, Peperzak L, Colijn F and Rademaker TWM (1994b) Phytoplankton monitoring by flow cytometry. *J Plankt Res* 16:1197-1224
- Holmes JJ, Weger HG, Turpin DH (1989) Chlorophyll *a* fluorescence predicts total photosynthetic electron flow to CO₂ or NO₃⁻/NO₂⁻ under transient conditions. *Plant Physiol* 91:331-337
- Holzwarth AR (1990) The functional organization of the antenna system in higher plants and green algae as studied by time resolved fluorescence techniques. In: Baltscheffsky M (ed) *Current Research in Photosynthesis*. Kluwer Academic Publisher, Dordrecht, NL. Vol 2:223-230
- Hormann H, Neubauer C and Schreiber U (1994) On the relationship between chlorophyll fluorescence quenching and the quantum yield of electron transport in isolated thylakoids. *Photosynth Res* 40:93-106
- Horton P and Hague A (1988) Studies on the induction of chlorophyll fluorescence in isolated barley protoplasts IV resolution of non-photochemical quenching. *Biochem Biophys Acta* 932:107-115
- Huppe HC and Turpin DH (1994) Integration of carbon and nitrogen metabolism in plant and algal cells. *Annu Rev Plant Physiol Plant Mol Biol* 45:577-607
- Kana TM (1990) Light-dependent oxygen cycling measured by an oxygen-18 isotope dilution technique. *Mar Ecol Prog Ser* 64:293-300
- Kana TM (1992) Relationship between photosynthetic oxygen cycling and carbon assimilation in *Synechococcus* WH7803 (cyanophyta). *J Phycol* 28:304-308

- Kana TM (1993) Rapid oxygen cycling in *Trichodesmium thiebautii* Limnol Oceanogr 38(1):18-24
- Kirk JTO (1994) Light and photosynthesis in aquatic ecosystems. second edition University Press, Cambridge
- Kolber Z, Zehr J, Falkowski P (1988) Effects of growth irradiance and nitrogen limitation on photosynthetic energy conversion in photosystem II. Plant Physiol 88:923-29
- Kolber Z and Falkowski PG (1993) Use of active fluorescence to estimate phytoplankton photosynthesis *in situ*. Limnol Oceanogr 38:1646-1665
- Kolbowski J and Schreiber U (1995) Computer controlled phytoplankton analyser based on a 4-wavelengths PAM chlorophyll fluorometer. Mathis P (ed) Photosynthesis: from light to biosphere. Proceedings of the 10th International Conference on Photosynthesis, Kluwer, Dordrecht, The Netherlands Vol. V: 825-828
- Krall JP and Edwards GE (1990) Quantum yields of Photosystem II electron transport and carbon dioxide fixation in C_4 plants. Aust J Plant Physiol 17:579-588
- Krause GH, Somersaldo S, Zumbusch E, Weyers B and Laasch H (1990) On the mechanism of photoinhibition in chloroplasts. Relationship between changes in fluorescence and activity of Photosystem II. J Plant Physiol 136:472-479
- Krause GH and Weis E (1991) Chlorophyll fluorescence and photosynthesis: the basics. Ann Rev Plant Physiol Plant Mol Biol 42:313-349
- Kroon BMA (1994) Variability of photosystem II quantum yield and related processes in *Chlorella pyrenoidosa* (Chlorophyta) acclimated to an oscillating light regime simulating a mixed photic zone. J Phycol 30:841-852
- Kroon B, Prézelin BB and Schofield O (1993) Chromatic regulation of quantum yields for photosynthetic Photosystem II charge separation, oxygen evolution and carbon fixation in *Heterocapsa pigmaea* (Pyrrophyta). J Phycol 29:453-462
- Lawlor DW (1993) Photosynthesis: molecular, physiological and environmental processes, 2nd edition, Longman Scientific & technical, England
- Ley A and Mauzerall DC (1982) Absolute absorption cross-sections for photosystem II and the minimum quantum requirement for photosynthesis in *Chlorella vulgaris*. Biochim Biophys Acta 680:95-106
- Lichtenthaler HK, Rinderle U (1988) The role of chlorophyll fluorescence in the detection of stress conditions in plants. CRC Critical Reviews in Chemistry. 19:529-585
- Lindblad P and Guerrero MG (1993) Nitrogen fixation and reduction. In: Hall DO, Scurlock JMO, Bolh r-Nordenkamp HR, Leegood RC and Long SP (eds) Photosynthesis and production in a changing environment: a field and laboratory manual. Chapman & Hall London UK 299-312
- Malkin S, Telfer A and Barber J (1986) Quantitative analysis of state 1-state 2 transitions in intact leaves using modulated fluorimetry - evidence for changes in the absorption cross-section of the two Photosystems during state transitions. Biochim Biophys Acta 848:48-57
- Mauzerall DC (1972) Light induced fluorescence changes in *Chlorella*, and the primary photoreactions for the production of oxygen. Proc Natl Acad Sci USA 69:1358-1393
- McLachlan J (1975) Growth media-marine. In Handbook of phycolgical methods culture methods and growth measurements, ed Stein JR, 25-51
- Oberhuber W, Dai Z-Y and Edwards GE (1993) Light dependence of quantum yields of photosystem II and CO_2 fixation in C_3 and C_4 plants. Photosynth Res 35:265-274
- Oilazola M, La Roche J, Kolber Z and Falkowski PG (1994) Non-photochemical fluorescence quenching and the diadinoxanthin cycle in a marine diatom. Photosynth Res 41:357-370
- Oxborough K and Horton P (1987) Characterisation of the effects of antimycin A upon high energy state

- quenching of chlorophyll fluorescence (q_e) in spinach and pea chloroplasts. *Photosynth Res* 12:119-128
- Owens TG and Wold ER (1986) Light harvesting function in the diatom *Phaeodactylum tricornutum*, I isolation and characterization of the pigment-protein complexes. *Plant Physiol* 80:732-738
- Owens TG (1986a) Photosystem II heterogeneity in the marine diatom *P. tricornutum*. *Photochem Photobiol* 43:535-544
- Owens TG (1986b) Light harvesting function in the diatom *Phaeodactylum tricornutum*. II Distribution of excitation energy between the photosystems. *Plant Physiol* 80:739-746
- Öquist G and Chow WS (1992) On the relationship between the quantum yield of Photosystem II electron transport, as determined by chlorophyll fluorescence and the quantum yield of CO_2 -dependent O_2 evolution. *Photosynth Res* 33:51-62
- Peeters JHC, Arts F, Ecaravage V, Haas HA, Jong IEA de, Loon R van, Moest B and Put A van der (1993) Studies on light climate, mixing and reproducibility of ecosystem variables in mesocosms: consequences for the design, in Peeters JHC, Joordens JCA, Smaal AC, Nienhuis PH (eds): The impact of marine eutrophication on phytoplankton and benthic suspension feeders: results of a mesocosms pilot study, Report GWAO-93.039, pp7-23, National Institute for Coastal and Marine Management/RIKZ, Middelburg, The Netherlands
- Peltier G, Ravenel J and Verméglio A (1987) Inhibition of a respiratory activity by short saturating flashes in *Chlamydomonas*: evidence for a chlororespiration. *Biochim Biophys Acta* 893:87-90
- Peltier G and Schmidt GW (1991) Chlororespiration: an adaptation to nitrogen deficiency in *Chlamydomonas reinhardtii* *Proc Natl Acad Sci* 88: 4791-4795
- Peterson BJ (1980) Aquatic primary productivity and the ^{14}C - CO_2 method: A history of the productivity problem. *Ann Rev Ecol Syst* 11:359-85
- Prasil O, Kolber Z, Berry JA, Falkowski PG (1996) Cyclic electron flow around Photosystem II *in vivo*. *Photosynth Res* 48:395-410
- Prézelin BB and Haxo FT (1976) Purification and characterization of peridinin-chlorophyll *a*-proteins from the marine dinoflagellates *Glenodinium sp.* and *Gonyaula polyedra*. *Planta (Berl)* 128:133-141
- Prins TC, Pouwer AJ and Escaravage V (1995) Nitrogen, phosphorus and oxygen balances of 1994 experiments, in Peeters, JHC, Smaal, AC, Haas HA, Heip, CHR (eds): The impact of marine eutrophication on phytoplankton and benthic suspension feeders: Progress report II: results of mesocosms experiments with reduced N-load and increased grazing pressure, Report RIKZ-95.048 pp 114-144, National Institute for Coastal and Marine Management/RIKZ, Middelburg, The Netherlands
- Quick WP and Stitt M (1989) An examination of factors contributing to non-photochemical quenching of chlorophyll fluorescence in barley leaves. *Biochem Biophys Acta* 977: 287-296
- Ravenel J and Peltier G (1991) Inhibition of chlororespiration by myxothiazol and antimycin A in *Chlamydomonas reinhardtii* *Phot Res* 28: 141-148
- Ravenel J and Peltier G (1992) Stimulation of the chlororespiratory electron flow by Photosystem II activity in *Chlamydomonas reinhardtii* *Biochem Biophys Acta* 1101:57-63
- Rees D, Lee CB, Gilmour DJ and Horton P (1992) Mechanisms for controlling balance between light input and utilisation in the salt tolerant alga *Dunaliella C9AA*. *Photosynth Res* 32:181-192
- Reid PC, Lancelot C, Gieskes WWC, Hagmeier E and Weichart G (1990) Plankton of the North Sea and its dynamics. A review. *Neth J Sea Res* 26:295-331
- Renger, G., Schreiber, U. (1986). Practical applications of fluorometric methods to algae and higher plant research. In Govindjee, Ames, J., Fork, D.C. (eds. Light Emission

- by Plants and Bacteria. Academic Press, New York, p. 587
- Rouag D and Dominy P (1994) State adaptations in the cyanobacterium *Synechococcus 6301* (PCC): dependence on light intensity or spectral composition? *Phot Res* 40:107-117
- Schansker G (1996) Photosynthetic performance of photoinhibited pea leaves: a photoacoustic and fluorescence study. In: Schansker G, Mechanistic aspects of the inhibition of photosynthesis by light. Ph. D Thesis, Wageningen Agricultural University, Netherlands
- Scherer S, Almon H and Böger P (1988) Interaction of photosynthesis, respiration and nitrogen fixation in cyanobacteria. *Phot Res* 15:95-114
- Schreiber U (1983) Chlorophyll fluorescence yield changes as a tool in plant physiology. I: The measuring system. *Photosynth Res* 4:361-73
- Schreiber U (1986) Detection of rapid induction kinetics with a new type of high-frequency modulated chlorophyll fluorometer. *Phot Res* 9: 261-272
- Schreiber U, Bilger W and Neubauer C (1995a) Chlorophyll fluorescence as a noninvasive indicator for rapid assessment of in vivo photosynthesis. In: Schulze E-D and Caldwell MM (eds) *Ecophysiology of photosynthesis*. Springer-Verlag, Berlin Heidelberg, Germany: 49-70
- Schreiber U, Hormann H, Neubauer C, Klughammer C (1995b) Assessment of Photosystem II photochemical quantum yield by chlorophyll fluorescence quenching analysis. *Aust Plant Physiol* 22:209-220
- Schreiber U, Neubauer C and Schliwa U (1993) PAM fluorometer based on medium frequency pulsed Xe-flash measuring light: A highly sensitive new tool in basic and applied photosynthesis research. *Photosynth Res* 36:65-72
- Schreiber U, Schliwa U and Bilger W (1986) Continuous recording of photochemical and non-photochemical chlorophyll fluorescence quenching with a new type of modulation fluorometer *Photosynth Res* 10:51-62
- Seidel-Guyenot W, Schwabe C and Büchel C (1996) Kinetic and functional characterization of a membrane-bound NAD(P)H dehydrogenase located in the chloroplasts of *Pleurochloris meiringensis* (Xanthophyceae). *Phot Res* 49:183-193
- Strasser RJ, Butler WL (1977) The yield of energy transfer and the spectral distribution of excitation energy in the photochemical apparatus of flashed bean leaves. *Biochim Biophys Act* 462:295
- Ting CS and Owens TG (1992) Limitations of the pulse-modulated technique for measuring the fluorescence characteristics of algae. *Plant Physiol* 100:367-373
- Ting CS and Owens TG (1993) Photochemical and nonphotochemical fluorescence quenching processes in the diatom *Phaeodactylum tricornutum*. *Plant Physiol* 101:1323-1330
- Tolber NE (1979) Glycolate metabolism by higher plants and algae. In Gibbs M and Latzko E (eds) *Photosynthesis II: photosynthetic carbon metabolism and related processes*. Springer-Verlag Heidelberg, Germany 338-352
- Turpin DH and Bruce D (1990) Regulation of light harvesting by nitrogen assimilation in the green alga *Selenastrum minutum*. *FEBS* 263:99-103
- Van Kooten O and Snel JFH (1990) The use of chlorophyll fluorescence nomenclature in plant stress physiology. *Photosynth Res* 25:147-150
- Van Wijk KJ and Krause GH (1991) O₂-dependence of photoinhibition at low temperature in intact protoplasts of *Locusta valerianella* L. *Planta* 186:135-142
- Weger HG, Birch DG, Elfiri IR, and Turpin DH (1988) Ammonium assimilation requires mitochondrial respiration in the light: A study with the green alga *Selenastrum minutum*. *Plant Physiol* 89:409-415
- Weger HG, Herzig R, Falkowski PG, Turpin DH (1989) Respiratory losses in the light in a marine diatom:

- Measurements by short-term mass spectrometry. *Limnol Oceanogr* 34:1153-1161
- Weger HG and Turpin DH (1989) Mitochondrial respiration can support NO_3^- and NO_2^- reduction during photosynthesis. *Plant Physiol* 89:409-415
- Wilhelm C (1993) Some critical remarks on the suitability of the concept of the photosynthetic unit in photosynthesis research and phytoplankton ecology. *Bot Acta* 106:287-293
- Williams PIIeB, Raine RCT and Bryan JR (1979) Agreement between the ^{14}C and oxygen methods of measuring phytoplankton production: reassessment of the photosynthetic quotient. *Oceanologica Acta* 2(4):411-416
- Williams PIIeB, Robinson C, Søndergaard M, Jespersen A-M, Bentley TL, Lefèvre D, Richardson K and Riemann B (1996) Algal ^{14}C and total carbon metabolisms. 2. Experimental observations with the diatom *Skeletonema costatum*. *J Plankton Res* 18(10):1961-1974
- Williams WP and Allen JF (1987) State1/state2 changes in higher plants and algae. *Phot Res* 13:19-45
- Yentsch CS, Phinney DA (1985a) Fluorescence spectral signatures for studies of marine phytoplankton. In Zirino, A. (ed.) Mapping Strategies in Chemical Oceanography. Advances in Chemistry Series, No. 209. American Chemical Society, Washington, DC, p. 259
- Yentsch CS, Phinney DA (1985b) Spectral fluorescence: an ataxonomic tool for studying the structure of phytoplankton populations. *J Plankton Res* 7:617-32
- Yentsch CS and Yentsch, CM (1979) Fluorescence spectral signatures: the characterization of phytoplankton populations by the use of excitation and emission spectra. *J Mar Res* 37:471-83
- Xue X, Gauthier DA, Turpin DH, Weger HG (1996) Interactions between photosynthesis and respiration in the green alga *Chlamydomonas reinhardtii*. *Plant Physiol* 112:1005-1014

CURRICULUM VITAE

Corine Geel werd op 4 juli 1967 geboren in Nuenen. In 1985 behaalde zij het VWO diploma aan het Rythoviuscollege te Eersel. Daarna begon zij met de studie Moleculaire Wetenschappen aan de Landbouwniversiteit te Wageningen. Het doctoraal examen met fysisch-chemische oriëntatie werd behaald in 1991. De hoofdvakken waren: fysische plantenfysiologie bij dr. J Snel en industriële microbiologie bij M. Smith. In november 1991 is zij begonnen als AIO aan de toenmalige vakgroep Plantenfysiologisch Onderzoek van de Landbouwniversiteit te Wageningen die nu gefuseerd is met de vakgroep Plantenfysiologie. Het onderzoeksproject 'energie conversie in fytoplankton' werd gefinancierd door het Rijksinstituut voor Kust en Zee (RIKZ) en de Cornelis Lely stichting en heeft geleid tot dit proefschrift.